

## CRITICAL REVIEW

[View Article Online](#)  
[View Journal](#) | [View Issue](#)Cite this: *J. Anal. At. Spectrom.*, 2017,  
32, 494

## Plasma source mass spectrometry for radioactive waste characterisation in support of nuclear decommissioning: a review

Ian W. Croudace,<sup>\*a</sup> Ben C. Russell<sup>ab</sup> and Phil W. Warwick<sup>a</sup>

The efficient characterization of nuclear waste materials represents a significant challenge during nuclear site decommissioning, with a range of radionuclides requiring measurement in varied and often complex sample matrices. Of the available measurement techniques, inductively coupled plasma mass spectrometry (ICP-MS) has traditionally been applied to long-lived radionuclides, particularly in the actinide series. With recent advances in the technique, both the sensitivities achievable and number of radionuclides potentially measurable has expanded, with the reduced procedural time offering significant economic benefits to nuclear site waste characterization compared with traditional radiometric (typically alpha and beta spectrometry) techniques. This review provides a broad assessment of recent developments, improvements in capability and describes the advantages and drawbacks of ICP-MS with regards to sample introduction and instrument design. The review will be of interest to international agencies concerned with nuclear decommissioning as well as nuclear site laboratories, project managers and sites involved in environmental monitoring and nuclear forensics.

Received 7th September 2016  
Accepted 20th December 2016DOI: 10.1039/c6ja00334f  
[www.rsc.org/jaas](http://www.rsc.org/jaas)

### 1 Introduction

Over the last 30 years, the application of ICP-MS for radionuclide quantification has grown significantly. Initially, ICP-MS techniques focused on longer lived radionuclides where their low specific activities favored atom-counting over radiometric techniques (typically alpha and beta spectrometry). For example, U, Th, Pu, <sup>99</sup>Tc, and <sup>237</sup>Np have been measured using ICP-MS since its early days. With the shift to decommissioning, other long lived but less abundant radionuclides such as <sup>93</sup>Zr have also been quantified using ICP-MS. In addition, improvements in instrument sensitivity achieved through advances in sample introduction, mass spectrometry configuration and design and vacuum pump technologies, has opened up the possibility of using ICP-MS for quantification of shorter-lived radionuclides such as <sup>90</sup>Sr, significantly reducing the analytical time for such analyses (Fig. 1).

Historically, radionuclide analysis within the nuclear sector has supported environmental monitoring programs, health physics, process control, effluent and waste characterization and personnel monitoring. Analytical programs tended to focus on relatively short-lived radionuclides that were likely to contribute significantly to personnel and public doses or contamination of the workplace, or which provided

information on reactor performance. However, in recent years, many first and second generation nuclear facilities worldwide have either entered or are approaching shutdown and decommissioning phases. This has led to a rapidly increasing demand for radionuclide analysis to characterize the wastes arising from site decommissioning programs (e.g. plant contamination assessments, radioactively contaminated land *etc.*)

As well as focusing on radionuclides that contribute to radiological worker dose and waste activity inventories in the short term, analytical strategies are now also required to quantify the low-abundance long lived radionuclides that will impact on waste repository safety cases over  $10^3$  to  $10^6$  years. The change in emphasis to decommissioning has resulted in a number of analytical challenges. These include the need for rapid radionuclide characterization of wastes prior to sentencing, the provision of techniques capable of measuring low-abundance long-lived radionuclides in the presence of other significantly higher abundance radionuclides and the requirement to analyze diverse and complex matrices. In all these cases, mass spectrometric techniques, and particularly ICP-MS, offer some unique capabilities, which help to address these challenges. Given the increasing expectations facing radioanalytical science arising from decommissioning and the expanding programme of decommissioning worldwide, it is timely to review the state-of-the-art regarding ICP-MS analysis of radionuclides and to explore how the technique could be more widely applied in the future.

<sup>a</sup>GAU-Radioanalytical, University of Southampton, NOCS, Southampton, SO14 3ZH, UK. E-mail: [iwc@noc.soton.ac.uk](mailto:iwc@noc.soton.ac.uk)

<sup>b</sup>National Physical Laboratory, Teddington, TW11 0LW, UK

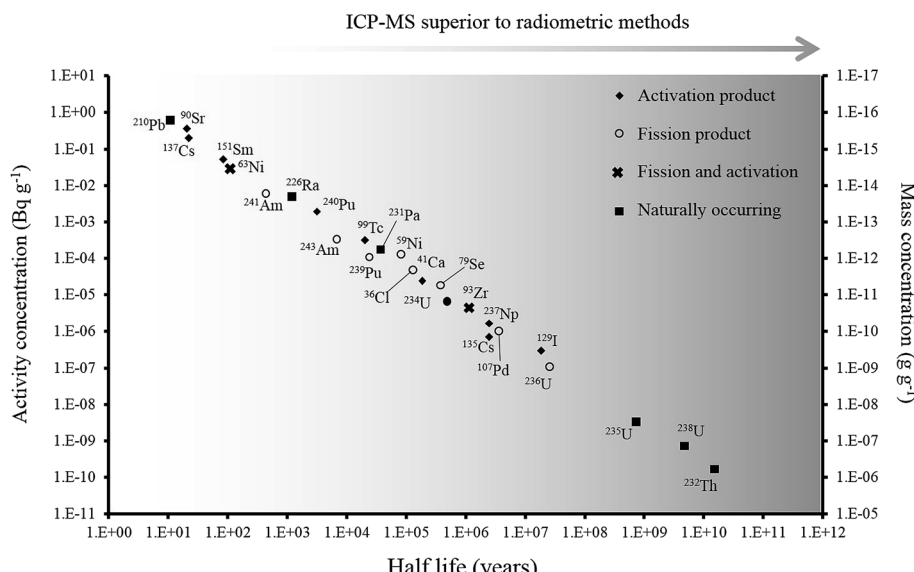


Fig. 1 Half-life versus minimum detectable activity (activity that gives count rate that is  $>3$  times standard deviation of the background count rate) and concentration of selected radionuclides, labelled according to their method of production. Adapted from Russell *et al.* (2014).<sup>1</sup>

## 2 History

There have been numerous developments in the field of mass spectrometry.<sup>2–20</sup> In 1983 a significant advance was the introduction of the first commercial ICP-QMS,<sup>21,22</sup> an instrument that allowed elements and isotope ratios to be

measured at high sensitivity. The ICP-QMS uses an inductively coupled argon plasma as an excitation source to ionize the sample and a quadrupole mass spectrometer as an analyser to separate and selectively transmit analyte ions of a single mass-to-charge ratio ( $m/z$ ) to the detector. During this process, sample ions rapidly undergo large temperature

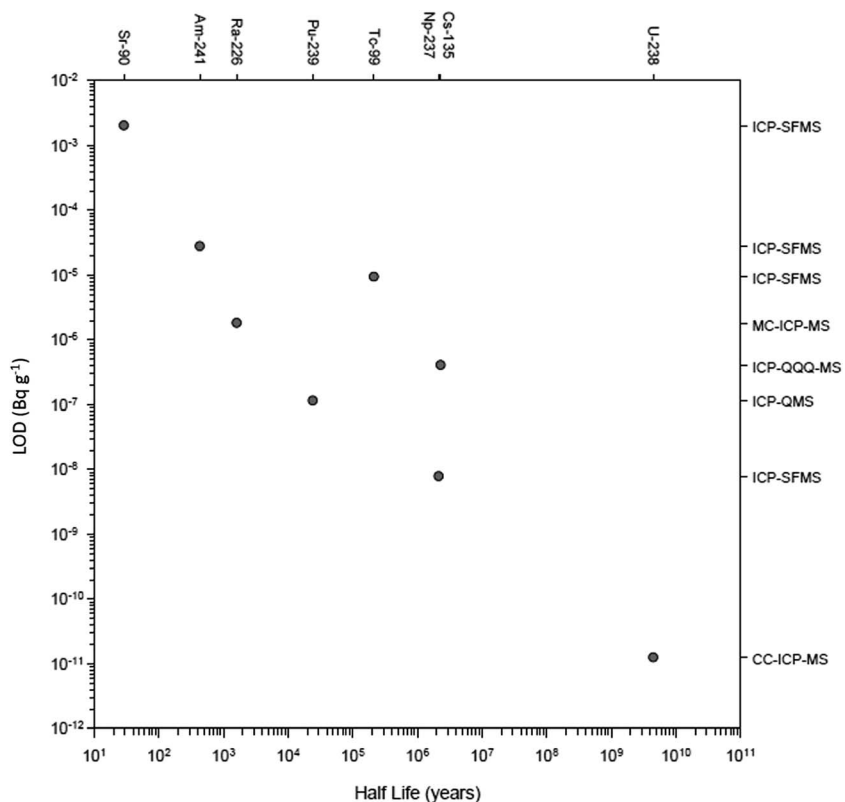


Fig. 2 Recent detection limits achieved for multiple radionuclides as a function of their half-life.

(6000 K-to-room temp.) and pressure (760 to  $10^{-6}$  Torr) reductions. In essence, ions are systematically transferred from the plasma to the detector in a highly controlled electrostatic field within a dynamically increasing vacuum which was followed several years later by early measurements of radionuclides.<sup>22–27</sup> The rapidity of ICP-QMS and ability to simultaneously measure multiple radionuclides were established as major advantages compared to alpha and beta counting techniques,<sup>28–30</sup> whilst the robustness of the technique better-suited to routine analysis compared to alternative mass spectrometric techniques, specifically thermal ionization mass spectrometry (TIMS).<sup>30,31</sup> Additionally, sample introduction into ICP-QMS could be achieved from a solid, liquid or gas.<sup>32</sup>

Early studies were critical in establishing the uncertainties associated with radionuclide detection by ICP-QMS and considerations for instrumental setup. This included sample pre-treatment prior to sample introduction to improve detection limits,<sup>23</sup> the impact of sample introduction on sensitivity and interference removal,<sup>27,29,33–35</sup> the importance of abundance sensitivity in removing peak tailing,<sup>26</sup> and the use of internal standardization to account for matrix effects.<sup>36</sup> As well as advances in quadrupole instrument design, the development of other ICP-MS setups including sector field (ICP-SFMS), collision/reaction cell instruments and multiple detector systems (MC-ICP-MS) has increased the sensitivity, interference-removal capability, and the number of nuclides measurable (Fig. 2). This has significantly expanded the toolbox for the radioanalytical chemist with regards to nuclear waste characterization and decommissioning.

### 3 Mass spectrometry vs. radiometric analysis

The specific activity (the rate of radioactive decay for a given mass of isotope) for a radionuclide is inversely proportional to the half-life and hence, for long lived radionuclides, more sensitive measurements can potentially be achieved by determining the concentration rather than the activity of the radionuclide (Fig. 1). More recently, there has been a growing interest in quantifying long-lived, low abundance radionuclides (e.g.  $^{41}\text{Ca}$ ,  $^{59}\text{Ni}$ ,  $^{63}\text{Ni}$ ,  $^{93}\text{Zr}$ ,  $^{135}\text{Cs}$ ,  $^{151}\text{Sm}$ ) formed through fission or neutron activation. These radionuclides were not considered significant during operational phases as their contribution to operator dose was significantly lower than for the short lived radionuclides such as  $^{90}\text{Sr}$  and  $^{137}\text{Cs}$  (Fig. 3). However, such radionuclides contribute significantly to the long-term nuclear waste repository dose estimates. Measurement of these radionuclides radiometrically is challenging as their emissions are often masked by the more abundant short-lived isotopes. For example, in fresh fission wastes the  $^{135}\text{Cs} : ^{137}\text{Cs}$  atomic ratio is approximately 1 : 1 whereas the activity ratio is 1 : 80 000. In such instances, mass spectrometric techniques are the best analytical approach and bring significant benefits through analytical cost saving and sample throughput.

In some cases, radiometric techniques are limited to measurement of radionuclides with relatively short half-lives. Consequently, isotope ratio measurements are limited to monitoring of nuclear incidents shortly after the event (e.g.  $^{134}\text{Cs} / ^{137}\text{Cs}$  measurements at Fukushima), and are no longer applicable to samples affected by atmospheric weapons test fallout or

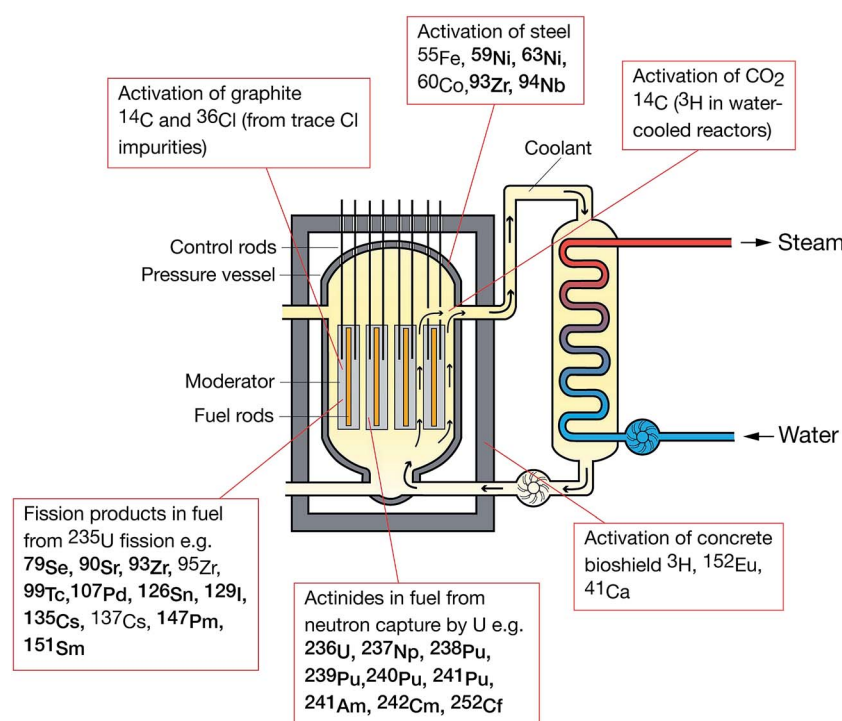


Fig. 3 Formation route of medium to long-lived radionuclides in a nuclear reactor.



Table 1 Summary of sample introduction techniques for ICP-MS

Technique	Comments	Radionuclide applications ref.
Solution nebulization	<ul style="list-style-type: none"> <li>Range of designs, some with high tolerance to solid content</li> <li>Sample uptake rate as low as 50 <math>\mu\text{L min}^{-1}</math></li> <li>Relatively high oxide and hydride formation</li> <li>Sample to plasma transfer efficiency can be 1–2%</li> </ul>	45–52
Desolvating sample introduction	<ul style="list-style-type: none"> <li>Reduced solvent loading, low oxide and hydride formation</li> <li>Ultrasonic nebulisers have high sample uptake rate (<math>\sim 1 \text{ mL min}^{-1}</math>)</li> </ul>	53–57
Direct injection	<ul style="list-style-type: none"> <li>100% sample to plasma efficiency</li> <li>Increased solvent loading into plasma increases oxide and hydride formation</li> </ul>	34, 41, 48 and 58
Flow injection (FI)	<ul style="list-style-type: none"> <li>Direct, real-time measurements</li> <li>Reduced sample preparation compared to offline separation</li> <li>100% sample to plasma efficiency</li> <li>High maintenance</li> <li>Ultra-trace measurement difficult</li> </ul>	59–62
Sequential injection (SI)	<ul style="list-style-type: none"> <li>Evolution of flow injection</li> <li>Delivery of eluents, washing solutions and standards without reconfiguring the manifold</li> <li>Potential cross-contamination using a single manifold</li> </ul>	63
Lab on chip	<ul style="list-style-type: none"> <li>Downscaling of sequential injection</li> <li>Reagent-based assay to sub-<math>\mu\text{L}</math> levels</li> </ul>	64
Laser ablation (LA-ICP-MS)	<ul style="list-style-type: none"> <li>Direct measurement of solid samples</li> <li>Surface and depth profiling, or measurement of single particles</li> <li>Reduced hydride and oxide formation because of 'dry' plasma</li> <li>Solution nebulization preferable for bulk sample composition</li> <li>Lack of reference materials</li> </ul>	65–76
Electro thermal vaporization (ETV)	<ul style="list-style-type: none"> <li>High analyte transport efficiency (20–80%)</li> <li>Low oxide and hydride formation</li> <li>Can handle complex sample matrices</li> <li>Inferior detection limit compared to solution nebulization</li> </ul>	77–81
Glow discharge	<ul style="list-style-type: none"> <li>Complete material characterization</li> <li>Interferences can arise from discharge gas and sample matrix</li> <li>Isobaric interferences prevents direct determination of radionuclides</li> </ul>	82 and 83
High performance liquid chromatography (HPLC)	<ul style="list-style-type: none"> <li>Rapid separation compared to offline chemical separation</li> <li>Separation and detection of multiple radionuclides from the same sample</li> </ul>	48, 74, 84 and 85
Cold plasma	<ul style="list-style-type: none"> <li>Rapid isobaric interference separation compared to offline chemical separation</li> <li>Sensitivity dependent on sample matrix</li> <li>Several potential applications e.g. <math>^{79}\text{Se}/^{79}\text{Br}</math>, <math>^{126}\text{Sn}/^{126}\text{Te}</math>, <math>^{129}\text{I}/^{129}\text{Xe}</math></li> </ul>	86 and 87
Capillary electrophoresis	<ul style="list-style-type: none"> <li>Low sample volumes (nL to <math>\mu\text{L}</math>)</li> <li>Rapid separation compared to offline chemical separation</li> </ul>	88–90

Chernobyl. Advances in ICP-MS have put this technique in a position where  $^{135}\text{Cs}$  (2.3 million year half-life) is measurable, enabling determination of the  $^{135}\text{Cs}/^{137}\text{Cs}$  ratio, expanding measurement options over longer timescales. In other cases, radiometric techniques are unable to separate isotopes with similar decay energies e.g.  $^{239}\text{Pu}$  and  $^{240}\text{Pu}$ , whereas ICP-MS is capable of accurate measurement of the  $^{239}\text{Pu}/^{240}\text{Pu}$  ratio, which can vary significantly depending on the source of contamination, and therefore represents a significant advance with regards to routine monitoring and nuclear forensics.

The significant reduction in counting time compared to radiometric techniques was identified as an early advantage of ICP-MS for particular radionuclides. As the technique has advanced, there has been a focus on reducing the sample preparation time using techniques such as online chemical separation coupled directly to the instrument, interference separation using an integrated collision or reaction cell, and

improvements in sensitivity and isotope ratio accuracies using sector-field and multi-collector instruments, respectively.

Accurate and low uncertainty measurements of the decay properties of radionuclides is of importance in numerous fields including decay heat calculations in the nuclear industry and calibration of instruments.<sup>37,38</sup> ICP-MS can achieve low uncertainty measurement of the number of atoms in a sample, which combined with radiometric activity measurements allow determination of the decay constant and half-life. This information is used as part of development of technical standards, which improves measurement with regards to measurement quality, reproducibility and comparison between studies<sup>39,40</sup>.

## 4 Sample introduction

Development of high sensitivity sample introduction has been a vital part of improving detection limits, and is potentially a key



factor in reducing isobaric, polyatomic and tailing interferences depending on the instrumental setup.<sup>41,42</sup> A number of studies have compared the performance of different sample introduction techniques<sup>41,43,44</sup> and these are summarised in Table 1.

## 5 Quadrupole ICP-MS (ICP-QMS)

ICP-QMS achieved the first successful measurements of radionuclides by ICP-MS. Early instruments were unable to achieve separation of isobaric and polyatomic interferences because of their limited abundance sensitivity. Their use was originally focused on higher mass radionuclides such as <sup>238</sup>U that do not suffer from the same number of interferences as lower mass radionuclides. However, advances in instrumental sensitivity, versatility with regards to sample introduction, and equipping certain instruments with a collision/reaction cell has improved detection limits and expanded applications over time.

MicroMass Ltd. (Wilmslow, UK) introduced an early version of a collision cell instrument (Platform ICP-MS), with the aim of thermalizing ions and dissociating disturbing molecular ions such as argides. Compared to operating without a collision cell, ion transmission, sensitivity and isotope ratio precision can be improved.<sup>74</sup> However, there are conflicting views on the impact of ICP-CC-MS on abundance sensitivity. On the one hand, collisions in the cell can reduce the ion kinetic energy, potentially improving the abundance sensitivity by increasing the residence time of ions in the mass analyser which results in better mass separation.<sup>49</sup> However, the collision gas increases pressure in the mass analyser, with residual gas ions leading to scattering of ions in the quadrupole, which at higher gas flow rates can have a negative impact on the abundance sensitivity.

The Perkin Elmer Elan 6100 Dynamic Reaction Cell (DRC) (based on Elan 6000 ICP-QMS) is an early example of a reaction cell instrument, capable of operating with multiple gases including NH<sub>3</sub>, CH<sub>4</sub>, H<sub>2</sub> and He. DRC instruments are equipped with a Bandpass Tuning feature, which offers mass discrimination against interfering by-products formed in the cell, whilst allowing analyte transmission. This compares to a collision cell setup that often operates with an energy filter to prevent newly formed interferences from leaving the cell. This can lead to an energy overlap between the analyte and interferences that may ultimately increase instrument backgrounds, decrease analyte signal and adversely impact detection limits.<sup>91</sup> Bandura *et al.* (2005) extensively studied cell-based separation of

radionuclides from overlapping isotopes using a Perkin Elmer Elan DRC, with the results outlining the cell gas used and the likelihood of the reaction occurring.<sup>92</sup> The DRC series has been updated with the NexION series, which is equipped with a quadrupole ion deflector that turns the ion beam 90° prior to the entrance to the collision/reaction cell. The NexION series is also equipped with an additional hyper skimmer cone to improve the removal of unionized material.

The Agilent 8800 Triple Quadrupole ICP-MS (ICP-QQQ-MS) consists of two quadrupoles positioned either side of a collision-reaction cell (termed the Octopole Reaction System, ORS). It is in effect an ICP-MS/MS or tandem mass spectrometer. Positioning a quadrupole before the entrance to the cell means the ion beam can be mass filtered prior to the cell entrance, enabling greater control over the ions entering the cell, preventing undesirable secondary polyatomic ions from forming in the cell. Secondly, the additional quadrupole improves the abundance sensitivity, with a theoretical value of 10<sup>-14</sup>. This is advantageous for radionuclides affected by tailing from a stable isotope of the same element *e.g.* <sup>88</sup>Sr on <sup>90</sup>Sr, and <sup>127</sup>I on <sup>129</sup>I. The 8800 has recently been superseded by the 8900, offering improvements including more rapid sample acquisition, measurement at higher masses (beneficial for actinide-based cell products) and introduction of samples with up to 25% total dissolved solid content.

## 6 Sector field ICP-MS (ICP-SFMS)

The introduction of ICP-SFMS offered lower background and higher sensitivity compared with ICP-QMS, enabling lower limits of detection for radionuclide measurement. The counting efficiency of ICP-SFMS is generally on the order of ~0.1%, with low background signals of <1 counts per second, compared to typical ICP-QMS values of 0.01% counting efficiency and several counts per second background.<sup>93,94</sup> ICP-SFMS can therefore theoretically analyze smaller bulk samples with lower analyte concentrations.<sup>95</sup> Operating at higher mass resolution can be used to reduce or remove isobaric and polyatomic interferences, however, this is at the expense of ion transmission and therefore sensitivity.<sup>94</sup> Reproducibility can also be affected, with typical values at low resolution of <0.02%, compared to <0.1% at medium and high resolution.<sup>96</sup> Additionally, overlapping peaks from stable isobars affecting radionuclide detection cannot be resolved, even at high resolution. Therefore, ICP-SFMS is

Table 2 Summary of main commercially available ICP-MS instruments

Instrument type	Thermo Scientific	Agilent	Perkin Elmer	Nu	Spectro
Collision/reaction cell	iCap Q	7800 7900 8900		NexION 300 series	
Sector field	Element 2 Element XR			Attom	Spectro MS
Multi-collector	Neptune Plus			Plasma II Plasma 1700	



generally operated at low mass resolution to maximize instrumental sensitivity,<sup>97,98</sup> with interference removal dependent on sample introduction and/or chemical separation.

Multi-collector instruments (MC-ICP-MS) are fitted with multiple ion counting detectors, which eliminates the need to cycle a number of small ion beams through a single detector. In addition, the effects of ion beam instability are eliminated, and flat-topped peaks and high precision isotope ratios ( $\sim 0.001\%$ ) are achievable, which is not possible using single detector instruments.<sup>51,54,99</sup> For example, the Thermo Neptune (equipped with eight Faraday cups that are interchangeable with ion counting detectors) are capable of flat-topped peaks at medium mass resolution (4000), unlike single detector ICP-SFMS instruments. Multiple collectors also increase the signal in proportion to the number of available ion counting channels. For example, Taylor *et al.* (2003) demonstrated that with two ion-counting channels, the dwell time of  $^{240}\text{Pu}/^{239}\text{Pu}$  is doubled, or only half the amount of plutonium is needed to give similar counting statistics to the peak jumping method.<sup>51</sup>

Finally, the Spectro-MS is a fully simultaneous, double focusing ICP-SFMS consisting of an entrance slit, ESA, energy slit, magnetic sector field and a solid state detector split into 4800 channels, which is capable of measuring the entire mass system.<sup>100</sup> For every analysis, the entire mass spectrum is captured, rather than focusing over a single mass unit. A summary of commercially available ICP-MS is given in Table 2.

## 7 Future developments in hardware

### 7.1 Miniaturization

Current applications of miniature instruments include drug screening of people, packages, luggage and vehicles, as well as forensics and environmental analysis.<sup>101–103</sup> The instruments developed can be self-contained with volumes of approximately  $50\text{ cm}^3$ , although this may exclude ionization sources and compressed gas cylinders.<sup>103</sup> There are a number of ionization techniques (Table 3) and commercially available instruments.<sup>104</sup> The pump and sample introduction system have a significant influence on instrument size and weight, whilst miniaturization can lead to a reduction in performance. Instruments typically have detection limits in the ppm to ppb range,<sup>105,106</sup> and to date there have been no applications for nuclear decommissioning. However, this approach potentially offers no sample preparation, and on-site, real-time analysis without having to return samples to an off-site laboratory.

### 7.2 Extreme environments

There have been a limited number of studies into instrument contamination following handling of active samples. Oak Ridge National Laboratory investigated contamination of ICP-QMS from  $^{90}\text{Sr}$  and  $^{137}\text{Cs}$  in the pump oil, and swabs of solid components.<sup>107</sup> No activity was measured on the detector, with the majority in the interface region. Whilst any activity on the sample cone was burned off by the torch, some was detected on the skimmer cone. Two separate studies found contamination on the quadrupoles.<sup>108,109</sup>

Table 3 Summary of atmospheric pressure ionization sources

Abbreviation	Full name
DBDI	Dielectric barrier discharge ion source
DESI	Desorption electrospray ionization
DART	Direct analysis in real time
LEMS	Laser electrospray mass spectrometry
FAPA	Flowing atmospheric pressure afterglow
LTP	Low temperature plasma
LP-DBDI	Low pressure dielectric barrier discharge ionization

There are a number of variables that must be considered, including the ion transmission, which is likely to vary depending on the age of the instrument. Contamination is also likely to vary with sample introduction system, instrument design, radionuclide and activity analyzed, and the sample throughput.<sup>110</sup> It is therefore good practice to monitor solid components such as cones, detectors and quadrupoles when they are replaced, prior to disposal. Some instruments have been modified in order to handle higher activity samples, with the nebulizer, torch and sliding interface situated inside a glovebox.<sup>97,111–116</sup>

## 8 Application to radionuclide measurement

The following radionuclides, of direct interest to the nuclear decommissioning, waste characterisation and repository safety cases, have been considered as part of this review:  $^{36}\text{Cl}$ ,  $^{41}\text{Ca}$ ,  $^{59}\text{Ni}$  and  $^{63}\text{Ni}$ ,  $^{79}\text{Se}$ ,  $^{90}\text{Sr}$ ,  $^{93}\text{Zr}$ ,  $^{99}\text{Tc}$ ,  $^{107}\text{Pd}$ ,  $^{129}\text{I}$ ,  $^{135}\text{Cs}$  and  $^{137}\text{Cs}$ ,  $^{151}\text{Sm}$ ,  $^{210}\text{Pb}$ ,  $^{226}\text{Ra}$  and  $^{228}\text{Ra}$ ,  $^{231}\text{Pa}$ , Th and U isotopes,  $^{237}\text{Np}$ , Pu isotopes,  $^{241}\text{Am}$ , and isotopes of Cm and Cf. The generalised origin of these radionuclides is indicated in Fig. 3.

### 8.1 Sample preparation

A range of possible dissolution methods exist (Table 4), with the choice of technique guided by the sample matrix and radionuclide(s) of interest. Some materials that will dissolve easily or with persistence in mineral acids (or in some cases using microwave-induced heating in pressurised vessels) followed that approach. Up to the mid-1990s, radioanalytical practitioners encountering samples that contained components resistant to acid digestion procedures would have followed a fusion-based approach where the sample matrix was completely opened-out using fluxes such as alkali carbonates and fluorides. In 1996, Croudace and co-workers,<sup>117</sup> effectively demonstrated the significant benefits of using lithium borate fusion as a rapid and effective digestion method to the radioanalytical community. Prior to this, borate fusion was almost exclusively employed for elemental analysis (X-ray fluorescence analysis and ICP-OES) where it was established for its broad sample dissolution capability in an effective, safe, rapid manner and where the glasses formed could be readily dissolved in mineral acids. Up to the 1996 study referred to, radioanalytical practitioners tended to use classical (and less effective) methods such as mineral acid leaching or fusions with alkali carbonates, fluorides or hydroxides. Croudace *et al.* (1998) noted that the chemical nature of the radionuclides and their

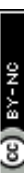


Table 4 Summary of sample digestion methods available adopted by radioanalytical practitioners

Digestion or analyte extraction method	Problems/comments	Silicates	Oxides	Sulphates	Carbonates	Borates	Phosphates	Metals, carbides, silicides <sup>a</sup>	References
Acids & alkalis	HCl and/or HNO <sub>3</sub>	Microwave digestion, heating in PTFE or PFA pressure vessels may be effective. Full recovery of analytes potentially low. Oxidation of sample may be required to prevent volatilization. Difficult to achieve full dissolution. Possible volatility issues with: As, Ge, Po, S, Sb, Se, Tc	X	X	X	X	X	X	120
HF/HClO <sub>4</sub> acid mix	Only small sample masses readily treatable. HF needs to be removed prior to analysis. Insoluble fluoride precipitates in large sample volumes. Perchlorates potentially explosive. Frequently requires the use of HCl and/or HNO <sub>3</sub> . Possible volatility issues with: As, B, Ge, Po, Sb, Tc	X	X	X	X	X	X	X	121
HF/H <sub>2</sub> SO <sub>4</sub> acid mix	Small sample volumes treatable. HF needs to be removed prior to analysis. Many evaporation stages					X		X	120
Traditional alkali fusions	Caustic digests NaOH fusion	Widely applied to dissolve halogens, Tc Opens out mineral lattices but requires lengthy post fusion treatment. Dissolution of Pt hardware possible	X			X		X	122
	NaCO <sub>3</sub> fusion	Opens out mineral lattices but requires lengthy treatment. Dissolution of Pt hardware possible. Elevated Pb or Fe(II) will alloy with Pt hardware. Possible volatility issues with: As, Hg, Po, Tc, Tl, Se	X		X	X		X	123
	Na <sub>2</sub> O <sub>2</sub> fusion or sinter with acid digestion	Attack of Pt hardware possible. Typical fusion temperature of 250–500 °C. Small sample volumes treatable. Time intensive procedure to dissolve the alkaline fusion cake. Possible volatility issues with Au & Ru				X		X	124
	Alkali fluoride followed by pyrosulfate	Hazardous as HF produced; requires treatment with pyrosulfate to remove fluorides. Will attack Pt hardware	X		X	X		X	125
Borate fusions	Borate fusion ± acid digestion	Flexible method with no problems. Effectively digests most materials (some may require an oxidant pretreatment) and is ideal for many elemental and isotopic analysis purposes. High purity lithium borate fluxes used to ensure low analytical blanks. Sample size can vary from 0.1–10 g. Sample: flux ratios from 1 : 1 upward. Pt–Au crucibles used which are easily cleaned. Typical fusion temperature <1000–1200 °C. Possible volatility issues with: Hg, Pb Po & Tl			X	X		X	117



Table 4 (Contd.)

Digestion or analyte extraction method	Problems/comments	Silicates	Oxides	Sulphates	Carbonates	Borates	Phosphates	Metals, carbides, silicides <sup>a</sup>	References
Fluxless fusion	Flux free fusion ± acid digestion	Small sample volumes treatable. Conducted in inert Ar atmosphere. Typical fusion temperature >1300 °C. May require addition of SiO <sub>2</sub> and MgO if silicate poor to help glass formation. Possible volatility issues with Hg, Pb & Tl	X	X	X	X	X	X	126
Thermal oxidation	Analyte(s) trapped in bubbler or condenser	Used to liberate volatile radionuclides e.g. pyrolyser, HBO <sub>2</sub>	X	X	X	X	X	X	
Laser ablation	Direct ablation, Viridiscan, LIBS/ICP-MS	Effective in liberating small quantities of elemental material in a controlled manner. Ablation can occur in carrier gas, by trapping in a filter medium or under acid to reduce later digestion problems	X	X	X	X	X	X	127-129

<sup>a</sup> Some samples (metals, carbides and disilicides may require an oxidative pretreatment prior to borate fusion. Adapted from Croudace *et al.* 2016.<sup>119</sup>

location (lattice-bound or adsorbed) needed to be considered and that some actinides such as Pu can often be digested using mineral acids, whereas high fired Pu was more intransigent and required a total dissolution techniques *e.g.* borate fusion.<sup>51,117</sup> Similarly, whilst <sup>135</sup>Cs and <sup>137</sup>Cs have been recovered by acid leaching for a range of sample matrices, it was proven that complete recovery in clay-rich sediments was only achievable using lithium borate fusion.<sup>1</sup> Additionally, certain radionuclides (<sup>99</sup>Tc and <sup>129</sup>I) suffer from losses due to volatility, which must be considered during sample preparation. A summary of sample digestion methods available for radionuclides has recently been published.<sup>119</sup>

## 8.2 Chlorine-36

Chlorine-36 (half-life  $3.02 \times 10^5$  years) is formed by neutron activation of stable <sup>35</sup>Cl, which is present as an impurity in concrete and other reactor components.<sup>130,131</sup> Concrete and graphite wastes generated from decommissioning are the main sample matrices of interest, with mg kg<sup>-1</sup> concentrations of <sup>35</sup>Cl in concrete, combined with the high neutron capture cross-section (43 barns) and high volume of waste concrete that must be characterised.<sup>130</sup> Chlorine-36 is sometimes measured alongside <sup>129</sup>I, and the volatility of both nuclides must be considered during sample preparation. Past separation techniques include leaching from concrete, followed by addition of oxidants to convert Cl and I to halides, which are then trapped in sodium hydroxide.<sup>130</sup> Alternatively, precipitation of Cl as AgCl followed by ion exchange chromatography has been applied to concrete, aluminium and graphite samples,<sup>132</sup> whilst an extraction chromatographic material (CL resin) was developed by Triskem International that is applicable to separation of <sup>36</sup>Cl and <sup>129</sup>I from decommissioning samples.<sup>133</sup>

Chlorine-36 is a beta emitting radionuclide ( $E_{\max} = 0.71$  MeV) that can be measured by liquid scintillation counting (LSC), with Ashton *et al.* (1999) achieving a minimum detectable activity of 9.7 mBq g<sup>-1</sup> in concrete samples when measured in combination with <sup>129</sup>I.<sup>130</sup> In a separate study, Hou *et al.* (2007) achieved a LOD of 14 mBq in various decommissioning samples, with the Cl chemical yield assessed by ICP-SFMS (MicroMass Plasma Trace 2).<sup>132</sup> The LOD for ICP-MS measurement for stable Cl was 0.01 mg kg<sup>-1</sup>, equivalent to 12.2 Bq kg<sup>-1</sup> <sup>36</sup>Cl. The specific activity of <sup>36</sup>Cl ( $1.07 \times 10^9$  Bq g<sup>-1</sup>) makes it well suited to mass spectrometric measurement, however, there is no known ICP-MS procedure for measurement of <sup>36</sup>Cl. Aside from isobaric <sup>36</sup>S (36.0% abundance), peak tailing from <sup>35</sup>Cl, and isobaric overlap <sup>36</sup>Ar in the plasma gas must be overcome, which will be dependent on the abundance sensitivity of the instrument and the use of a collision or reaction cell, respectively. AMS is capable of separating <sup>36</sup>Cl from the <sup>36</sup>S isobar, and has achieved a detection limit of 0.1 Bq kg<sup>-1</sup> in food for sample sizes of 3-4 g,<sup>131</sup> with good reproducibility (<2%) for samples with a <sup>36</sup>Cl/Cl ratio  $>10^{-12}$ .<sup>134</sup>

## 8.3 Calcium-41

Calcium-41 ( $t_{1/2} = 1.03 \times 10^5$  years) is formed through thermal neutron capture of stable <sup>40</sup>Ca (natural abundance 96.94%), and

also naturally through cosmic ray spallation. The latter has led to interest in measurement in the fields of cosmochemistry and geomorphology, whilst the high bioavailability is of interest in biomedical tracing in the progress of bone disease.<sup>135–141</sup> Calcium-41 is present in reactor shield concrete, and is therefore a key radionuclide with regards to high-volume low and intermediate level waste originating from decommissioning, as well as in long-term monitoring of nuclear waste repositories.<sup>140,142–144</sup>

Decay of <sup>41</sup>Ca to <sup>41</sup>K ground state by electron capture emits low energy X-rays and Auger electrons (0.3–0.6 keV), and is therefore measurable by X-ray spectrometry or LSC.<sup>139,142</sup> X-ray spectrometry is straightforward but the low counting efficiency and low abundance of X-rays (11.4% for 3.31 keV) results in low sensitivity.<sup>142</sup> This also impacts measurement by LSC, which requires separation of other radionuclides prior to measurement.<sup>142,143</sup> A detection limit of 0.02 Bq g<sup>−1</sup> was achieved for a 5 g concrete sample following a 60 minute count time.<sup>142</sup> Calcium-41 has been successfully separated from the bulk matrix and radiometric interferences by numerous techniques including ion exchange, liquid–liquid extraction, liquid membrane separation, and precipitations including calcium fluoride, carbonate and oxalate.<sup>139,143,145</sup>

The long half-life of <sup>41</sup>Ca and low energy X-ray and Auger electrons makes it well-suited to mass spectrometric determination, with an additional interest in measurement of the <sup>41</sup>Ca : <sup>40</sup>Ca ratio in nuclear samples. There is no known ICP-MS application for detection of <sup>41</sup>Ca, due to significant tailing effects from <sup>40</sup>Ca, as well as <sup>40</sup>Ar (99.60% natural abundance) in the plasma gas, with additional interferences from isobaric <sup>41</sup>K (natural abundance 6.73%) and instrument-generated <sup>40</sup>CaH.<sup>136</sup> Even in highly contaminated samples, a <sup>41</sup>Ca isotopic abundance of 10<sup>−9</sup> relative to <sup>40</sup>Ca must be determined<sup>118</sup> (compared to natural terrestrial ratios of ~10<sup>−14</sup> to 10<sup>−15</sup>).<sup>137,139</sup> A half-life value of 9.94 ± 0.15 × 10<sup>4</sup> years was recently determined using multiple techniques including TIMS.<sup>144</sup> A <sup>42</sup>Ca–<sup>48</sup>Ca double spike as well as two NIST reference materials of known isotopic composition were used to correct for isotopic fractionation. A mathematical correction was applied to account for tailing from <sup>40</sup>Ca, and isobaric <sup>40</sup>K using <sup>39</sup>K (natural abundance 93.26%) by monitoring at mass 41 when processing natural Ca samples.

RIMS is a highly sensitive technique for isotopic <sup>41</sup>Ca/<sup>40</sup>Ca measurements in the 10<sup>−10</sup> to 10<sup>−11</sup> range,<sup>136,139</sup> whilst AMS is capable of isotope ratio measurements as low as 10<sup>−15</sup>.<sup>139,145</sup> Given the difficulty in routinely measuring <sup>41</sup>Ca, Nottoli *et al.* (2013) estimated the activity from measurement of <sup>60</sup>Co in ion exchange resins used for primary fluid purification in pressurized water reactors (PWR's).<sup>145</sup> AMS has been compared to LSC for detection of <sup>41</sup>Ca in concrete and other solid samples including sediment and soil.<sup>139,143</sup> Given the fundamental difference in the two techniques, there was good agreement between results in both studies, however Hampe *et al.* noted significant deviations at lower activities.<sup>139</sup>

#### 8.4 Nickel-59 and nickel-63

Neutron irradiation of Ni, Ni alloys and stainless steels result in the formation of two long-lived Ni radioisotopes, <sup>59</sup>Ni

( $t_{1/2} = 7.6 \times 10^4$  years) and <sup>63</sup>Ni ( $t_{1/2} = 99$  years). Irradiation of <sup>63</sup>Cu can also result in the formation of <sup>63</sup>Ni via <sup>63</sup>Cu(n,p)<sup>63</sup>Ni reaction. Typical <sup>59</sup>Ni/<sup>63</sup>Ni activity ratios are ~1 : 100 and most published methodologies have focused on the quantification of <sup>63</sup>Ni as the dominant radionuclide in recently irradiated materials. However, the long-lived <sup>59</sup>Ni will have a more long-term impact on waste radionuclide inventories and its characterization is becoming of greater interest. Measurement of <sup>63</sup>Ni is relatively straightforward through measurement of the 66.95 keV beta emissions by liquid scintillation analysis, with detection limits of typically 14 mBq.<sup>146</sup> Thin window beta counting has also been used, achieving limits of detection of 1 mBq for a 3000 min count time.<sup>147</sup> Measurement of <sup>59</sup>Ni is more complicated. Theoretically, it should be possible to detect the associated X-ray emissions (5.88–6.49 keV) using liquid scintillation analysis, but in practice these emissions are indistinguishable from the more abundant beta emissions arising from the associated <sup>63</sup>Ni. X-ray spectrometry using LECG of Si(Li) detectors has therefore typically been employed for <sup>59</sup>Ni measurement although such approaches are relatively insensitive with detection limits of 1–2 Bq being reported.<sup>148</sup> In all cases, chemical purification of the Ni fraction is required prior to measurement of the Ni radioisotopes. Purification of Ni is most commonly achieved using dimethylglyoxime (DMG) at pH 8–9, either *via* precipitation or solvent extraction of the Ni-DMG complex, or *via* adsorption of Ni onto an extraction chromatographic material incorporating DMG loaded onto an inert support. Co-adsorption of other transition metals (notably Co, Fe and Cu) can be prevented by including ammonium acetate in the load solution. Ni/Co decontamination factors of 10<sup>3</sup> have been reported using such separations.<sup>146</sup> Further purification of Ni from Co can be achieved using anion exchange chromatography, with Co being retained from 9 M HCl solutions, with Ni/Co decontamination factors approaching 10<sup>4</sup>.<sup>149</sup> Purification of Ni prior to AMS measurement through the formation of volatile Ni(CO)<sub>4</sub> has also been described and this could have significance in the development of robust Ni/Co separation procedures prior to ICP-MS measurement.<sup>150</sup>

Given the long half-life of <sup>59</sup>Ni, the radionuclide should be measurable with reasonable sensitivity using mass spectrometric techniques. In practice, <sup>59</sup>Ni is always associated with stable Ni with a maximum <sup>59</sup>Ni/Ni ratio of 10<sup>−7</sup>. In addition, mass spectrometric measurement of <sup>59</sup>Ni is impacted by an isobaric interference from the only stable isotope of Co, <sup>59</sup>Co. Measurement of <sup>59</sup>Ni and <sup>63</sup>Ni by AMS following chemical separation of the Co interference has been reported.<sup>150,151</sup> AMS was considered in preference to ICP-MS for the measurement of <sup>59</sup>Ni to detect nuclear waste container leaks in the Kara Sea<sup>152</sup> with proposed detection limits of 2–5 fg (6–15 µBq). Although less sensitive, ICP-MS should still be of use for general waste characterization, yet application of ICP-MS to <sup>59</sup>Ni measurement has not been reported to date. This most likely reflects the challenges in measuring the low abundance <sup>59</sup>Ni in the presence of a significantly higher signal of <sup>58</sup>Ni and the associated abundance sensitivity interference along with the isobaric interference from <sup>59</sup>Co. The extremely low abundance sensitivities (theoretically 10<sup>−10</sup>) associated with ICP-QQQ-MS



may ultimately permit measurement of  $^{59}\text{Ni}$  by ICP-MS. Isobaric interference from  $^{59}\text{Co}$  cannot be resolved using high resolution mass spectrometry as a resolution of  $>50\,000$  would be required to achieve this. Effective separation of Ni and Co must therefore be achieved either through chemical separation prior to ICP-MS measurement or *via* reaction gas technologies to remove the  $^{59}\text{Co}$  interference. To date, effective separation of Ni and Co using dynamic reaction cell-based techniques has not been extensively investigated. Bandura *et al.* (2006) suggested  $\text{N}_2\text{O}$  as a reaction gas for Co/Ni separation.  $\text{Co}^+$  reacts at a faster rate with  $\text{N}_2\text{O}$  compared with  $\text{Ni}^+$ .<sup>92</sup> However, formation of  $\text{NiO}^+$  was still observed and a Co/Ni separation factor of only 6 was determined. Efficient off-line chemical separation of Ni and Co therefore appears critical to the application of ICP-MS for  $^{59}\text{Ni}$  determination.

### 8.5 Selenium-79

Selenium-79 is a long lived ( $t_{1/2} = 6.0 \times 10^5$  years) fission product with a low energy beta emission ( $E_{\text{max}} = 0.151$  MeV). The radionuclide is of interest for post-closure repository performance assessments given its potentially mobile nature. Measurement of  $^{79}\text{Se}$  is potentially well suited to ICP-MS, however this is problematic given its low abundance in nuclear wastes, its relatively high ionisation potential (9.75 eV) and isobaric interference arising from  $^{79}\text{Br}$  (50.6% abundance), as well as polyatomic interferences arising from  $^{39}\text{K}^{40}\text{Ar}$  and  $^{38}\text{Ar}^{40}\text{ArH}$ . Aguerre and Frechou (2006) developed a scheme to effectively separate Se from Br and associated fission products (although  $^{125}\text{Sb}$  was co-extracted with the Se) with final Se measurement by ICP-QMS (Perkin Elmer Elan 6000).<sup>153</sup> Plasma power was increased to 1300 W to maximise sensitivity, with a detection limit of  $0.15\, \mu\text{g L}^{-1}$ , equivalent to  $50\, \text{Bq L}^{-1}$   $^{79}\text{Se}$ . There is also the potential to use cold plasma conditions (reduced RF power) in combination with chemical separation to separate  $^{79}\text{Se}$  from  $^{79}\text{Br}$ , although there is no known application of this approach. Compte *et al.* (1995) developed a method for determination of  $^{79}\text{Se}$  in high activity fission product solutions ( $10^{10}\, \text{Bq L}^{-1}$ ) using ETV-ICP-MS, following single stage chemical separation, with  $^{79}\text{Se}$  measured at a concentration of  $0.43\, \text{mg L}^{-1}$  ( $120.01\, \text{Bq L}^{-1}$ ).<sup>154</sup> ETV-ICP-MS has also been used in combination with LSC for determining the half-life of  $^{79}\text{Se}$ , following separation from a reprocessing solution using liquid-liquid extraction and ion exchange chromatography.<sup>155</sup>

### 8.6 Strontium-90

Strontium-90 is a beta-emitting radionuclide (decay energy 0.546 MeV) with a half-life of 28.8 years that decays to  $^{90}\text{Y}$  (half-life 2.67 days) and then on to stable  $^{90}\text{Zr}$ . Strontium-90 is of critical importance in nuclear waste management, environmental monitoring and radiation protection. Additionally,  $^{90}\text{Sr}$  is a mobile element that can accumulate in soils and plants *via* precipitation and ion exchange mechanisms,<sup>62,77,86</sup> as well as in bones and teeth if inhaled or ingested, because of its similar chemical properties to calcium. This increases the risk of leukemia and bone cancer.<sup>86,87,156</sup> An extensive review of sample preparation and measurement techniques for  $^{90}\text{Sr}$  is presented

elsewhere,<sup>62</sup> with a recent review paper focusing on mass spectrometric measurement of  $^{90}\text{Sr}$ , along with  $^{135}\text{Cs}$  and  $^{137}\text{Cs}$ .<sup>157</sup>

The primary limitation affecting ICP-MS measurement of  $^{90}\text{Sr}$  is an isobaric interference from stable  $^{90}\text{Zr}$  (natural abundance 51.45%). The similarity in mass requires a resolution of  $\sim 30\,000$  for effective separation, which is beyond the capabilities of ICP-SFMS.<sup>86</sup> Even in highly  $^{90}\text{Sr}$ -contaminated soils surrounding the Chernobyl Nuclear Power Plant, a  $^{90}\text{Zr}$  decontamination factor of  $\sim 10^6$  is still required.<sup>77,158</sup> An additional interference is peak tailing from stable  $^{88}\text{Sr}$  (natural abundance 82.6%), which is present at high concentrations in environmental samples ( $20\text{--}300\, \text{mg kg}^{-1}$  in soils,  $7\text{--}9\, \text{mg L}^{-1}$  in seawater).<sup>87</sup> Finally, multiple polyatomic interferences can arise from reactions of elements in the plasma.<sup>54</sup>

Beta-counting techniques are applicable to highly sensitive detection of  $^{90}\text{Sr}$ , either through direct measurement of  $^{90}\text{Sr}$ , or *via*  $^{90}\text{Y}$ .<sup>62</sup> The overlapping spectra of these two radionuclides can be resolved by calculating an ingrowth of  $^{90}\text{Y}$ , or more commonly waiting for 2–3 weeks for the establishment of secular equilibrium, followed by long count times, depending on the detection limits required. The short measurement time for ICP-MS means the concentration of  $^{90}\text{Y}$  daughter product is negligible ( $\sim 0.02\%$  of the total intensity at  $m/z = 90$  in nuclear fuel samples) and will not interfere with  $^{90}\text{Sr}$  determination.<sup>158</sup>

Chemical separation is commonly based on extraction chromatography using commercially available Sr-resin (Triskem International). For more complex sample matrices, this is commonly preceded by a pre-concentration stage such as calcium oxalate precipitation.<sup>77,86,158–160</sup> Online chemical separation is advantageous when a rapid response is required, for example in the prompt assessment of contamination following the Fukushima accident in 2011.<sup>160,161</sup> A lab-on-valve based setup successfully removed 99.8% Zr using Sr-resin prior to measurement with a Perkin Elmer Elan II DRC-ICP-MS, whilst an automated solid phase elution (SPE) system coupled to the same instrument reduced the chemical separation and analysis time by  $\sim 50\%$  compared to offline separation.<sup>160</sup> Grinberg *et al.* (2007) investigated ETV-based separation of Sr from Zr and Y using a commercial graphite tube in combination with DRC-ICP-MS.<sup>77</sup> In Zr-free samples, ETV using a graphite tube achieved a Sr detection limit of  $1.8\, \text{ng kg}^{-1}$  ( $9.2 \times 10^3\, \text{Bq kg}^{-1}$ ), compared to  $0.1\, \text{ng kg}^{-1}$  ( $513.2\, \text{Bq kg}^{-1}$ ) using solution nebulization. However, in the presence of  $100\, \text{mg kg}^{-1}$  Zr, the detection limit for solution nebulization increased to  $89\, \text{ng kg}^{-1}$  ( $4.5 \times 10^5\, \text{Bq kg}^{-1}$ ) compared to  $2.9\, \text{ng kg}^{-1}$  ( $1.4 \times 10^4\, \text{Bq kg}^{-1}$ ) using ETV.

A Perkin Elmer Elan II DRC-ICP-MS is the most commonly applied instrument to  $^{90}\text{Sr}$  measurement (Table 5). With  $\text{O}_2$  as the reaction gas,  $^{90}\text{Zr}$  is oxidized to  $^{90}\text{Zr}^{16}\text{O}$ , while the same oxidation reaction with  $^{90}\text{Sr}$  is not energetically favorable and would require a stronger oxidant such as  $\text{N}_2\text{O}$ , or a higher  $\text{O}_2$  flow rate.<sup>87,160</sup> DRC-ICP-MS has been applied to detection of  $^{90}\text{Sr}$  in soil samples in the vicinity of the Chernobyl nuclear power plant.<sup>158</sup> A Zr decontamination factor of  $>10^7$  was achieved by a combination of Sr-resin and DRC-ICP-MS. The abundance sensitivity was calculated as  $\sim 3 \times 10^{-9}$ , with a detection limit



of  $4 \text{ pg L}^{-1}$  in Zr-free solutions, increasing to  $200 \text{ pg L}^{-1}$  ( $1026.5 \text{ Bq L}^{-1}$ ) in digested soils. Strontium-90 has also been measured in soil contaminated by the accident at the Fukushima nuclear power plant, using on-line Sr-resin separation combined with DRC-ICP-MS, with a detection limit of  $0.77 \text{ pg L}^{-1}$  ( $4.0 \text{ Bq L}^{-1}$ ).<sup>160</sup> Taylor *et al.* (2007) measured  $^{90}\text{Sr}$  by DRC-ICP-MS in samples collected from Perch Lake, Ontario, with detection limits of  $0.1 \text{ ng kg}^{-1}$  ( $513.2 \text{ Bq kg}^{-1}$ )  $0.04 \text{ ng kg}^{-1}$  ( $205.3 \text{ Bq kg}^{-1}$ ) and  $0.003 \text{ ng L}^{-1}$  ( $15.4 \text{ Bq L}^{-1}$ ) for sediments, plants and water, respectively.<sup>159</sup> There was a good agreement in the values measured for a standard reference material by Cerenkov counting and DRC-ICP-MS, with detection limits for the two techniques of  $13.7 \text{ pg kg}^{-1}$  ( $70.3 \text{ Bq kg}^{-1}$ ) and  $97.7 \text{ pg kg}^{-1}$  ( $501.4 \text{ Bq kg}^{-1}$ ), respectively. A recent study by Amr *et al.* (2016) measured  $^{90}\text{Sr}$  (along with  $^{137}\text{Cs}$  and Pu isotopes) by triple quadrupole ICP-MS (Agilent 8800) in Qatar soils and sediments.<sup>162</sup> Following acid leaching and extraction chromatography using Sr-resin (Triskem International),  $^{90}\text{Sr}$  was separated from  $^{90}\text{Zr}$  using oxygen in the collision-reaction cell, with  $^{90}\text{Sr}$  measured at an average concentration of  $0.61 \text{ fg g}^{-1}$  ( $3.1 \text{ Bq g}^{-1}$ ).

A less common approach to  $^{90}\text{Sr}$  measurement is ICP-SFMS operating with cold plasma conditions (forward power = 650–750 W) and medium mass resolution ( $R = 4000$ –4500).<sup>86,87</sup> Cold plasma conditions are applicable to separation of Sr from Zr based on the difference in ionization potential (5.7 eV and 6.8 eV, respectively), although sensitivity becomes more dependent on the sample matrix under these conditions. Medium mass resolution reduces instrument sensitivity compared to low resolution, but also reduces tailing from stable  $^{88}\text{Sr}$ .<sup>132</sup> When a combination of medium mass resolution and cold plasma are applied, peak tailing of  $^{88}\text{Sr}$  is considered the critical factor affecting accurate detection of  $^{90}\text{Sr}$ . Abundance sensitivity values of  $6 \times 10^{-7}$  and  $0.8 \times 10^{-7}$  have been recorded at medium resolution, which is an improvement of 2 orders of magnitude compared to low mass resolution,<sup>76</sup> but is lower than that of DRC-ICP-MS. A detection limit of  $0.4 \text{ pg L}^{-1}$  ( $2.1 \text{ Bq L}^{-1}$ ) was achieved for urine samples by ICP-SFMS, compared to  $2 \text{ ng L}^{-1}$  ( $10.5 \text{ Bq L}^{-1}$ ) for ICP-QMS operating with a collision cell (Platform, Micromass Ltd).<sup>86</sup>

## 8.7 Zirconium-93

Zirconium-93 is a fission product (6.35% thermal neutron fission yield) and is also produced *via* the neutron irradiation of  $^{92}\text{Zr}$  (natural abundance 17.1%  $\sigma_{\text{therm}}$  – 0.2 barns). Although theoretically predicted previously,  $^{93}\text{Zr}$  was first positively identified in irradiated uranium by Steinberg and Glendenin in 1950.<sup>163</sup> The long half-life ( $t_{1/2} = 1.53 \times 10^6$  years) and corresponding low specific activity ( $9.3 \times 10^7 \text{ Bq g}^{-1}$ ) means that the nuclide is ideally suited to mass spectrometric detection. In addition, the low beta energy ( $E_{\text{max}} = 56 \text{ keV}$ ) and lack of gamma emission and, in recently irradiated materials, potential interference from  $^{95}\text{Zr}$  makes radiometric detection less attractive. Given the low ionisation efficiency of Zr, ICP-MS-based techniques are preferable to TIMS-based approaches. Measurement of atomic percentages of a range of fission products, including

$^{93}\text{Zr}$ , in spent nuclear fuel dissolver solutions by direct measurement has been reported using a Perkin Elmer Elan 250 ICP-MS,<sup>164</sup> although isobaric interferences were identified as an issue. In general, isobaric interferences arising from  $^{93}\text{Nb}$  (100% abundance),  $^{93m}\text{Nb}$  and  $^{93}\text{Mo}$  (both activation products) and polyatomic  $^{92}\text{MoH}^+$  must be mitigated by chemically separating the interfering species from  $^{93}\text{Zr}$  prior to measurement. Chemical separations of  $^{93}\text{Zr}/^{93}\text{Nb}$  have been reported based on solvent extraction into benzoylphenylhydroxylamine-trichloromethane–HCl<sup>165</sup> and ion-exchange chromatography in HCl/HF media.<sup>166</sup> Isobaric interference suppression on-line using ICP-DRC-MS has not been employed. Bandura *et al.* (2006) noted that no reactions had been identified that would permit separation of  $^{93}\text{Nb}/^{93}\text{Mo}$  interferences in a reaction cell.<sup>92</sup>

Chartier *et al.* (2008) reported an isotope-dilution MC-ICP-MS (Isoprobe) approach using a  $^{96}\text{Zr}$  spike.<sup>165</sup> A mass bias of  $3\% \text{ amu}^{-1}$  was observed for Zr and corrected for through measurement of  $^{94}\text{Zr}/^{90}\text{Zr}$  ratios (reference value  $0.3378 \pm 0.0002$ ) in a natural Zr standard.<sup>165</sup> The relative uncertainty of measured  $[^{93}\text{Zr}]$  was estimated as 0.6% ( $k = 2$ ). The procedure was subsequently applied to the determination of the half-life of  $^{93}\text{Zr}$ .<sup>167</sup>

## 8.8 Technetium-99

Technetium-99 is a pure-beta emitting radionuclide with a half-life of  $2.13 \times 10^5$  years, and is a high yield fission product (6.1% and 5.9% fission yield from thermal neutron fission of  $^{235}\text{U}$  and  $^{239}\text{Pu}$ , respectively) of significant interest with regards to nuclear waste characterization and decommissioning. The relatively high mobility is a concern with regards to waste storage and disposal, whilst the high solubility in seawater (as  $\text{TCO}_4^-$ ) makes it an important seawater tracer.<sup>168</sup> A comprehensive review of analytical methods for  $^{99}\text{Tc}$  is published elsewhere.<sup>169</sup>

Low level gas flow GM counter or LSC are applicable to  $^{99}\text{Tc}$  measurement. The long half-life and low decay energy ( $E_{\text{max}} = 292 \text{ keV}$ ) means long count times for LSC if detection limits in the  $\text{pg g}^{-1}$  range are required,<sup>169</sup> whilst interferences from  $^{103}\text{Ru}$ ,  $^{106}\text{Ru}$  and  $^{90}\text{Sr}$  must be removed prior to measurement. ICP-MS measurement of  $^{99}\text{Tc}$  is impacted by an isobaric interference from stable  $^{99}\text{Ru}$  (natural abundance 12.76%), which can be corrected for by chemical separation, or monitoring  $^{101}\text{Ru}$  (natural abundance 17.06%). Several isotopes have been used for drift correction, including  $^{103}\text{Rh}$  and  $^{115}\text{In}$ . Issues with  $^{103}\text{Rh}$  are memory effects, and instability in dilute  $\text{HNO}_3$  for long analytical runs.<sup>168,170</sup> By comparison,  $^{115}\text{In}$  does not suffer from memory effects and has minimal disturbance from  $^{99}\text{Tc}$ / $^{16}\text{O}$ .<sup>169</sup> There are no stable isotopes of Tc, although long-lived  $^{97}\text{Tc}$  and  $^{98}\text{Tc}$  (both with  $4.2 \times 10^6$  year half-lives) can be used as both a yield tracer and internal standard.<sup>169</sup>

Solvent extraction, ion exchange chromatography and extraction chromatography are all effective approaches to separation of  $^{99}\text{Tc}$ , with extraction chromatography using TEVA resin the most commonly used.<sup>169</sup> The volatility of Tc must be considered during sample preparation, with losses noted when



Table 5 Summary of recent procedures for  $^{90}\text{Sr}$  measured by ICP-MS

Reference	Instrument	Model	Matrix	Chemical separation	LOD, $\text{pg L}^{-1}$ ( $\text{Bq L}^{-1}$ )
86	SFMS	Element	Urine	$\text{CaPO}_4$ pptate, Sr-resin, medium res, cold plasma	0.4 (2.1)
64	SFMS	Element	Groundwater	Medium res, cold plasma	11 (56.5)
161	DRC-MS	Perkin Elmer Elan DRC II	Soils	On-line solid phase elution, reaction cell	600 (3079.4)
160	DRC-MS	Perkin Elmer Elan DRC II	Soils	Sr resin, reaction cell	0.8 (3.9)
77	DRC-MS		Environmental samples	Sr resin, ETV sample introduction, reaction cell	1800 (9238.3)
158	DRC-MS	Perkin Elmer Elan DRC II	Soils	Sr resin, reaction cell	200 (1026.5)
	CC-QMS			Collision cell	900 (4619.1)
86	CC-QMS	Platform, Micromass Ltd	Urine	$\text{CaPO}_4$ pptate, Sr-resin, collision cell	2000 ( $1.0 \times 10^4$ )

the temperature of a  $\text{HNO}_3$  solution (up to 8 M concentration) increased from 100 °C to 150 °C.<sup>169</sup> Such losses must also be considered when dry ashing samples to decompose organic matter in solid samples.<sup>171</sup> No significant losses were observed when ashing at 800 °C for less than 6 hours for a seaweed sample. Technetium-99 has been measured in a range of environmental and biological samples by ETV-ICP-MS (Perkin Elmer HGA-600 MS), using  $\text{NH}_4\text{OH}$  as matrix modifier to form an alkaline solution and minimize loss of Tc during drying and ashing. Depending on the daily performance, the detection limit ranged from 0.5–1.0  $\text{pg mL}^{-1}$  ( $3.2 \times 10^{-4}$  to  $6.3 \times 10^{-4}$   $\text{Bq mL}^{-1}$ ) compared to 5–50  $\text{pg mL}^{-1}$  ( $3.2 \times 10^{-4}$  to  $3.2 \times 10^{-2}$   $\text{Bq mL}^{-1}$ ) using radiochemical techniques.

A modular automated separator (MARS Tc-99; Northstar Technologies, Madison WI, USA) was developed for rapid analysis of groundwater samples from boreholes at a low and intermediate waste repository. The system was coupled to ICP-QMS (Varian 810), with an activity of  $1658 \pm 7 \text{ mBq L}^{-1}$  ( $2.6 \text{ ng mL}^{-1}$ ) measured for a method standard, which was in good agreement with the certified value of  $1598 \pm 40 \text{ mBq L}^{-1}$  ( $2.5 \text{ ng mL}^{-1}$ ).<sup>172</sup> The detection limit of the procedure developed was  $0.12 \text{ mBq mL}^{-1}$  ( $0.19 \text{ pg mL}^{-1}$ ), whilst the system developed was potentially applicable to other radionuclides. In a separate study, large volume water samples were measured by ICP-QMS (Thermo X-series II) following chemical separation by ferrous hydroxide co-precipitation, and online SI using 2 TEVA columns.<sup>168</sup> Decontamination factors of  $1 \times 10^6$  and  $5 \times 10^5$  were achieved for Ru and Mo, with a detection limit of  $11.5 \text{ pg m}^{-3}$  ( $7.5 \text{ mBq m}^{-3}$ ) for a 200 L sample. Slightly lower decontamination factors of  $4 \times 10^4$  and  $1 \times 10^5$  for Mo and Ru, respectively, were recorded following 2 TEVA column-separations of environmental samples prior to ICP-QMS (Thermo X-series II) measurement, with a detection limit of  $0.15 \text{ mBq g}^{-1}$  ( $0.24 \text{ pg mL}^{-1}$ ).<sup>171</sup> Samples were left for 1 week following separation to allow for decay of  $^{99\text{m}}\text{Tc}$  (half-life 6.0 hours).

Measurement of  $^{99}\text{Tc}$  in waste stream samples was carried out at the Lan-Yu low level waste storage site, Taiwan, where Tc was previously estimated from a scaling factor based on the activity of  $^{137}\text{Cs}$ .<sup>173</sup> Following acid digestion and TEVA resin separation, samples were measured by ICP-QMS (Agilent 7500a), with a detection limit of  $0.021 \text{ ng g}^{-1}$  ( $0.013 \text{ Bq g}^{-1}$ ). Accurate quantification meant a revision of the scaling factors

being used was recommended, to the extent that reclassification of historical waste should also be carried out. The performance of ICP-QMS (Thermo X-series II) and ICP-SFMS (Thermo Element 2) was compared for low-level radioactive waste following digestion and separation using TEVA extraction chromatography resin.<sup>170</sup> Instrumental detection limits of  $0.024 \text{ ng L}^{-1}$  ( $0.015 \text{ Bq L}^{-1}$ ) and  $0.015 \text{ ng L}^{-1}$  ( $0.0095 \text{ Bq L}^{-1}$ ) were measured for ICP-QMS and ICP-SFMS, respectively. The minimum detectable activity for LLW samples was  $<8.5 \text{ mBq g}^{-1}$  ( $13.4 \text{ pg g}^{-1}$ ) for ICP-QMS,  $<5.9 \text{ mBq g}^{-1}$  ( $9.3 \text{ pg g}^{-1}$ ) for ICP-SFMS and  $<414\text{--}511 \text{ mBq g}^{-1}$  ( $806.8 \text{ pg g}^{-1}$ ) for a gas proportional counter, whilst the method detection limit (for a 0.1 g waste sample) was  $13.6 \text{ ng L}^{-1}$  ( $8.5 \text{ Bq L}^{-1}$ ) for ICP-QMS, and  $1.19 \text{ ng g}^{-1}$  ( $745 \text{ mBq g}^{-1}$ ) for LSC (no value was given for ICP-SFMS).

## 8.9 Palladium-107

Palladium-107 is a long lived ( $t_{1/2} = 6.5 \times 10^6$  years) low energy beta emitting radionuclide ( $E_{\text{max}} = 33 \text{ keV}$ ). The radionuclide is produced with a thermal neutron fission yield of 0.15%. The specific activity of  $1.9 \times 10^7 \text{ Bq g}^{-1}$  indicates that mass spectrometric measurement would be favorable. Isobaric interferences would arise from natural  $^{107}\text{Ag}$  (51.8% abundance), as well as a potential polyatomic interference from  $^{91}\text{ZrO}^+$ . There are few published procedures based on ICP-MS for measurement of  $^{107}\text{Pd}$ . Bibler *et al.* (1997) used a ICP-QMS (Fisons/VG Plasmaquad) to measure fission products including  $^{107}\text{Pd}$  in HLW sludge's and glass.<sup>174</sup> It was noted that direct measurement of  $^{107}\text{Pd}$  was not possible due to isobaric interference from silver which is used to scavenge iodine and is therefore present in the waste stream. Bannochie *et al.* (2009) noted a similar problem and calculated  $^{107}\text{Pd}$  activities *via* measurement of  $^{105}\text{Pd}$  and correcting for the relative fission yield of the two isotopes.<sup>175</sup> Interference from Ag could also be overcome through chemical separation, with Bienvenu *et al.* (1998) noting that Pd could be separated from Ag using liquid-liquid extraction into triphenyl phosphine in nitro-2-phenylpentyl ether from 2 M  $\text{HNO}_3$  with Pd being back-extracted into 4 M ammonia.<sup>176</sup> However, decontamination factors were not sufficient for high Ag containing samples, and an electrothermal vaporization approach was subsequently developed whereby Ag was volatilized at  $<1000$  °C and Pd volatilized at 1500 °C.



## 8.10 Iodine-129

Iodine-129 is a fission product (0.6% yield), and is also produced naturally *via* cosmic-ray-induced spallation of Xe, spontaneous fission of  $^{238}\text{U}$ , neutron bombardment of Te in the geosphere, and *via* thermal neutron-induced fission of stable I in the lithosphere.<sup>177–180</sup> Iodine-129 decays with a half-life of  $1.57 \times 10^7$  years to stable  $^{129}\text{Xe}$ , and is a weak beta-gamma emitter with maximum beta decay energy of 29.78 keV (37.2%) and gamma energy of 39.58 keV (7.42%).

Iodine is a redox-sensitive element, which controls speciation and exchange between the ocean/atmosphere terrestrial environment.<sup>177,181</sup> The high concentration and solubility in water makes  $^{129}\text{I}$  a useful oceanographic tracer,<sup>179,182</sup> and has also been used in distinguishing the discharge pathways from European reprocessing facilities at Sellafield and La Hague,<sup>182</sup> and more recently following the Fukushima accident.<sup>183</sup> Measurement of  $^{129}\text{I}$  in Fukushima-contaminated samples has also been applied as an analogue for reconstruction of the distribution and activity of shorter-lived  $^{131}\text{I}$  (half-life 8.02 days).<sup>184</sup>

Traditionally, radiochemical neutron activation analysis (RNAA) was the only method applied to  $^{129}\text{I}$  detection in environmental samples for a number of years.<sup>185</sup> Beta, gamma and X-ray-based techniques are limited by interferences and shielding issues, as well as long count times for low activity samples.<sup>191</sup> For mass spectrometric determination, the primary concern is accurate detection of  $^{129}\text{I}$  in the presence of high concentrations of stable  $^{127}\text{I}$  (natural abundance 100%). Isotopic  $^{129}\text{I}/^{127}\text{I}$  ratios range from  $10^{-13}$  to  $10^{-12}$  prior to anthropogenic nuclear activities, compared to  $10^{-11}$  to  $10^{-9}$  in the marine and terrestrial environment, with ratios as high as  $10^{-8}$  to  $10^{-3}$  at reprocessing sites.<sup>178,180,182,186–188</sup> The  $^{129}\text{I}/^{127}\text{I}$  ratio measurable by the instrument is therefore a critical factor. Decomposition of solid samples and chemical separation prior to quantification are additional challenges, with losses due to volatilization and/or transformation to an undesirable chemical form.<sup>197</sup> Separation techniques include ion chromatography, and phyrohydrolysis and solvent extraction for soil samples.<sup>179,184,189</sup>

Until recently, ICP-MS was generally used for detection of stable  $^{127}\text{I}$ , while AMS was the favored technique for  $^{129}\text{I}$  detection, because it can achieve instrumental background ratios of  $10^{-15}$  to  $10^{-13}$  (Table 6).<sup>181,182,184–186</sup> ICP-MS was considered not to be capable of distinguishing between iodine isotopes, with applications limited to more contaminated samples with  $^{129}\text{I}/^{127}\text{I}$  ratios greater than  $\sim 10^{10}$ .<sup>177,180,187,189</sup> Additional interferences include the low ionization efficiency of I (33.9%) owing to its high first ionization energy (10.45 eV),<sup>190</sup> isobaric  $^{129}\text{Xe}$  (natural abundance 26.40%) present as an impurity in the plasma gas, and polyatomic interferences (particularly from collision or reaction cell instruments) including  $^{127}\text{IH}_2$ ,  $^{97}\text{MoO}_2$ ,  $^{113}\text{CdO}$ ,  $^{115}\text{In}^{14}\text{N}$  and  $^{89}\text{Y}^{40}\text{Ar}$ .<sup>179,191</sup> An additional challenge is selection of an appropriate internal standard, with possible options including Cs, Re and Te.<sup>179</sup> One study selected Te owing to the similarity in ionization energy with I (9.01 eV),<sup>190</sup> whilst another did not use an internal standard owing to limitations with the elements listed.<sup>179</sup>

Iodine-129 was detected in vegetation to a detection limit of  $1.4 \text{ ng kg}^{-1}$  (9.2 mBq  $\text{kg}^{-1}$ ) using a Plasma Quad PQ2 ICP-QMS,<sup>191</sup> with the  $^{129}\text{Xe}$  interference corrected for using  $^{131}\text{Xe}$  (natural abundance 21.23%). The volatility of iodine was seen as an advantage that partially overcame the low transport efficiency (2–4% with pneumatic nebulization), as the formation of droplets in the spray chamber increased surface area and rate of vaporization, with vapors then taken up into the ICP. More recently, a Perkin Elmer Elan DRCe was applied to measurement of soils in land surrounding a fuel reprocessing site in Tokai, Japan.<sup>187</sup> Using oxygen as a reactive gas, the  $^{129}\text{Xe}$  interference was reduced, however ion transport was generally suppressed, and the instrument  $^{129}\text{I}/^{127}\text{I}$  background of  $\sim 10^{-8}$  was not improved in DRC mode due to  $^{127}\text{IH}_2$  formation with trace impurities in the reaction gas. The background was improved to  $10^{-10}$  using Axial Field Technology, which applies an accelerating axial field to ions in the DRC, improving instrument stability and reducing matrix effects. Fukushima-contaminated soil samples were measured using an Agilent 8800 ICP-QQQ-MS,<sup>189</sup> with  $\text{O}_2$  used for  $^{129}\text{Xe}$  removal, and in-cell polyatomic interferences reduced by the additional quadrupole mass filter positioned before the entrance to the cell. A sample standard bracketing technique was used to correct for mass discrimination and improve reproducibility, with good agreement between ICP-MS and AMS.

ICP-SFMS (Thermo Element 2) detection of  $^{129}\text{I}$  was achieved in Fukushima-contaminated Greenland snow samples.<sup>179</sup> Clean laboratory conditions (class 10–100) were used for sample preparation, whilst separation of Mo, In and Cd using online ion chromatography reduced polyatomic interference formation. A desolvating sample introduction system (Apex-Q (ESI)) tripled the sensitivity compared a cyclonic Peltier-cooled spray chamber, however the nitrogen carrier gas increased Xe background by an order of magnitude. The formation of  $^{127}\text{I}^+\text{H}$  was controlled by the instrumental setup *e.g.* sample uptake and gas flow rate, and plasma temperature. This is compared to an 'on-peak' baseline subtraction by Ohno *et al.* (2013) when using ICP-QQQ-MS, with a  $^{127}\text{IH}_2/^{127}\text{I}$  ratio of  $3 \times 10^{-8}$  calculated from aspiration of a  $100 \text{ mg L}^{-1}$  stable I solution.<sup>189</sup> The inability of ICP-SFMS to eliminate  $^{129}\text{Xe}$  was resolved by monitoring changes in the background Xe signal in Ar plasma gas to determine whether a background correction was necessary.

## 8.11 Caesium 135 and 137

High yield fission products  $^{135}\text{Cs}$  and  $^{137}\text{Cs}$  (6.58% and 6.22%, respectively) are present in environmental samples as a result of releases from nuclear power plants and reprocessing sites, nuclear accidents, and fallout from atmospheric weapons testing. Caesium-137 ( $t_{1/2} = 30.07$  years) is established as an important radionuclide in radiation protection, environmental monitoring and waste disposal. By comparison,  $^{135}\text{Cs}$  is a long-lived radioisotope ( $t_{1/2} = 2.3 \times 10^6$  years) with a comparatively low radiation risk; however it is a significant contributor to the long term radiological risk associated with deep geological disposal. Furthermore, the  $^{135}\text{Cs}/^{137}\text{Cs}$  ratio varies with reactor, weapon and fuel type, and recent studies have achieved precise



determination of  $^{135}\text{Cs}/^{137}\text{Cs}$  ratios as a forensic tool to identify the source of radioactive contamination.<sup>195–200</sup>

Caesium-137 decays by beta emission to short-lived metastable isomer  $^{137\text{m}}\text{Ba}$ , with maximum energies of 514 keV (94.4% yield) and 1175 keV (5.4% yield). This is immediately accompanied by gamma ray emission of 661.7 keV (85.1% yield) to form  $^{137}\text{Ba}$ . Gamma spectrometry is generally favored because it exploits the good gamma yield of the 661.6 keV energy that is not susceptible to significant absorption, whilst the ability to directly count most samples without any chemical separation is also beneficial. Caesium-135 decays with a maximum beta particle energy of 269 keV, however, measurement by beta counting is restricted by any  $^{137}\text{Cs}$  also present in the sample with a radioactivity concentration that is typically 5 orders of magnitude higher. Measurement of  $^{135}\text{Cs}$  by mass spectrometry offers a considerable advantage because of the larger atom population compared with radioactive decays. A review of measurement of  $^{135}\text{Cs}$  and  $^{137}\text{Cs}$  and  $^{135}\text{Cs}/^{137}\text{Cs}$  isotope ratios in environmental samples has been published recently,<sup>201</sup> and Table 7 gives a summary of recent procedures for  $^{135}\text{Cs}/^{137}\text{Cs}$  measurement.

A key challenge for mass spectrometric measurement is removal of isobaric interferences from naturally occurring  $^{135}\text{Ba}$  and  $^{137}\text{Ba}$  (isotopic abundances 6.6% and 11.2%, respectively), peak tailing from stable  $^{133}\text{Cs}$  (isotopic abundance 100%), and polyatomic interferences including  $^{95}\text{Mo}^{40}\text{Ar}$ ,  $^{97}\text{Mo}^{40}\text{Ar}$ ,  $^{119}\text{Sn}^{16}\text{O}$  and  $^{121}\text{Sb}^{16}\text{O}$ . For mass spectrometric measurement, Cs separation has commonly been achieved using ammonium molybdate phosphate (AMP) followed by anion exchange and/or cation exchange chromatography, most commonly Dowex AG1 and Dowex AG50W (both Bio-Rad, USA), respectively.<sup>1,195,197,198,200,202</sup> Other techniques include extraction chromatography using calixarenes,<sup>203</sup> and potassium nickel hexacyanoferrate (KNiFC).<sup>200</sup> Barium-138 (natural abundance 71.7%) has been used to assess the effectiveness of separation at masses 135 and 137, however any interference correction will reduce the accuracy of  $^{135}\text{Cs}/^{137}\text{Cs}$  values. Caesium-137 values can be verified by gamma spectrometry, however if a significant correction is required this will not validate the  $^{135}\text{Cs}$  result.<sup>204–206</sup>

Online separation has been applied to Cs and Ba separation prior to ICP-MS analysis. For example, Isnard *et al.* (2009) achieved a  $^{135}\text{Cs}$  and  $^{137}\text{Cs}$  detection limit of  $2 \text{ pg L}^{-1}$  ( $8.2 \times 10^{-8} \text{ Bq L}^{-1}$ )

Table 6 Summary of recent procedures for measurement of  $^{127}\text{I}/^{129}\text{I}$

Reference	Iodine isotope	Instrument	Model	Matrix	Chemical separation	LOD, $\text{pg L}^{-1}$ ( $\text{Bq L}^{-1}$ )
192	127 129	QMS AMS	X series II	Lake sediments		
181	127 129	AMS		Aerosol particles		
193	127 129	AMS		Environmental samples		
177	127 129	QMS AMS	X series II	Scandinavian soil and sediment	Sequential extraction into soil/sediment fractions	
178	127 129	QMS AMS	X series II	Baltic sea seawater		
187	127 129	DRC-MS	Elan DRCe	Soil	$\text{O}_2$ -based extraction with heating, extraction from activated carbon	
188	127 129	CC-QMS AMS	Agilent 7500ce/cx	Baltic sea, lake and rain waters from Finland	Anion exchange, solvent extraction	
182	127 129	QMS AMS		Seawater and aerosol filters	Liquid-liquid exchange for air filters Seawater samples anion exchange Matrix adjustment for I-127, but no matrix separation	
194	127 129	AMS		Pacific ocean and Japan seawater	Solvent extraction	
190	127 129	SFMS	Element 2	Japanese coastal seawater (pre-Fukushima)		2300 (0.015)
183	127 129	QMS AMS	X series II	Fukushima seawater samples	Anion exchange	
189	127 129	QQQ-MS	Agilent 8800	Fukushima soil samples	Pyrohydrolysis and solvent extraction	
189	127 129	ORS-QMS	Agilent 7700X	Fukushima soil samples	Pyrohydrolysis and solvent extraction	1500 (0.0098)
179	127 129	SFMS	Element 2	Snow samples from Greenland (Fukushima contaminated)	Online IC separation (anion exchange)	700 (0.0046)
184	127 129	ORS-QMS QQQ-MS	Agilent 7700 Agilent 8800	Fukushima soil samples	Pyrohydrolysis	
180	127 129	AMS AMS		Woodward iodine corporation		



and  $1 \text{ pg L}^{-1}$  ( $3.2 \times 10^{-3} \text{ Bq L}^{-1}$ ), respectively, using on-line chromatographic separation with a CG3 IonPac guard column (Dionex, USA) for a spiked groundwater matrix.<sup>207</sup> Following AMP and anion exchange separation, Taylor *et al.* (2008) achieved online Cs/Ba separation in sediment samples by attaching a Dionex CS12A  $3 \times 150$  mm cation exchange column onto a high performance liquid chromatography (HPLC) module, and coupling this system with ICP-MS.<sup>195</sup>

Sample introduction-based separation has also been applied to Cs/Ba separation. Song *et al.* used ETV with potassium thiocyanate (KSCN) as a chemical modifier.<sup>79</sup> At a volatilization temperature of  $1100^\circ\text{C}$ , Cs was vaporized in a  $10^4$  excess of Ba, with a Ba signal increase at mass 135 of only 1%. The detection limit of  $^{135}\text{Cs}$  using QMS (Perkin Elmer Elan 5000) was calculated as  $0.2 \text{ ng L}^{-1}$  ( $0.01 \text{ Bq L}^{-1}$ ). An alternative online separation technique is capillary electrophoresis (CE-ICP-MS), which was effectively applied to  $^{135}\text{Cs}/^{137}\text{Cs}$  measurement in plutonium uranium redox extraction (PUREX) and mixed oxide fuel (MOX) samples.<sup>208</sup> The procedure achieved  $^{133}\text{Cs}$  detection limits of  $6000 \text{ ng L}^{-1}$  ( $245.0 \text{ Bq L}^{-1}$ ) and  $4 \text{ ng L}^{-1}$  ( $0.2 \text{ Bq L}^{-1}$ ) in ICP-QMS (Perkin Elmer Elan 5000) and ICP-SFMS (Thermo Element 2), respectively.

A reaction cell has been applied to Cs separation, with  $\text{N}_2\text{O}$ , and  $\text{CH}_3\text{Cl}$  both effectively used as reactive gases.<sup>195,209</sup> For example, kinetic data from Lavrov *et al.* (2004) indicates the reaction for Ba with  $\text{N}_2\text{O}$  has an efficiency of 32%, compared to 0.01% for Cs.<sup>210</sup> An Agilent 8800 ICP-QQQ-MS has been used for  $^{135}\text{Cs}/^{137}\text{Cs}$  detection in rainwater and environmental samples contaminated following the accident at the Fukushima Daiichi NPP.<sup>198–200</sup> Using  $\text{N}_2\text{O}$  as a reactive gas, a  $^{135}\text{Cs}$  and  $^{137}\text{Cs}$  detection limit of  $10 \text{ pg L}^{-1}$  (equivalent to  $4.1 \times 10^{-7} \text{ Bq L}^{-1}$  and  $3.2 \times 10^{-2} \text{ Bq L}^{-1}$ , respectively) was achieved in a Ba-free solution, compared to  $100 \text{ pg L}^{-1}$  ( $4.1 \times 10^{-6} \text{ Bq L}^{-1}$ ) and  $270 \text{ pg L}^{-1}$  ( $8.6 \times 10^{-1} \text{ Bq L}^{-1}$ ) for  $^{135}\text{Cs}$  and  $^{137}\text{Cs}$ , respectively, in solutions containing  $100 \mu\text{g L}^{-1}$  Ba. These values are higher than the instrumental and method detection limits achievable using ICP-SFMS.<sup>1</sup> However, the ICP-QQQ-MS offers the combination of chemical and instrument-based separation, whilst the two quadrupoles have measured a  $^{133}\text{Cs}/^{135}\text{Cs}$  abundance sensitivity of  $\sim 10^{-10}$ .

A procedure using a Thermo Element 2XR ICP-SFMS achieved an instrumental detection limit of  $1 \text{ pg L}^{-1}$  for stable  $^{133}\text{Cs}$ . The absence of instrument-based separation meant highly efficient chemical separation techniques using high purity reagents and clean laboratory conditions was required to minimize Ba contamination prior to sample introduction. Following chemical separation, a higher method detection limit of  $20 \text{ pg L}^{-1}$  was calculated (equivalent to  $8.2 \times 10^{-7} \text{ Bq L}^{-1}$  and  $6.4 \times 10^{-2} \text{ Bq L}^{-1}$  for  $^{135}\text{Cs}$  and  $^{137}\text{Cs}$ , respectively).<sup>1</sup> Time independent fractionation is an issue affecting accurate isotope ratio measurements by ICP-MS. One cause of this is space charge effects, as lighter ions are deflected to a greater extent than heavier ions during ion extraction.<sup>207</sup> The absence of a  $^{135}\text{Cs}/^{137}\text{Cs}$  certified reference material makes accurate mass bias correction challenging, and limits the ability to compare results between studies. Isnard *et al.* (2009) applied a sample standard bracketing technique using natural  $^{121}\text{Sb}$ ,  $^{123}\text{Sb}$  and  $^{151}\text{Eu}$ ,  $^{153}\text{Eu}$  to correct for mass bias, as the average mass of

these isotopes is close to that of  $^{137}\text{Cs}$ .<sup>207</sup> The isotopic fractionation affecting TIMS and ICP-MS, as well as the absence of a certified reference material to verify accuracy of  $^{135}\text{Cs}/^{137}\text{Cs}$  measurements, led to a comparison of the two techniques for uranium oxide and mixed oxide fuel samples.

Of the alternative mass spectrometric techniques, Lee *et al.* (1993) were the first to develop a procedure for measuring  $^{135}\text{Cs}/^{137}\text{Cs}$  in environmental samples using TIMS.<sup>211</sup> There have been multiple recent TIMS applications including sediment core samples to highlight fractionation of  $^{135}\text{Cs}$  and  $^{137}\text{Cs}$  following aboveground nuclear tests at the Nevada Nuclear test site,<sup>196</sup> and environmental samples contaminated by the Fukushima Daiichi accident.<sup>202</sup> TIMS is affected by time-dependent isotopic fractionation, as lighter isotopes are preferentially evaporated from the filament. The lack of an available certified Cs isotopic standard makes it difficult to measure mass fractionation, however has been anticipated to be small relative to estimated uncertainties.<sup>196</sup> Alternatively, mass fractionation can be corrected by measuring  $^{133}\text{Cs}/^{137}\text{Cs}$  and  $^{135}\text{Cs}/^{137}\text{Cs}$  ratios during the analysis.<sup>207</sup>

Pibida *et al.* used both RIMS and TIMS to determine the chronological age of nuclear fuel burn up samples through measurement of  $^{135}\text{Cs}/^{137}\text{Cs}$ .<sup>212</sup> For low-level detection in environmental samples, improvements in overall efficiency and chemical separation were required, whilst the absence of a commercially available instrument and time-consuming optimization of instrument efficiency and chemical preparation are the main limitations to this approach. AMS measurement is limited by the high energies required to separate Cs and Ba isobars, which makes separation a complex and costly process.<sup>206</sup> A method to produce a beam of Cs anions, and production of suitable yield tracers to determine the efficiency of the process are also required.<sup>213</sup>

## 8.12 Samarium-151

Samarium-151 is a lanthanide element fission product, with a  $^{235}\text{U}$  thermal neutron fission yield of 0.53%. The radionuclide has a half-life of 94.7 years giving a specific activity of  $9.25 \times 10^{11} \text{ Bq g}^{-1}$ . Quantification of  $^{151}\text{Sm}$  is typically required in determining nuclear fuel burn up and in nuclear waste characterization. Samarium-151 is a pure beta emitting radionuclide ( $E_{\text{max}} = 76 \text{ keV}$ ), which is typically analyzed using liquid scintillation counting following separation of  $^{151}\text{Sm}$  from other rare earth radionuclides and  $^{241}\text{Am}$ . Separation of Sm from other lanthanides is usually achieved using either extraction chromatographic materials such as HDEHP-based resins,<sup>218</sup> ion exchange chromatography, or HPLC<sup>219,220</sup> based techniques. More recently, isotachophoretic separation coupled with ICP-MS has been developed for lanthanide quantification of spent nuclear fuel.<sup>221</sup>

There are only a limited number of papers relating to measurement of  $^{151}\text{Sm}$  by ICP-MS, although ICP-MS has also been used in nuclear fuel burn up assessments to measure the variation in stable Sm isotopic composition.<sup>85</sup> Isobaric interferences arise from stable  $^{151}\text{Eu}$  (47.81%) and polyatomic species  $^{119}\text{Sn}$ ,  $^{16}\text{O}_2$ ,  $^{133}\text{Cs}$ ,  $^{18}\text{O}$ ,  $^{134}\text{Ba}$ ,  $^{17}\text{O}$ ,  $^{135}\text{Ba}$ ,  $^{16}\text{O}$  and  $^{150}\text{Nd}$ ,  $^{18}\text{O}$ . Due to the potential for interference from Eu and Nd and their



Table 7 Summary of recent procedures for measurement of  $^{135}\text{Cs}/^{137}\text{Cs}$ 

Reference	Instrument	Model	Matrix	Chemical separation	LOD, $\text{pg L}^{-1}$ ( $\text{Bq L}^{-1} \text{ }^{135}\text{Cs}/\text{ }^{137}\text{Cs}$ )
214	QMS		Spent fuel pellets and solutions	Cation exchange	
215	QMS	VG Elemental Plasma Quad 2	Waste tank sludge and supernatants	$\text{Ba}(\text{OH})_2$ precipitation	209 000 (8.53/6.7 $\times 10^5$ )
216	QMS	Perkin Elmer Elan 5000	High activity waste	Cation exchange	16 000 (0.65/5.12 $\times 10^5$ )
79	QMS	Perkin Elmer Elan 5000	Cs-137 standard	ETV sample introduction	200 (0.01/640.1)
217	QMS	PQ Excell	Groundwater	On-line cation exchange	2 (8.2 $\times 10^{-5}$ /6.4)
207 and 209 1	MC-ICP-MS	GV Isoprobe	Spent fuel pellets	Anion exchange and HPLC, reaction cell	
208	SFMS	Element 2XR	Fission product standard	AMP, cation exchange, extraction chromatography	50 (2.0 $\times 10^{-3}$ /160.0)
195	DRC-MS	Perkin Elmer Elan 5000 Perkin Elmer Elan DRC II	Simulated spent fuel Soil and sediment	Capillary electrophoresis AMP, anion exchange, online cation exchange, reaction cell	4000 (0.16/1.3 $\times 10^4$ ) 200 (0.01/640.1)
198	QQQ-MS	Agilent 8800	Rainwater	Reaction cell	270 (0.01/864.2)
199	QQQ-MS	Agilent 8800	Environmental samples	AMP, anion exchange, cation exchange, reaction cell	
200	QQQ-MS	Agilent 8800	Environmental samples	AMP, anion exchange, cation exchange, reaction cell	10/6 (4.1 $\times 10^{-4}$ /19.2)

chemical similarity to Sm, reliable  $^{151}\text{Sm}$  measurements by ICP-MS rely on robust chemical separation of the rare earth elements.

Alonso *et al.* (1995) measured actinides and fission products in spent nuclear fuel using HPLC coupled to an Elan 5000 ICP-QMS.<sup>214</sup> Lanthanide separation was performed using CG5/CS5 guard/separation columns and isocratic elution with 0.1 M oxalic acid and 0.19 M LiOH. The HPLC eluent was introduced into the ICP-MS *via* a cross flow nebulizer and Scott type, double pass spray chamber. Plasma RF power was optimized at 1050 W. Spent nuclear fuel  $^{151}\text{Sm}/^{150}\text{Sm}$  values of 0.0119–0.0175 were reported. The same experimental set-up was used to measure fission products, including  $^{151}\text{Sm}$ , in  $\text{UO}_2$  and MOX fuel pellets.<sup>204</sup>

Wolf *et al.* (2004) coupled HPLC and ICP-MS to separate rare earth elements prior to measurement.<sup>84</sup> HPLC separation was achieved using an Amberlite CG50 (2  $\times$  50 mm<sup>2</sup>) guard column coupled with a Dionex CS5A (2  $\times$  250 mm<sup>2</sup>) analytical column, a linear gradient elution of 0.040–0.26 M hydroxyisobutyric acid (HIBA) with a 0.30 mL min<sup>-1</sup> flow rate. The eluent from the HPLC was introduced directly into the ICP-MS *via* a CETAC MCN-100, Model M-2 pneumatic microconcentric nebulizer. Measurements were performed using a Fison PlasmaQuad 2+ quadrupole ICP-MS. The within-sample precision of  $^{151}\text{Sm}$  measurement was quoted as 6%.

Isnard *et al.* (2005) separated Sm and Gd off-line using HPLC, followed by MC-ICP-MS measurement of Sm isotopes, including  $^{151}\text{Sm}$ , using a GV Isoprobe-N MC-ICP-MS.<sup>222</sup> Sample introduction was *via* a microconcentric nebulizer and cyclonic spray chamber. Plasma RF power was set at 1350 W, with measurements performed *via* static Faraday detectors. Analysis of MOX spent nuclear fuel gave mean  $^{151}\text{Sm}/^{150}\text{Sm}$  atom ratios of 0.04319 with a standard deviation of 0.2%. Pitois *et al.* (2008) coupled capillary electrophoretic separation with both ICP-QMS

(PerkinElmer ELAN 5000) and ICP-SFMS (Thermo Element 2) to measure rare earth fission products although not  $^{151}\text{Sm}$ .<sup>208</sup> Detection limits of 8 ng mL<sup>-1</sup> (ICP-QMS) and 7 pg mL<sup>-1</sup> (ICP-SFMS) were reported for rare earth elements, which would be equivalent to 6500 Bq mL<sup>-1</sup> and 6.5 Bq mL<sup>-1</sup> of  $^{151}\text{Sm}$ .

### 8.13 Lead-210

The longest lived radioisotopes of Pb are  $^{202}\text{Pb}$  ( $t_{1/2} = 5.3 \times 10^4$  years),  $^{205}\text{Pb}$  ( $t_{1/2} = 1.5 \times 10^7$  years), and  $^{210}\text{Pb}$  ( $t_{1/2} = 22.23$  years). Lead-210 is naturally occurring as part of the  $^{238}\text{U}$  decay series, and has been measured in the fields of geochronology, air flux measurements of radon<sup>223,224</sup> radiation protection associated with uranium mining, and environmental contamination from the iron and steel industry.<sup>225</sup> Lead-210 is a beta emitting radionuclide (Emax 63.5 keV, 100% intensity), and is also a weak alpha (decay energy 3.72 MeV,  $1.9 \times 10^{-6}\%$  intensity) and gamma emitter (12.56 keV, 22.0% intensity). Measurement is therefore potentially achievable by multiple radiometric techniques. Gamma spectrometry measurement is affected by limited sample throughput, and prior knowledge of the sample geometry and composition is required. The low energy gamma ray, self-absorption and interferences from other gamma emitters and X-rays must also be considered.<sup>224</sup> Lead-210 measurement by beta counting using a GM counter is achieved through measuring the  $^{210}\text{Bi}$  daughter (1.2 MeV Emax), following an ingrowth period of 8–9 days. Finally, measurement by alpha spectrometry is achievable through measurement of  $^{210}\text{Po}$ , however an ingrowth time of greater than 3 months is required.<sup>224</sup>

Mass spectrometric measurement of  $^{210}\text{Pb}$  is affected by peak tailing from stable  $^{208}\text{Pb}$  (52.4% abundance), and polyatomic interferences associated with Pt, Hg, Bi and Pb.<sup>226</sup> Polyatomic interferences combined with the relatively short half-life of  $^{210}\text{Pb}$  have been highlighted as the causes for measurement precision being inferior to that of alpha



spectrometry.<sup>223</sup> Pre-concentration of  $^{210}\text{Pb}$  prior to measurement is achievable by co-precipitation with cobalt-ammonium pyrrolidine dithiocarbonate,<sup>226</sup> or as lead sulphate,<sup>225</sup> whilst chemical separation from interferences can be performed by extraction chromatography using Sr-resin.<sup>226</sup> Given the Pt-based interferences, Pt sampler and skimmer cones should be avoided, as high backgrounds have been reported at  $m/z = 210$ .<sup>225</sup>

Larivière *et al.* compared ICP-QMS (Perkin Elmer Elan 5000), ICP-DRC-MS (Perkin Elmer Elan 6100) and ICP-SFMS (Thermo Element 2) for measurement of  $^{210}\text{Pb}$  in water.<sup>226</sup> All instruments were equipped with an Apex-Q sample introduction system, and a detection limit of 90 mBq L<sup>-1</sup> (0.03 pg L<sup>-1</sup>) was recorded for final measurements. The tailing removal was greatest using ICP-DRC-MS ( $>3 \times 10^9$ ), compared to  $>2 \times 10^6$  for QMS, and  $1 \times 10^5$  for SFMS. In a separate study, CC-ICP-MS (Agilent 7500ce) was applied to measurement of standards and solutions spiked with  $^{210}\text{Pb}$ , and sediment samples from waste associated with an oil and gas production field in Egypt.<sup>224</sup> The recovery was assessed using isotope dilution with  $^{206}\text{Pb}$ . The results showed good agreement with those obtained by gamma spectrometry, with a detection limit of 0.21 ng L<sup>-1</sup> (593.24 Bq L<sup>-1</sup>). The formation of polyatomic interferences was reduced using krypton as a collision gas at a flow rate of 0.4 mL min<sup>-1</sup>, which was determined by assessing the  $^{208}\text{Pb}/^{206}\text{Pb}$  ratio with the change in gas flow rate. It was also noted that potential lead hydride formation could be removed using a desolvating sample introduction system. Technologically enhanced  $^{210}\text{Pb}$  as a result of iron and steel manufacture has been measured along with  $^{210}\text{Po}$  using a combination of ICP-QMS (Perkin Elmer Elan 9000), gamma spectrometry and alpha spectrometry,<sup>225</sup> with a Pb activity range of  $<7$  Bq kg<sup>-1</sup> (2.5 pg kg<sup>-1</sup>) to 4240 Bq kg<sup>-1</sup> (1.5 ng kg<sup>-1</sup>).

#### 8.14 Radium-226 and 228

Radium-226 and 228 are naturally occurring radioactive materials, with large amounts produced from mining and extraction of fossil fuels, as well as from the phosphate industry and uranium mine tailings.<sup>227,228</sup> Radium-228 is also continually produced from the decay of  $^{232}\text{Th}$  in shelf sediments.<sup>229</sup> The natural occurrence of these nuclides has led to application as a tracer for ocean circulation, seawater sediment fluxes and particulate residence times.<sup>229</sup> Radium-226 decays with a half-life of 1599 years, with maximum alpha decay energy of 4.79 MeV (94.6%) and gamma emission of 186 keV (32.8%). The half-life of  $^{228}\text{Ra}$  is comparatively short (5.76 years), with a maximum beta decay energy of 39 keV.

Radiometric detection is achievable by alpha or gamma spectrometry, however both require a lengthy ingrowth period for secular equilibrium to be established between  $^{228}\text{Ra}$  and  $^{228}\text{Th}$ .<sup>229,230</sup> Whilst ICP-MS measurement needs lengthy sample treatment to remove multiple potential polyatomic interferences prior to sample introduction (including  $^{88}\text{Sr}$ ,  $^{138}\text{Ba}$ ,  $^{87}\text{Sr}$ ,  $^{139}\text{La}$ ,  $^{86}\text{Sr}$ ,  $^{140}\text{Ce}$ ,  $^{208}\text{Pb}$ ,  $^{18}\text{O}$ , and  $^{186}\text{W}$ ,  $^{40}\text{Ar}$ ), no ingrowth time is required, and the sample analysis time is also significantly lower than radiometric measurements.<sup>228,229</sup> Chemical separation is generally achieved by diffusive gradients in thin films

(DGT) or manganese dioxide ( $\text{MnO}_2$ ) combined with ion exchange and/or extraction chromatography.<sup>227,230-233</sup>

Measurement of the  $^{228}\text{Ra}$  is challenging given the significantly shorter half-life and lower concentration in environmental samples compared to  $^{226}\text{Ra}$ . Recent applications have taken advantage of the high instrumental sensitivity of ICP-SFMS for  $^{226}\text{Ra}$ / $^{228}\text{Ra}$  detection, using either single<sup>227,231-233</sup> or multi-collector instruments<sup>229,230,233</sup> (Table 8). Instruments have been successfully operated at both low resolution,<sup>231-233</sup> and medium resolution,<sup>227</sup> with the latter setup improving polyatomic interference removal at the expense of one order of magnitude sensitivity loss when analysing seawater samples (1200 cps per ng L<sup>-1</sup> at low resolution compared to 100 cps per ng L<sup>-1</sup> at medium resolution). A recent study of  $^{226}\text{Ra}$  in high salinity seawater using a Perkin Elmer NexION 300x achieved a detection limit of 100 pg L<sup>-1</sup> (3.7 Bq L<sup>-1</sup>),<sup>228</sup> which is several orders of magnitude higher than that of ICP-SFMS. Multiple elements have been applied for mass bias correction, given the absence of a certified  $^{226}\text{Ra}$ / $^{228}\text{Ra}$  reference material, including  $^{207}\text{Pb}$ / $^{208}\text{Pb}$ ,  $^{238}\text{U}$ / $^{235}\text{U}$ , and  $^{229}\text{Th}$ / $^{232}\text{Th}$ .<sup>229,230</sup>

#### 8.15 Protactinium-231

Protactinium-231 is the longest lived intermediate daughter of  $^{235}\text{U}$ , with a half-life of  $3.28 \times 10^4$  years, and can also be produced as a by-product in the thorium fuel cycle *via* a fast neutron reaction with  $^{232}\text{Th}$  or  $^{232}\text{U}$ . Protactinium-231 is an alpha emitting radionuclide (5.149 MeV), decaying to  $^{227}\text{Ac}$ . A major application of  $^{231}\text{Pa}$  is in precise isotope ratio calculations for uranium-series age dating, and as an indicator of climate change, and is commonly measured in combination with Th and U isotopes. This required high precision measurements of isotopic ratios, which can be achieved using TIMS (typically 2–3% precision).<sup>234-236</sup> However, extensive matrix separation, and challenges associated with sample loading limit sample throughput.<sup>234</sup> Alpha spectrometry has been used for measurement of  $^{231}\text{Pa}$  in seawater samples, however cubic-metre levels of sample are required, followed by extensive chemical separation, with low final measurement precision (5–10%).<sup>234</sup> ICP-MS measurement can rival the precision of TIMS, whilst achieving a significant improvement in sample throughput. The main interference is peak tailing from  $^{232}\text{Th}$ , which can be removed by chemical separation prior to measurement if necessary. Protactinium-234 ( $t_{1/2} = 26.97$  days) has been used as a spike in some studies,<sup>234,237</sup> however, consideration must be given to decay to  $^{233}\text{U}$ , leading to changes in the  $^{231}\text{Pa}$ / $^{233}\text{Pa}$  ratio over time, with losses of Pa to beaker walls also highlighted as an issue.

Applications include a fossil coral fragment measured by MC-ICP-MS (FISONS PLASMA 54), with samples introduced by a CETAC MCN6000 desolvating nebulizer.<sup>238</sup> The reduced sample handling, sample size and increased throughput compared to TIMS were highlighted as advantages. Choi *et al.* (2001) measured  $^{231}\text{Pa}$  along with  $^{230}\text{Th}$  in seawater by ICP-SFMS (Element) equipped with a desolvating nebulizer (Cetac MCN-6000), with a detection limit of 0.4 fg, corresponding to 0.02 fg g<sup>-1</sup> ( $3.5 \times 10^{-8}$  Bq g<sup>-1</sup>) in 20 L seawater samples.<sup>234</sup> In a separate

Table 8 Summary of recent procedures for measurement of  $^{226}\text{Ra}$ 

Reference	Instrument	Model	Matrix	Chemical separation	LOD $\text{pg L}^{-1}$ ( $\text{Bq L}^{-1}$ )
228	CC-QMS	Perkin Elmer NexION 300x	High salinity wastewater	AG50 (IE)	100 (3.7)
227	SFMS	Element II	Seawater		
231	SFMS	Element II	Water and sediment pore water	DGT	0.5 (0.02)
232	SFMS	Element II	Water and sediments	DGT, $\text{MnO}_2$ pptate, Sr resin (EC)	0.5 (0.02)
233	MC-ICP-MS	Nu plasma	Natural waters	$\text{MnO}_2$ , AG50 (IE), Sr resin (EC)	0.05 (0.002)
					0.05 (0.002)
230	MC-ICP-MS	Neptune	Seawater and suspended particles	$\text{MnO}_2$ , AG50, AG1, Sr resin	0.091 (0.003)
229	MC-ICP-MS	Nu instruments	Seawater		

study, silicate rock samples were measured following anion exchange and extraction chromatography (TRU (Triskem International)) separation by MC-ICP-MS (Thermo Neptune) equipped with a desolvating nebulizer (Cetac Aridus), with a detection limit of  $200 \text{ fg L}^{-1}$  ( $3.5 \times 10^{-6} \text{ Bq L}^{-1}$ ).<sup>237</sup>

### 8.16 Thorium isotopes

Thorium is a naturally occurring element, with an abundance in the earth's crust 3–4 times higher than uranium, and has also been used as an alternative fuel for nuclear fission. The most abundant isotope is  $^{232}\text{Th}$  with a half-life of  $14.02 \times 10^9$  years, and undergoes alpha decay to  $^{228}\text{Ra}$ . Additional radioisotopes with long half-lives measurable by ICP-MS are  $^{229}\text{Th}$  ( $t_{1/2} = 7340$  years) and  $^{230}\text{Th}$  ( $t_{1/2} = 7.5 \times 10^4$  years). Thorium is commonly measured as  $^{232}\text{Th}$  along with isotopes of U and Pu in bioassay samples, as well as with uranium in chronology, paleoclimatology, archaeology, hydrology, geochemistry and oceanography.<sup>239,240</sup> Alternative mass spectrometric measurement techniques include TIMS and SIMS.<sup>241</sup> When Th is measured by ICP-MS in combination with U, the  $^{232}\text{Th}$  tailing can impact measurement of  $^{233}\text{U}$ , as can the formation of  $^{232}\text{Th}^1\text{H}$ .<sup>242</sup> A summary of recent measurement of Th isotopes by ICP-MS is given in Table 9, with a review of mass spectrometric determination of Th published elsewhere.<sup>243</sup>

As instrument sensitivity has improved, the low-level measurement of Th is potentially impacted by environmental contamination during sample preparation. The concentrations of Th, U and their progenies in the reagents and labware used has become an increasingly important issue, with clean laboratory conditions and cleaning of materials prior to use required for some applications. Hoppe *et al.* (2013) investigated the use of low background materials and maintenance of low background levels of Th and U.<sup>244</sup> It was concluded that sample preparation is the limiting factor affecting sensitivity for very low level measurements, and thorough cleaning and acid leaching of these materials has made very sensitive measurements possible.

Several studies have measured Th in combination with U and/or Pu in urine.<sup>242,245,246</sup> Becker *et al.* (2004) measured Th and U using LA-ICP-MS, which minimized sample preparation, whilst quantification issues associated with laser ablation were resolved with matrix-matched standards.<sup>245</sup> Measurements were performed by both ICP-QMS (Perkin Elmer Elan 6000) and

ICP-SFMS (Thermo Element) coupled to laser ablation (CETAC LSX 200). The Th recovery ranged from 97–104% at doping concentrations of  $0.52\text{--}2.49 \text{ ng L}^{-1}$  ( $2.1 \times 10^{-6} \text{ Bq L}^{-1}$  to  $1.0 \times 10^{-5} \text{ Bq L}^{-1}$ ) with detection limits of  $0.4 \text{ ng L}^{-1}$  ( $3.5 \times 10^{-8} \text{ Bq g}^{-1}$ ) and  $0.2 \text{ ng L}^{-1}$  ( $8.1 \times 10^{-7} \text{ Bq g}^{-1}$ ) for ICP-QMS and ICP-SFMS, respectively. The study highlighted the advantages of ICP-MS for actinide measurement over alpha spectrometry, which was a less sensitive approach that required more extensive sample preparation. In a separate study, Shi *et al.* (2013) measured Th, U and Pu in urine samples with regards to dose assessment, as well as measuring decommissioning samples including tape and paint.<sup>242</sup> Samples were measured by ICP-SFMS (Thermo Element XR) with an Elemental Scientific Apex desolvating sample introduction system, which reduced the  $^{232}\text{Th}^1\text{H}$  formation rate to  $1.3 \times 10^{-5}$ , compared to  $6.6 \times 10^{-5}$  for solution nebulization using a Micromist nebulizer. Cozzella and Pelttirossi (2013) measured Th, U and Pu in urine by ICP-MS rather than alpha spectrometry, highlighting the ability to process a large number of samples whilst maintaining an acceptable measurement uncertainty.<sup>246</sup> Samples were measured by ICP-QMS (Thermo X-series) with a Burgener nebulizer. Prior to sample introduction, Th was stabilized in urine with Triton X-100 and then mixed with MICROTENE-TOPO, shaken vigorously and then loaded onto a column prior to elution. Thorium recovery ranged from  $93 \pm 0.2\%$  to  $120 \pm 1.2\%$  over a spiked concentration range of  $0.5\text{--}2 \text{ }\mu\text{g L}^{-1}$  ( $2.0 \times 10^{-3}$  to  $8.1 \times 10^{-3} \text{ Bq g}^{-1}$ ).

Thorium and U were measured along with multiple rare earth elements in natural spring water samples in Brazil, in relation to supplying safe potable water to nearby towns.<sup>247</sup> Water samples were measured by ICP-DRC-MS (Perkin Elmer ELAN DRC-e) equipped with a sea spray nebulizer and cyclonic spray chamber. The method detection limit was  $0.5 \text{ ng L}^{-1}$  ( $2.0 \times 10^{-6} \text{ Bq g}^{-1}$ ). Avivar *et al.* (2011) measured Th and U in multiple environmental samples (different water samples, a phosphogypsum sample, and a channel sediment reference material) using multi-syringe FIA (MSFIA), using UTEVA resin (Triskem International) for online separation and pre-concentration.<sup>248</sup> The system was coupled to ICP-DRC-MS (Perkin Elmer Elan DRC-e) equipped with a Scott spray chamber and cross-flow nebulizer. Combination of LOV with MSFIA achieved a  $^{232}\text{Th}$  detection limit of  $2.8 \text{ ng L}^{-1}$  ( $1.1 \times 10^{-5} \text{ Bq L}^{-1}$ ), compared to  $120 \text{ ng L}^{-1}$  ( $4.9 \times 10^{-4} \text{ Bq L}^{-1}$ ) using FIA only. Tuovinen (2015) compared ICP-MS to XRF, ERD,



EPMA, gamma spectrometry and alpha spectrometry for determination of Th and U in ore and mill tailing samples collected in Finland.<sup>249</sup> Thorium was measured over a concentration range of 7–157 mg L<sup>−1</sup> (2.8–637.2 Bq L<sup>−1</sup>) by ICP-QMS (Agilent 7500 ce/cx), with the results showing generally good agreement with other techniques. The lowest values were measured by ICP-MS compared to other techniques, which was the result of challenges with sample preparation.

### 8.17 Uranium isotopes

Uranium is naturally occurring, with an average concentration of ~4 µg g<sup>−1</sup> in the terrestrial crust, 3 µg L<sup>−1</sup> in seawater (uniformly distributed in the world's oceans) and ranging from 0.5–500 µg L<sup>−1</sup> in surface freshwater depending on the extent of contamination.<sup>78</sup> The environmental occurrence of uranium is mostly in hexavalent form, associated with oxygen in nature as the uranyl ion UO<sub>2</sub><sup>2+</sup>. Under strongly reducing conditions, uranium is present in tetravalent form in strongly reducing medium such as high organic material (UO<sub>2</sub>). Uranium-238 is the major isotope (99.27%), with additional minor isotopes of <sup>234</sup>U (0.006%) and <sup>235</sup>U (0.72%).

Uranium was one of the early nuclides to be measured by ICP-MS, with studies initially focusing on the elemental concentration of <sup>238</sup>U. As instrumental performance improved, there was an increasing focus on isotopic ratio measurements, initially <sup>235</sup>U/<sup>238</sup>U, and more recently <sup>234</sup>U/<sup>238</sup>U, and <sup>236</sup>U/<sup>238</sup>U, with isotopic analysis enabling distinction between exposure to natural and anthropogenic U sources. Reviews of uranium determination using atomic spectrometric techniques, and in environmental samples, are published elsewhere,<sup>78,251</sup> and Table 10 gives a summary of recent ICP-MS procedures for U isotopic measurements.

Several spectral interferences must be considered for uranium analysis, with Ir, Bi, Th or Ru effectively used for interference correction.<sup>78</sup> Potential platinum-argide interferences from the use of platinum cones can be avoided by using nickel cones,<sup>252</sup> whilst chloride-based interferences with

elements including Au and Hg must also be considered.<sup>78</sup> Uranium-236 detection is potentially affected by both <sup>235</sup>UH formation, and tailing from <sup>238</sup>U. Sector field instruments are a popular choice for uranium determination due to low background, high sensitivity at low resolution, and ability to remove interferences at high resolution.<sup>78</sup> Additionally, the simultaneous data acquisition of MC-ICP-MS combined with sector field sensitivity leads to more precise isotope ratio determination.<sup>253</sup> Determination of uranium concentration and/or isotopic ratios in bioassay samples is commonly carried out through measurement of urine samples, as it is non-invasive, whilst the complexity of the sample matrix represents a challenge for isotope ratio determination.<sup>252–254</sup> For example, uranium was measured as part of the Baltimore VA Depleted Uranium Clinical Follow-up Program by ICP-SFMS (Thermo Element 2).<sup>252</sup> Measurement of <sup>235</sup>U/<sup>238</sup>U and <sup>236</sup>U/<sup>238</sup>U was compared for a quartz concentric nebulizer with a cyclonic spray chamber, and APEX Q (Elemental Scientific) sample introduction system. Superior sensitivity was recorded using the Apex Q, which was preferable for low U concentrations, whilst the concentric nebulizer and cyclonic spray chamber was more robust and suitable for higher U concentrations. The limited abundance sensitivity and <sup>235</sup>UH formation meant the background equivalent concentration of <sup>236</sup>U was 25 times higher than for <sup>235</sup>U and <sup>238</sup>U, with more scattered <sup>236</sup>U/<sup>238</sup>U ratios at total uranium concentrations <10 ng L<sup>−1</sup>. Additionally, the accuracy of <sup>235</sup>U measurements was poor when total U concentrations were less than 5 ng L<sup>−1</sup>.

In a separate study, Arnason *et al.* (2015) carried out an inter-laboratory comparison for uranium concentration and multiple isotope ratio values in urine, with results from sites using ICP-QMS or ICP-SFMS.<sup>254</sup> As the total uranium concentration decreased, the concentration measured by isotope dilution only were higher than those that used chemical separation or digestion prior to measurement. At a concentration of 50 ng L<sup>−1</sup>, the predicted <sup>234</sup>U/<sup>238</sup>U value was 0.000053. Sites that carried out digestion and chemical separation prior to measurement yielded values from  $5.2 \times 10^{-5}$  to  $7.2 \times 10^{-5}$ ,

Table 9 Summary of recent procedures for measurement of Th isotopes

Reference	Instrument	Model	Matrix	Chemical separation	LOD <sup>a</sup> , pg L <sup>−1</sup> (Bq L <sup>−1</sup> )
246	QMS	X-series	Urine	MICROTENE-TOPO chromatography	
250	QMS	X-series II	River water	Stacked TEVA and DGA	<sup>229</sup> Th: 4490 (34.9) <sup>230</sup> Th: 4490 (3.4) <sup>232</sup> Th: 694 000 ( $2.8 \times 10^{-3}$ )
249	QMS	Agilent 7500 ce/cx	Ores and mill tailings		
245	QMS	Perkin Elmer Elan 6000	Urine	TiCl <sub>4</sub> precipitation and Dowex 1-x8	QMS-400 ( $1.6 \times 10^{-6}$ )
	SFMS	Element			SFMS-200 ( $8.1 \times 10^{-7}$ )
242	SFMS	Element 2XR	Urine, decommissioning samples including paint and tape		
247	DRC-MS	Perkin Elmer DRC-e	Natural waters		500 ( $2.0 \times 10^{-6}$ )
248	DRC-MS	Perkin Elmer DRC-e	Environmental samples	FIA, UTEVA	2800 ( $1.1 \times 10^{-5}$ )

<sup>a</sup> LOD for <sup>232</sup>Th unless indicated otherwise.



compared to  $1.5 \times 10^{-3}$  to  $1.8 \times 10^{-2}$  for isotope-dilution-only methods. A significant positive bias was also seen for  $^{235}\text{U}/^{238}\text{U}$  for dilution only-methods, accounted for by polyatomic interference at  $m/z = 235$ . Finally, for  $^{236}\text{U}/^{238}\text{U}$ , only studies that applied chemical separation were considered, and, of these five studies, four either did not report a result or reported a non-detect result. The conclusion from this study was that accurate and precise isotope ratio measurements was more dependent on the analytical methodology and instrument capability than measurement of total U concentration. Arnason *et al.* also measured uranium isotopes in urine samples at volumes from 1–8 mL by ICP-SFMS (Element 2) equipped with a Cetac Aridus desolvating sample introduction system, following chemical separation using UTEVA extraction chromatography separation.<sup>253</sup> At spike concentrations of 2.5–25 ng L<sup>-1</sup>,  $^{235}\text{U}/^{238}\text{U}$  was successfully detected, with an improvement in precision as U concentration increased. By comparison,  $^{234}\text{U}/^{238}\text{U}$  was only detected in samples spiked with 25 ng L<sup>-1</sup>. It was also realized that whilst a higher urine volume achieved better precision, the uranium recovery was lower.

Liu *et al.* (2011) applied extractive electrospray ionization mass spectrometry (EESI-MS) to determination of  $^{235}\text{U}/^{238}\text{U}$  in uranyl nitrate solutions, prepared from samples including natural water, uranium ore and soil.<sup>255</sup> EESI-MS is typically used for organic compounds, and in this study samples were directly measured without pre-concentration or separation. The resulting mass spectrum looked for detection of uranyl nitrate at  $m/z$  456 [ $^{238}\text{UO}_2(\text{NO}_3)_3^-$ ], as well as peaks for 234 and 235. There was a relative error in isotope ratios of 0.21–0.25%, and RSD of 1.54–1.81%. This approach overcomes the extensive sample preparation that can lead to U losses, and also offers fast analysis speed (~5 minutes per sample). Results were comparable between EESI-MS and ICP-QMS (Agilent 7500ce) over a U concentration range of  $\sim 2.6 \mu\text{g L}^{-1}$  to  $\sim 3.1 \text{ mg L}^{-1}$ . Results from EESI-MS returned a RSD of 1.25–3.26%, compared to 0.71–1.46% for ICP-MS. The EESI used in this study was home-made, and it was suggested that improvements in RSD would be realized using a commercial EESI source.

Uranium-236 was measured in soil samples in the vicinity of Chernobyl by ICP-SFMS (Thermo Element), ICP-QMS (Perkin Elmer Elan 6000) and ICP-CC-MS (Micromass Platform ICP), with high precision isotope ratio measurements were performed using a MC-ICP-MS (Nu Instruments).<sup>256</sup> Multiple sample introduction systems (micro-concentric Micromist nebulizer, Q-DIHEN or MCN equipped with an Aridus desolvating sample introduction (CETAC)) were investigated. An abundance sensitivity for  $^{236}\text{U}/^{238}\text{U}$  of  $5 \times 10^{-6}$ ,  $3 \times 10^{-7}$ ,  $6 \times 10^{-7}$  and  $3 \times 10^{-7}$  was measured for ICP-SFMS, MC-ICP-MS, ICP-QMS and ICP-CC-MS, respectively. The precision ranged from 0.28–0.34% for  $^{236}\text{U}/^{238}\text{U}$  for single collector instruments, improving to up to 0.07% for MC-ICP-MS equipped with USN or MCN with an Aridus. Ultra-low  $^{236}\text{U}/^{238}\text{U}$  ratios were recently measured at isotopic ratios of  $< 10^{-7}$  by ICP-QQQ-MS (Agilent 8800).<sup>257</sup> The two mass filters effectively removed tailing from the peak at  $^{238}\text{U}$ , whilst the  $^{235}\text{U}^{\text{H}}$  interference was removed by reacting UH with O<sub>2</sub> in the collision–reaction cell. The interference-removal capability meant that accurate isotopic ratios

could be measured without the need for spectral interference correction.

### 8.18 Neptunium-237

Neptunium-237 is an alpha emitting radionuclide (maximum decay energy 4.78 MeV (47.6%) with a half-life of 2.1 million years. Neptunium is present in the environment as a result of atmospheric weapons test fallout and nuclear fuel reprocessing. A review of  $^{237}\text{Np}$  measurement in nuclear and environmental samples was recently published.<sup>266</sup> Samples investigated include soils, sediment, groundwater, seawater and various other environmental samples.<sup>82,267–277</sup>

Neptunium occurs in both tetra- and pentavalent states, and the variation in oxidation state depending on the reagents and conditions used makes sample preparation challenging.<sup>278</sup> Bulk separation from the sample matrix has been achieved by techniques including iron hydroxide precipitation<sup>272</sup> and lanthanum hydroxide precipitation,<sup>275</sup> followed by ion exchange or extraction chromatography.<sup>82,268–272,275,278</sup> Neptunium is often measured along with Pu following chemical separation, given the similar chemical behavior of the two elements in HNO<sub>3</sub> and HCl on anion exchange and extraction chromatography resins.<sup>63,268–271,274–276,279</sup> A micro-flow injection sample introduction system combined with membrane desolvation improved the instrument sensitivity, and the detection limit by concentrating the analyte into a smaller volume.<sup>276</sup> In a separate study, Qiao *et al.* incorporated TEVA resin into a sequential injection (SI) system for simultaneous Np and Pu measurement in environmental samples, or Bio-RAD AG MP-1M for soil, sediment and seaweed.<sup>279</sup>

The major interference impacting  $^{237}\text{Np}$  detection is tailing from  $^{238}\text{U}$ , which must be removed by chemical separation, or by the instrument if abundance sensitivity is sufficient.<sup>276</sup> The  $^{237}\text{Np}$  detection limit has been noted to increase with increasing U concentration (0.32 fg ( $8.3 \times 10^{-9}$  Bq) with no uranium, compared to 10 fg ( $2.6 \times 10^{-7}$  Bq) with 2500 pg of U, with a negative impact on detection limit once the U concentration exceeded 30 pg).

The lack of a suitable tracer for  $^{237}\text{Np}$  has been identified as a limitation,<sup>266,276</sup> particularly for isotope dilution applications.<sup>274,280</sup> Neptunium-236 (154 000 year half-life) is potentially suitable,<sup>269,274</sup> but suffers from a lack of commercial availability and production difficulties.<sup>280,281</sup> Alternative isotopes of neptunium ( $^{239}\text{Np}$  and  $^{235}\text{Np}$ ) are less well suited given their short half-lives (2.35 days and 396 days, respectively) and suffer from potential isobaric interferences from  $^{239}\text{Pu}$  and  $^{235}\text{U}$ , respectively.<sup>63</sup> Plutonium-242 (half-life  $3.75 \times 10^5$  years) has been used as a tracer for determination of both  $^{237}\text{Np}$  and Pu isotopes,<sup>276</sup> given its similar chemical behavior and commercial availability.<sup>269,270,274,275,280</sup> An issue with this is variation in chemical fractionation between Np and Pu during analysis, which will increase uncertainty,<sup>280</sup> and an isotope of the same element is desirable.

Neptunium-237 has frequently been determined using ICP-SFMS<sup>268,270–274</sup> (Table 11). Kim *et al.* (2004) simultaneously measured  $^{237}\text{Np}$  with  $^{239}\text{Pu}$  and  $^{240}\text{Pu}$  in environmental samples





Table 10 Summary of recent procedures for measurement of U isotopes

Reference	Instrument	Model	Sample matrix	Chemical separation	LOD <sup>a</sup> , pg L <sup>-1</sup> (Bq L <sup>-1</sup> )
78	QMS	Plasma Quad 2+	Environmental samples (oyster tissue and pine needles)		Pneumatic nebulizer: 5400 ( $6.7 \times 10^{-5}$ ) to 48 000 ( $6.0 \times 10^{-4}$ ) ETV: 900 ( $1.1 \times 10^{-5}$ ) to 21 000 ( $2.6 \times 10^{-4}$ )
255	Ion trap MS	LTQ-XL	Water, U ore, soil		
97	QMS	Elan 5000	Uranium oxide leachate		
258	QMS		Environmental samples		
259	QMS	Yokogawa PMS-2000	Urine		
250	QMS	Perkin Elmer Elan 6000 X-series II	River water	Stacked TEVA and DGA resins	$4000 (5.0 \times 10^{-5})$ $^{233}\text{U}: 6.5 (2.3 \times 10^{-3})$ $^{234}\text{U}: 6.5 (1.5 \times 10^{-3})$ $^{235}\text{U}: 23.8 (1.9 \times 10^{-6})$ $^{236}\text{U}: 6.5 (1.6 \times 10^{-5})$ $^{238}\text{U}: 2820 (3.5 \times 10^{-5})$
260	QMS	Agilent 7500	Urine	Ca phosphate, stacked TEVA, TRU, DGA resin	
261	DRC-MS	Perkin Elmer Elan 6100 DRC	Urine		Instrument LOD: 4 ( $5.0 \times 10^{-8}$ ) Method LOD: 22 ( $2.2 \times 10^{-11}$ ) 200 ( $2.5 \times 10^{-6}$ )
262	SFMS	Element 2	Urine	Sample dilution only	
263	SFMS	Element	Standard solutions		
49	SFMS	Element	Soil samples 4–20 km north and west of Chernobyl	Instrument LOD: 60 ( $7.5 \times 10^{-7}$ ) Method LOD: <3000 ( $3.7 \times 10^{-5}$ )	
259	SFMS	Element	Urine		
264	SFMS CC-MC-ICP-MS MC-ICP-MS	Plasma Trace 2 Micromass Isoprobe VG Elemental P54 Element XR	Urine	Phosphate precipitation 2× TRU UTEVA resin	$5 (6.2 \times 10^{-8})$ $1 (1.2 \times 10^{-8})$ 200 ( $2.5 \times 10^{-6}$ )
265	SFMS	Swab samples		Stacked ion exchange and extraction chromatography Ca and Mg co-precipitation UTEVA resin	
265	SFMS	Element 2	Urine		$^{235}\text{U}: 0.8 (6.4 \times 10^{-8})$
266	SFMS	Element 2	Urine		$^{236}\text{U}: 0.05 (1.2 \times 10^{-7})$
					$^{238}\text{U}: 100 (1.2 \times 10^{-9})$

<sup>a</sup> LOD for  $^{238}\text{U}$  unless indicated otherwise.

Table 11 Summary of recent procedures for measurement of  $^{237}\text{Np}$ 

Reference	Instrument	Model	Matrix	Chemical separation	LOD, pg L <sup>-1</sup> (Bq L <sup>-1</sup> )
283	QMS	Perkin Elmer Elan 5000	Natural groundwater	Capillary electrophoresis	50 000 000 (1.3 $\times$ 10 <sup>3</sup> )
260	QMS	Agilent 7500	Urine	Ca phosphate, stacked TEVA, TRU, DGA resin	
275	QMS	Agilent 7500 X-series II	Large soil samples	Hydroxide precipitate, sequential injection (TEVA resin)	8700 (0.2)
63	QMS	X-series II	Environmental samples	Iron hydroxide precipitation, sequential injection (anion exchange)	1.5 (3.9 $\times$ 10 <sup>-5</sup> )
279	QMS	VG Elemental PlasmaQuad PQ2+	Soil, sediment, seaweed	TOA extraction chromatography	460 (1.2 $\times$ 10 <sup>-2</sup> )
267	SFMS	Finnigan MAT Element	Environmental samples	TRU resin	80 000 (2.1)
268	SFMS	Not given	Environmental samples	Glow discharge	0.5 (1.3 $\times$ 10 <sup>-5</sup> )
82	SFMS	Finnigan-MAT Element	Irish sea sediments	La(OH) <sub>3</sub> coprecipitation, TEVA resin	2.5 (6.5 $\times$ 10 <sup>-5</sup> )
269	SFMS	Micromass PlasmaTrace 2	Environmental samples	Automated sequential injection (TEVA resin)	
270	SFMS	Finnigan MAT Element 2	Soil	TEVA resin	0.2–0.4 (5.2 $\times$ 10 <sup>-6</sup> to 1.0 $\times$ 10 <sup>-5</sup> )
272	SFMS	Element 2	Soils and sediments from river Yenisei	TEVA resin	
284	SFMS				

by ICP-SF-MS (Micromass Plasma Trace 2) equipped with an Aridus desolvating sample introduction system and T1-H microconcentric nebulizer.<sup>270</sup> Chemical separation of Np and Pu was achieved using an automated SI system using TEVA extraction chromatography resin, with a  $^{237}\text{Np}$  detection limit of 2.5 pg L<sup>-1</sup> (6.5  $\times$  10<sup>-5</sup> Bq L<sup>-1</sup>). In a separate study, an Agilent 7500 QMS equipped with an Octopole Reaction System was operated in 'no gas' mode for Np measurement.<sup>275</sup> However, there was evidence that Np would behave similarly to Pu with CO<sub>2</sub> as the reactive gas, which could be used as a basis for separation of Np and Pu from U.<sup>282</sup> It was noted that applying chemical separation prior to ICP-SFMS measurement could lower the detection limit.

Sediments have been measured by glow discharge mass spectrometry.<sup>82</sup> The instrument was operated at a mass resolution of around 6000, resulting in high transmission (>75%) and removal of tailing interferences, as well as reduced sample preparation time compared to chemical separation. Irish Sea sediment samples were measured after being compacted into pellets. Neptunium was determined in groundwater at the Nevada National Security Site (NNSS) by ICP-SFMS (NuPlasma) at concentrations ranging from  $<4 \times 10^{-4}$  to 2.6 mBq L<sup>-1</sup> (0.015–99.7 pg L<sup>-1</sup>) with all values below the US Environment Protection Agency drinking limits of 560 mBq L<sup>-1</sup>.<sup>277</sup> The outcome was used to evaluate retardation of Np relative to other radionuclides in NNSN groundwater.

### 8.19 Plutonium isotopes

Plutonium is present in the environment as a result of nuclear weapons tests, reactor accidents, and discharges from reprocessing facilities, and is arguably the most frequently studied transuranic element. Isotopes of particular interest with regards to ICP-MS measurement are  $^{238}\text{Pu}$  ( $t_{1/2} = 87.7$  years),  $^{239}\text{Pu}$  ( $t_{1/2} = 24\,110$  years) and  $^{240}\text{Pu}$  ( $t_{1/2} = 6561$  years) (Table 13). Several reviews on the determination of plutonium isotopes are given elsewhere.<sup>95,120,285</sup>

Isotope ratio measurements by ICP-MS (most commonly  $^{240}\text{Pu}/^{239}\text{Pu}$ ) have been effectively used to determine the source of nuclear contamination<sup>286</sup> (Table 12). This is a significant advance over traditional alpha spectrometry detection, which is unable to resolve the similar alpha energies of  $^{239}\text{Pu}$  and  $^{240}\text{Pu}$  (5.24 and 5.25 MeV, respectively). Measurement of Pu isotopes by alpha spectrometry also requires extensive chemical separation and counting times on the order of days to weeks.

Measurement of  $^{239}\text{Pu}$  is affected by tailing from  $^{238}\text{U}$ , with decontamination factors of 10<sup>8</sup> or higher required depending on the sample matrix.<sup>285,286</sup> A detection limit of 1.0 fg (2.3  $\times$  10<sup>-6</sup> Bq) was achieved for  $^{239}\text{Pu}$  at U concentrations from 0–30 pg using ICP-SFMS (Thermo Element XR), compared to 8.6 fg (2.0  $\times$  10<sup>-5</sup> Bq) when U concentration was increased to 2500 pg.<sup>276</sup> There is an additional polyatomic interference from  $^{238}\text{U}^{\text{1H}}$ , which can be removed by U/Pu separation, or by reducing hydride formation using a desolvating sample introduction system. Plutonium-238 measurement is challenging owing to low concentrations, and an isobaric interference from  $^{238}\text{U}$ , whilst  $^{241}\text{Pu}$  can be affected by isobaric  $^{241}\text{Am}$ . Chemical separation of Pu prior to sample introduction is generally a 2

Table 12  $^{240}\text{Pu}$  :  $^{239}\text{Pu}$  atom ratios for different sources<sup>286,299</sup>

Source	$^{240}\text{Pu}$ / $^{239}\text{Pu}$
Integrated weapon test fallout	0.18
Weapon production	0.01–0.07
Chernobyl accident	0.40
MAGNOX reactor	0.23 <sup>a</sup>
Pressurized heavy water reactor	0.41 <sup>a</sup>
Advanced gas-cooled reactor (AGR)	0.57 <sup>a</sup>
Pressure tube boiling water reactor	0.67 <sup>a</sup>
Boiling water reactor (BWR)	0.40 <sup>a</sup>
Pressurized water reactor (PWR)	0.43 <sup>a</sup>
Fukushima prefecture coast sediments	0.19–0.26

<sup>a</sup> After fuel burn up (the amount of energy extracted from the primary fuel source).<sup>48,287</sup>

stage process-bulk matrix co-precipitation, followed by actinide pre-concentration and separation using extraction chromatography.<sup>63,275,282,288–290</sup> More rapid FI or SI techniques have been effectively applied to urine,<sup>291</sup> soils,<sup>275,289</sup> and environmental samples.<sup>63</sup> A number of Pu isotopes including  $^{236}\text{Pu}$ ,  $^{242}\text{Pu}$  and  $^{244}\text{Pu}$  have been effectively used as tracers,<sup>63</sup> with isotope dilution a common technique that can also address issues with plasma instability and ion intensity drift.<sup>95</sup>

Carbon dioxide has been used as a reactive gas for U separation from Pu for a  $^{235}\text{U}$  target using CC-ICP-MS (GV Isoprobe MC-ICP-MS).<sup>282</sup> At  $\text{CO}_2$  gas flow rates  $>0.5 \text{ mL min}^{-1}$ , U is present as  $\text{UO}^+$  (~95%) and  $\text{UO}_2^+$  (~5%), compared to Pu, which was present as  $\text{Pu}^+$  (40%),  $\text{PuO}^+$  (~60%), and  $\text{PuO}_2^+$  (~2%). A recent study used lab-on-valve separation of Pu using bead injection extraction chromatography micro-flow system was coupled to ICP-QMS (Thermo X-series II) equipped with Xs skimmer cone and Burgener nebulizer.<sup>292</sup> The design enabled processing of large urine volumes (1 L), Pu chemical yields >90%, and completion of the analytical procedure in less than 3 hours, compared to 1–2 days for manual processing. A detection limit of  $1.0\text{--}1.5 \text{ pg L}^{-1}$  (equivalent to  $2.3 \times 10^{-3}$  to  $3.4 \times 10^{-3} \text{ Bq L}^{-1}$  for  $^{239}\text{Pu}$  and  $1.5 \times 10^{-4}$  to  $2.2 \times 10^{-4} \text{ Bq L}^{-1}$  for  $^{242}\text{Pu}$ ) was achieved for  $^{239}\text{Pu}$  and  $^{242}\text{Pu}$ , however, potential improvements to the procedure were suggested, including overcoming the limited flow rate ( $<1 \text{ mL min}^{-1}$ ) due to back-pressure build up and settling of beads within the system, which could lead to leakage and/or malfunctioning for long-term operations.

Plutonium isotope ratios ( $^{239}\text{Pu}$ / $^{240}\text{Pu}$ ) were determined from alpha planchettes originally prepared from samples from the Mayak nuclear facility, Russia.<sup>293</sup> The aim was to show that direct analysis of samples was possible without the time-consuming dissolution and chemical separation associated with solution ICP-MS. A potential advantage is that this approach can be applied to planchette samples round the world, to generate a large amount of new data from existing samples. Samples had previously been separated from the sample matrix, and were measured by ICP-QMS (Agilent 7700X). If the  $^{239+240}\text{Pu}$  activity on the planchette was  $<1 \text{ Bq}$ , the

statistical variation in isotope ratios was too high and reliable determination of  $^{240}\text{Pu}$  was not possible. It was noted that the likelihood of distinguishing between sources of Pu could be improved by chemical separation to remove U from the sample prior to measurement.

Varga *et al.* investigated rapid and direct measurement of U and Pu,  $^{235}\text{U}$ / $^{239}\text{Pu}$  and  $^{236}\text{U}$ / $^{240}\text{Pu}$  chronometers without chemical separation using a Thermo Element 2 ICP-SFMS equipped in a glovebox.<sup>294</sup> The instrument was run in low resolution mode with a low-flow micro concentric nebulizer, and a quartz glass spray chamber. A second method incorporating extraction chromatography prior to measurement was also tested, with multiple U/Pu ratios measured. Results from two Pu CRM's were in good agreement with archive purification dates.

Bu *et al.* measured Pu isotopes in lichen, kelp, moss and horse mussel collected from Alaska by ICP-SF-MS (Thermo Element XR).<sup>295</sup> The instrument was operated in low resolution, equipped with an Apex (Elemental Scientific) sample introduction system and PFA nebulizer. A  $^{242}\text{Pu}$  tracer was used, and a correction factor was applied to correct for uranium hydride interference, however this was expected to be low as chemical separation was applied prior to sample introduction. Mass discrimination was determined from measurement of  $^{235}\text{U}$ / $^{238}\text{U}$  in a natural U solution, with the overall procedure validated by measuring  $^{239+240}\text{Pu}$  in a CRM. A measured value of  $5.18 \pm 0.10 \text{ Bq kg}^{-1}$  was in good agreement with the certified value of  $5.30 \pm 0.16 \text{ Bq kg}^{-1}$ . The total  $^{239+240}\text{Pu}$  content in sample measured ranged from 3.8 to  $573 \text{ Bq kg}^{-1}$  dry weight. The difference in isotope ratio values measured showed isotopically heavier  $^{240}\text{Pu}$ / $^{239}\text{Pu}$  values in marine samples compared to terrestrial samples, accounted for as being a large input of Pu into the Pacific Ocean, most likely Marshall Islands high yield tests.

A comparison of liquid scintillation and ICP-SFMS for  $^{241}\text{Pu}$  measurement in nuclear waste slurries was reported by Jäggi *et al.* (2012).<sup>296</sup> ICP-MS measurements were performed using a double focusing ICP-SFMS (Thermo Element 2). Samples were introduced via an Apex nebulizing system connected to an ACM desolvation system and a self-aspirating PFA-ST nebulizer. Correction for tailing and hydride formation were performed following measurement of a  $^{238}\text{U}$  standard. Correction factors for mass 239, 240 and 241 arising from  $^{238}\text{U}$  were typically  $9 \times 10^{-6}$ ,  $1 \times 10^{-6}$  and  $3 \times 10^{-7}$ . A detection limit of  $0.27 \text{ Bq g}^{-1}$  ( $117.6 \text{ pg g}^{-1}$ ) for a 0.1 g slurry sample was achieved.

Isotope ratios were measured from multiple environmental samples collected in Finland by ICP-SFMS (Thermo Element 2) operating in low resolution, fitted with a coaxial nebulizer and cyclonic spray chamber.<sup>297</sup> Instrument performance was carried out using a certified reference material containing natural U, and quality of  $^{240}\text{Pu}$ / $^{239}\text{Pu}$  measurements was validated from a CRM. For surface air samples collected in 1963, values mostly fell in the range 0.15–0.25, indicative of global weapons fallout. Results from environmental samples showed a wider range in values from  $0.13 \pm 0.1$  to  $0.53 \pm 0.03$ , indicative of both global fallout and the Chernobyl accident. As well as digestion and



Table 13 Summary of recent procedures for measurement of Pu isotopes

Reference	Instrument	Model	Matrix	Chemical separation	LOD, pg L <sup>-1</sup> (Bq L <sup>-1</sup> ) <sup>a</sup>
42	SFMS	Plasma Trace 2	Environmental samples	Sr resin and TEVA resin	3 (6.5 × 10 <sup>-5</sup> Bq L <sup>-1</sup> )
283	QMS	Perkin Elmer Elan 5000	Natural groundwater	Capillary electrophoresis	50 000 000 (1.2 × 10 <sup>-2</sup> )
300	QMS	PlasmaQuad2+	Environmental samples		<sup>239/240</sup> Pu: 10 (2.3 × 10 <sup>-2</sup> /8.4 × 10 <sup>-2</sup> )
289	QMS	PQ Excel-s	Soil		4.3 (9.9 × 10 <sup>-3</sup> )
301	QMS	Varian 810 MS	Environmental samples	Flow injection (UTEVA resin)	3 (6.9 × 10 <sup>-3</sup> )
302	QMS	Perkin Elmer Elan 6000	Environmental samples	Flow injection (TEVA resin)	
260	QMS	Agilent 7500	Urine	TEVA resin	
275	QMS	Agilent 7500	Large soil samples	Ca phosphate precipitation, stacked	
63	QMS	X-series II	Environmental samples, sequential injection	TEVA, TRU, DGA resins	700 (1.6)
279	QMS	X-series II	Soil, sediment, seaweed, sequential injection	Hydroxide precipitation, sequential injection (TEVA resin)	
250	QMS	X-series II	River water	Iron hydroxide precipitation, SI-based AG1	1.5 (3.5 × 10 <sup>-3</sup> )
97	QMS	Elan 5000	Uranium oxide leachate	Stacked TEVA and DGA resin	<sup>239/240/242</sup> Pu: 0.3 (6.2 × 10 <sup>-4</sup> , 2.3 × 10 <sup>-3</sup> , 4.0 × 10 <sup>-5</sup> )
283	QMS	Perkin Elmer Elan 5000	Natural groundwater		30 000 (6.8)
282	CC-QMS	GV Isoprobe	U-235 target		
268	SFMS	Finnigan MAT Element	Environmental samples	Anion exchange	50 000 000 (1.2 × 10 <sup>6</sup> )
49	SFMS	Element	Soil samples 4–20 km north and west of Chernobyl	Capillary electrophoresis	
291	SFMS	Element 2	Urine		
270	SFMS	Micromass PlasmaTrace 2	Environmental samples	Automated sequential injection (TEVA resin)	2.1 (4.8 × 10 <sup>-3</sup> )
300	SFMS	Axiom SC	Environmental samples		<sup>239/240</sup> Pu: 0.42 (9.7 × 10 <sup>-4</sup> )
303	SFMS	Thermo Element	Urine		SFMS: <sup>239/240</sup> Pu: 0.1 (2.3 × 10 <sup>-4</sup> /8.4 × 10 <sup>-4</sup> )
57	SFMS	Element 2			<sup>241</sup> Pu: 0.05 (0.2)
304	SFMS	Micromass PlasmaTrace 2			1.0 × 10 <sup>-3</sup> (2.3 × 10 <sup>-6</sup> )
284	SFMS	Element 2	Soils and sediments from river Yenisei	Ca phosphate precipitation and TEVA resin	9.2 (2.1 × 10 <sup>-2</sup> ) to 15 (3.5 × 10 <sup>-2</sup> )
					<sup>240/241/242</sup> Pu: 3–4 (2.5 × 10 <sup>-2</sup> to 3.4 × 10 <sup>-2</sup> /11.4–15.2/4.4 × 10 <sup>-4</sup> to 5.9 × 10 <sup>-4</sup> )
					<sup>239/240</sup> Pu: 8–9 (1.8 × 10 <sup>-2</sup> to 2.1 × 10 <sup>-2</sup> /6.7 × 10 <sup>-2</sup> to 7.6 × 10 <sup>-2</sup> )

<sup>a</sup> LOD for <sup>239</sup>Pu unless indicated otherwise.

chemical separation, old alpha planchettes were wet-ashed and purified by extraction chromatography prior to measurement.

Both airborne Pu and U originating from the Fukushima Daiichi NPP were identified in the atmosphere 120 km from the site through measurement of aerosol samples, with a sampling time of approximately one week.<sup>298</sup> Following ashing and chemical separation, samples were analyzed by a combination of AMS and ICP-SFMS. Whilst the amount of environmental U and Pu increased, the dose from airborne Pu was negligible. ICP-SFMS was used for analysis of  $^{234}\text{U}/^{238}\text{U}$  and  $^{235}\text{U}/^{238}\text{U}$ , however AMS was advantageous for Pu measurement due to excellent suppression of hydride interferences. No Pu spike was added because of the low levels being investigated, and the potential negative impact on detection limit that adding a spike could have. Zheng *et al.* presented the first data on distribution of Pu isotopes in surface sediments 30 km off Fukushima.<sup>287</sup> The  $^{240}\text{Pu}/^{239}\text{Pu}$  ratios were measured using ICP-SFMS with Apex (Elemental Scientific) sample introduction. Chemical separation was performed using anion exchange chromatography, and several reference materials were used for method validation. Isotope ratio results were compared to background data in Japanese estuaries and the western North Pacific, and it was found that no Pu contamination was detected outside the 30 km zone around the plant. A more comprehensive assessment of Pu isotope measurements in seawater and sediments within the 30 km zone was recommended, to improve understanding of marine environmental behavior.

Detection limits in the attogram range in sediment and seaweed reference materials was achieved using ICP-SFMS (Element XR) equipped with the Jet interface,<sup>56</sup> comparable to sensitivities achievable by AMS. Despite the larger orifice of the Jet sample cone, the Jet interface did not increase the hydride formation rate when operating with a desolvating sample introduction system. Without the Jet interface, the precision of  $^{240}\text{Pu}/^{239}\text{Pu}$  was 20.5% and accuracy  $-3.3\%$ , compared to 5.0% and 0.83% when equipped with the Jet interface and Cetac Aridus II desolvating sample introduction system. Plutonium has also been determined in urine samples by multiple techniques-alpha spectrometry, ICP-SFMS (Thermo Element XR) and AMS.<sup>299</sup> The minimum detectable activity for SF-ICP-MS (23 fg) was two times better than alpha spectrometry (50 fg), but inferior to AMS (0.44 fg).

## 8.20 Americium-241

Americium-241 is produced as an activation product, and from beta decay of  $^{241}\text{Pu}$ , with a half-life of 432.2 years. Americium-241 is an alpha emitter (5.44 MeV, 12.8% yield and 5.49 MeV, 85.2% yield), and gamma emitter (59.5 keV, 36% abundance), with gamma spectrometry considered inadequate for low-level  $^{241}\text{Am}$  determination.<sup>62</sup> Alpha spectrometry is the most sensitive and frequently used approach, and measurement is generally combined with chemical yield tracer  $^{243}\text{Am}$  ( $t_{1/2} = 7.4 \times 10^3$  years), which decays by alpha emission (5.28 MeV, 87.4% yield and 5.23 MeV, 11% yield), and gamma emission (74.7 keV, 62.8% abundance). A comprehensive review of analytical

methods for americium determination is published elsewhere.<sup>62,305</sup>

Measurement of  $^{241}\text{Am}$  is affected by an isobaric interference from  $^{241}\text{Pu}$ , and from  $^{240}\text{PuH}^+$ , with Pu typically present at comparable or higher concentrations than that of  $^{241}\text{Am}$  in materials of reactor origin. There are also multiple polyatomic interferences, and  $^{243}\text{Am}$  (half-life 3730 years) has been applied as an internal standard,<sup>57,306</sup> with  $^{242}\text{Pu}$  used to assess  $^{241}\text{Pu}$  contamination.<sup>98</sup> Alternatively, a mixed elemental standard can be used for external calibration of the instrument.<sup>116</sup> Chemical separation techniques prior to sample introduction include precipitation/co-precipitation and/or liquid-liquid extraction, ion exchange chromatography and extraction chromatography.<sup>57,306</sup> Providing these interferences can be effectively removed, ICP-SFMS can match the detection limits of alpha spectrometry.<sup>62</sup>

Krachler *et al.* (2014) noted the absence of matrix-matched reference materials, leading to determination of Am in spent nuclear fuels using both high resolution ICP-OES and ICP-SFMS (Thermo Element 2) installed in a glovebox.<sup>116</sup> The absence of a certified reference material meant instrumental mass bias was estimated based on the difference in sensitivity between  $^{232}\text{Th}$  and  $^{238}\text{U}$  in the internal standard, and assuming the same instrument sensitivity for all actinides. The mean concentration differed by a maximum of 4% between ICP-OES and ICP-MS.

Isotope-dilution ICP-SFMS has been used for the determination of  $\text{pg kg}^{-1}$  concentrations of  $^{241}\text{Am}$  in sediments (Agarande *et al.*, 2001).<sup>307</sup> Measurements of  $^{241}\text{Am}$  relative to a  $^{243}\text{Am}$  spike were performed using a VG Elemental Axiom ICP-MS with single collector and MCN6000 desolvating microconcentric nebulizer. Plutonium-242 was also added to confirm effective separation of Pu and Am prior to measurement. Measurements were performed in low resolution mode and mass bias was corrected using the U isotopic standard IRMM-72/1. Limits of detection of  $0.2 \text{ Bq kg}^{-1}$  ( $1.6 \text{ pg kg}^{-1}$ ) were reported. Americium was analyzed along with Pu in Chernobyl-contaminated samples by ICP-SFMS (Thermo Element 2) in comparison to alpha spectrometry.<sup>62</sup> Good agreement was observed between the two techniques for Certified Reference Materials (IAEA-384 and IAEA-385). The measurement time for ICP-SFMS was several minutes, compared to count times of days by alpha spectrometry. ICP-SFMS achieved a detection limit of  $13.2 \mu\text{Bq g}^{-1}$  ( $0.1 \text{ fg g}^{-1}$ ) for ICP-SFMS, with a precision of 0.8–3%, compared to  $4 \mu\text{Bq g}^{-1}$  ( $0.03 \text{ fg g}^{-1}$ ) and a precision of 1–5% by alpha spectrometry. Mass discrimination was again determined by applying a linear correction using a natural uranium solution. The combined measurement of Pu and Am allowed calculation of date of contamination based on the  $^{241}\text{Pu}/^{241}\text{Am}$  ratio, assuming release of radionuclides was over a short time rather than continuous, as  $^{241}\text{Am}$  is also produced by decay of  $^{241}\text{Pu}$ . In a separate study, Varga measured  $^{241}\text{Am}$  in two environmental reference materials (sediment and seaweed) by ICP-SFMS (Thermo Element),<sup>98</sup> with alpha spectrometry used to validate the procedure. The removal of polyatomic interferences was tested using stable element standards of Bi, Pb, Hg and Tl, whilst isobaric  $^{241}\text{Pu}$  removal was monitored using a  $^{242}\text{Pu}$  isotopic tracer. A detection limit of  $0.86 \text{ fg g}^{-1}$  ( $0.11 \text{ mBq g}^{-1}$ )



was achieved, which was comparable to that of alpha spectrometry 0.79 fg (0.10 mBq).

A method for  $^{241}\text{Am}$  determination in urine was developed and validated at the Centre for Disease Control and Prevention (CDC).<sup>306</sup> Measurements were performed using ICP-SFMS (Thermo Element XR) equipped with a CETAC Aridus desolvating sample introduction system, with a detection limit of 0.22 pg L<sup>-1</sup> (0.028 Bq L<sup>-1</sup>). These values were in good agreement with liquid scintillation counting (LSC), and NIST CRM target values. The analytical bias from -0.3 to 1.7% for observed values compared to target values, and 2.1–3% for samples run in an internal comparison with LSC. The previous procedure using LSC returned a detection limit of 32.3 pg L<sup>-1</sup> (4.2 Bq L<sup>-1</sup>), higher than the CDC action level of 0.73 pg L<sup>-1</sup> (0.09 Bq L<sup>-1</sup>). It was noted that if U concentrations exceeded 10  $\mu\text{g L}^{-1}$ , more aggressive rinsing was required to eliminate U from solution, with analytical bias increasing to between -0.62 and -5.61% compared to NIST target values.

On-line extraction chromatographic separation of actinides, including  $^{241}\text{Am}$ , from urine matrices coupled with ICP-QMS has also been evaluated (Hang *et al.*, 2004).<sup>308</sup> Detection limits of 0.15 pg mL<sup>-1</sup> (0.02 Bq mL<sup>-1</sup>) were reported for a 25 mL urine sample volume. Coupling of flow injection analysis with ICP-SFMS has also been reported for the analysis of environmental samples, with detection limits down to 0.6 fg being reported.<sup>268</sup>

Wang *et al.* recently developed a method for  $^{241}\text{Am}$  measurement in large (2–20 g) soil samples using ICP-SFMS (Thermo Element XR) equipped with a high efficiency nebulizer (HEN).<sup>309</sup> Multiple chemical separation techniques were investigated for separation of Am from soil matrix components, rare earth elements, and ICP-MS interferences (Bi, Tl, Hg, Pb, Hf and Pt). A good chemical recovery of Am (76–82%) and detection limit of 0.012 mBq g<sup>-1</sup> was achieved, whilst decontamination factors of  $7 \times 10^5$  for Pu was the highest reported for  $^{241}\text{Am}$  studies, enabling measurement in Fukushima sourced soils contaminated with  $^{241}\text{Pu}$ .

## 8.21 Curium/californium

Curium isotopes are produced *via* successive neutron capture by Am and subsequent beta decay. The main Cm isotopes produced in nuclear reactors are  $^{242}\text{Cm}$  ( $t_{1/2} = 162.9$  days),  $^{243}\text{Cm}$  ( $t_{1/2} = 28.9$  years),  $^{244}\text{Cm}$  ( $t_{1/2} = 18.2$  years),  $^{245}\text{Cm}$  ( $t_{1/2} = 8480$  years),  $^{246}\text{Cm}$  ( $t_{1/2} = 4760$  years) and  $^{248}\text{Cm}$  ( $t_{1/2} = 3.48 \times 10^5$  years). For Cf, the main isotopes are  $^{249}\text{Cf}$  ( $t_{1/2} = 351$  years),  $^{250}\text{Cf}$  ( $t_{1/2} = 13.1$  years),  $^{251}\text{Cf}$  ( $t_{1/2} = 898$  years) and  $^{252}\text{Cf}$  ( $t_{1/2} = 2.6$  years). To date, there are no reported applications of ICP-MS for Cm or Cf measurement in nuclear wastes. Kurosaki *et al.* (2014) reported the measurement of  $^{243}\text{Cm}$ ,  $^{244}\text{Cm}$ ,  $^{245}\text{Cm}$ ,  $^{246}\text{Cm}$  and  $^{240}\text{Pu}$  using a Thermo Finigan Element 2 for nuclear forensics applications.<sup>310</sup> Gourgiotis *et al.* (2010) used ICP-QMS (Thermo Electron X-series) for Cm and Cf isotope measurement in transmutation studies.<sup>311</sup> Sample introduction was *via* a quartz Peltier-cooled impact bead spray chamber (natural aspiration) and micro concentric nebulizer. Two peak jump routines were employed to separately measure high abundance ( $^{248}\text{Cm}/^{246}\text{Cm}$ ) and low abundance

( $^{245}\text{Cm}/^{246}\text{Cm}$ ,  $^{247}\text{Cm}/^{246}\text{Cm}$ ,  $^{249}(\text{Bk} + \text{Cf})/^{251}\text{Cf}$ ,  $^{250}\text{Cf}/^{251}\text{Cf}$ , and  $^{252}\text{Cf}/^{251}\text{Cf}$ ) isotope ratios. High precision isotope ratio measurement was achieved using corrected peak centering (3 points per peak with the central point associated with the maximum count rate). Dead time and mass bias corrections (using sample standard bracketing) were also applied. Peak tailing and hydride interferences were corrected by measuring the  $^{237}/^{238}\text{U}$  ratio and  $^{238}\text{UH}/^{238}\text{U}$  ratio for a U010 standard. Abundance sensitivities of  $1.97 \pm 0.02$  ppm and hydride formation of  $(35.7 \pm 0.1) \times 10^{-6}$  were reported. Chromatographic separation of  $^{249}\text{Bk}$  and  $^{249}\text{Cf}$  using Dionex HPLC was developed to permit separate determination of  $^{249}\text{Bk}/^{248}\text{Cm}$  and  $^{249}\text{Cf}/^{248}\text{Cm}$  ratios.<sup>312</sup>

## 9 Conclusions

Advances in the capability and sensitivity of recent ICP-MS instruments have stimulated new interest from the nuclear sector. This stems from the potential of these instruments to routinely and swiftly measure a range of key radionuclides considered important in nuclear decommissioning programmes. ICP-MS has proven itself as a versatile technique with regards to sample introduction and instrument setup, both of which can be used to improve sensitivity and/or interference removal. For the majority of radionuclides suitable for ICP-MS measurement, interference removal is the critical aspect affecting optimised detection limits. Effective measurement must be combined with robust, effective sample digestion and chemical separation (either through wet chemistry techniques, sample introduction and/or using an instrument with collision/reaction cell capabilities).

For long-lived radionuclides, ICP-MS offers significant benefits in sample throughput compared to the traditional radiometric methods (alpha and beta counting techniques). These benefits arise from reduced measurement time per sample, and reduced preparation time with the use of on-line separation and collision/reaction cell instruments and provide significant potential economic benefits to nuclear sites. The improvements in ICP-MS means that a number of long-lived radionuclides are now measurable that are very challenging or even not measurable by radiometric techniques *e.g.*  $^{93}\text{Zr}$ ,  $^{107}\text{Pd}$ ,  $^{135}\text{Cs}$ ,  $^{41}\text{Ca}$  and  $^{59}\text{Ni}$ . These radionuclides are of increasing interest to regulatory agencies concerned with long-term nuclear waste storage and disposal. Additionally, ICP-MS (particularly multi-collector instruments) offers the ability to accurately measure isotopic ratios *e.g.*  $^{239}\text{Pu}/^{240}\text{Pu}$  and  $^{236}\text{U}/^{238}\text{U}$ , enabling the determination of the source of contamination, rather than the activity concentration alone.

## Acknowledgements

The authors warmly thank Bob Nesbitt, Rex Taylor and Andy Milton for ICP-MS collaborations over the years. Ben Russell thanks the NDA for partial support *via* an NDA Bursary (awarded to Profs Croudace and Warwick), and funding through the National Measurement System by the Department of Business, Energy and Industrial Strategy.



## References

1 B. C. Russell, I. W. Croudace, P. E. Warwick and J. A. Milton, *Anal. Chem.*, 2014, **86**, 8719–8726.

2 W. Wien, *Ann. Phys.*, 1898, **65**, 440.

3 J. J. Thomson, *Philos. Mag.*, 1897, **44**, 29.

4 A. J. Dempster, *Phys. Rev.*, 1918, **11**, 316.

5 F. W. Aston, *Philos. Mag.*, 1919, **38**, 709.

6 F. W. Aston, *Philos. Mag.*, 1920, **39**, 449.

7 F. W. Aston, *Proc. R. Soc. A*, 1927, **115**, 487.

8 W. Bartky and A. J. Dempster, *Phys. Rev.*, 1929, **33**, 1019.

9 J. Mattauch and R. Hertzog, *Z. Phys.*, 1934, **89**, 786.

10 K. T. Bainbridge and E. B. Jordan, *Phys. Rev.*, 1936, **50**, 282.

11 A. O. Nier, *Rev. Sci. Instrum.*, 1940, **11**, 212.

12 A. O. Nier, *Rev. Sci. Instrum.*, 1947, **18**, 39.

13 J. A. Hippel, *J. Appl. Phys.*, 1942, **13**, 551.

14 H. Ewald and H. Hintenberger, *Methoden und Anwendungen der Massenspektroskopie*, Verlag Chemie GmbH, Weinheim, Germany, 1953.

15 S. Penner, *Rev. Sci. Instrum.*, 1961, **32**, 150.

16 H. Ewald, E. Konecny, H. Opower and H. Rösler, *Z. Naturforsch., C: Biochem., Biophys., Biol., Virol.*, 1964, **19**, 194.

17 S. Fukumoto, T. Matsuo and H. Matsuda, *J. Phys. Soc. Jpn.*, 1968, **25**, 946.

18 J. Frantzen, *Jahrbuch der Witheit zu Bremen 2006/2007*, Hauschild Verlag, Bremen, Germany, 2008, vol. 181, ISBN 978-3-89757-529-5.

19 *A History of European Mass Spectrometry*, ed. K. R. Jennings, IM Publications LLP, Chichester, UK, 2012, ISBN 978-1-906715-04-5, pp. 285.

20 K. S. Sharma, *Int. J. Mass Spectrom.*, 2013, **349–350**, 3–8.

21 G. P. Russ and J. M. Bazan, *Spectrochim. Acta, Part B*, 1987, **42**, 49–62.

22 D. W. Boomer and M. J. Powell, *Anal. Chem.*, 1987, **59**, 2810–2813.

23 R. M. Brown, S. E. Long and C. J. Pickford, *Sci. Total Environ.*, 1988, **70**, 265–274.

24 G. L. Beck and O. T. Farmer, *J. Anal. At. Spectrom.*, 1988, **3**, 771–773.

25 C. K. Kim, A. Takaku, M. Yamamoto, H. Kawamura, K. Shiraishi, Y. Igarashi, S. Igarashi, H. Takayama and N. Ikeda, *J. Radioanal. Nucl. Chem.*, 1989, **132**(1), 131–137.

26 A. S. Hursthouse, M. S. Baxter, K. McKay and F. R. Livens, *J. Radioanal. Nucl. Chem.*, 1992, **157**(2), 281–294.

27 C. K. Kim, R. Seki and S. Morita, *J. Anal. At. Spectrom.*, 1991, **6**, 205–209.

28 J. S. Crain and B. L. Mikesell, *Appl. Spectrosc.*, 1992, **46**(10), 1498–1502.

29 C. Riglet, O. Provitina, J. L. Dautheribes and D. Revy, *J. Anal. At. Spectrom.*, 1992, **7**, 923–927.

30 M. R. Smith, E. J. Wyse and D. W. Koppenaal, *J. Radioanal. Nucl. Chem.*, 1992, **160**(2), 341–354.

31 R. J. Rosenberg, *J. Radioanal. Nucl. Chem.*, 1993, **171**(2), 465–482.

32 J. S. Crain, J. S. Yaeger, F. P. Smith, J. A. Alvarado, L. L. Smith, J. T. Kiely and D. G. Graczyk, *Argonne National Laboratory 4<sup>th</sup> CIRMS Meeting*, NIST, Gaithersberg, 28–30 Nov 1995.

33 J. S. Crain and J. Alvarado, *J. Anal. At. Spectrom.*, 1994, **9**, 1223–1227.

34 E. J. Wyse and D. R. Fisher, *Radiat. Prot. Dosim.*, 1994, **55**(3), 199–206.

35 J. S. Crain, L. L. Smith, J. S. Yaeger and J. A. Alvarado, *J. Radioanal. Nucl. Chem.*, 1995, **194**(1), 133–139.

36 Y. Igarashi, C. K. Kim, Y. Takaku, K. Shiraishi, M. Yamamoto and N. Ikeda, *Anal. Sci.*, 1990, **6**, 157–164.

37 S. Collins, S. Pommé, S. M. Jerome and A. K. Pearce, *Appl. Radiat. Isot.*, 2015, **104**, 203–211.

38 S. M. Collins, A. K. Pearce, K. Ferreira, A. Fenwick, P. H. Regan and J. Keightley, *Appl. Radiat. Isot.*, 2015, **99**, 46–53.

39 NPL Radioactivity Group, <http://www.npl.co.uk/science-technology/radioactivity/products-and-services/primary-and-secondary-standards>, accessed 17/08/16.

40 NIST Radionuclide Half-Life measurements, <http://www.nist.gov/pml/data/halflife.cfm>, accessed 17/08/16.

41 J. S. Becker and H. J. Dietz, *Fresenius' J. Anal. Chem.*, 1999, **364**, 482–488.

42 C. S. Kim, C. U. Kim, J. I. Lee and K. J. Lee, *J. Anal. At. Spectrom.*, 2000, **15**, 247–255.

43 S. F. Boulyga and J. S. Becker, *Fresenius' J. Anal. Chem.*, 2001, **370**, 612–617.

44 K. K. Falkner, G. P. Klinkhammer, C. Ungerer and D. M. Christie, *Annu. Rev. Earth Planet. Sci.*, 1995, **23**, 409–449.

45 C. M. Barshick, D. C. Duckworth and D. H. Smith, *Inorganic Mass Spectrometry Fundamentals and Applications*, Oak Ridge National Laboratory, Marcel Dekker Inc., Oak Ridge, Tennessee, 2000.

46 R. Thomas, A Beginner's Guide to ICP-MS, Part II: The Sample Introduction System, *Spectroscopy*, 2001, **16**(5), 56–60.

47 W. Kerl, J. S. Becker, H.-J. Dietze and W. Dannecker, *Fresenius' J. Anal. Chem.*, 1997, **359**, 407–409.

48 J. S. Becker and H. J. Dietz, *J. Anal. At. Spectrom.*, 1999, **14**, 1493–1500.

49 S. F. Boulyga and J. S. Becker, *J. Anal. At. Spectrom.*, 2002, **17**, 1143–1147.

50 N. Jakubowski, L. Moens and F. Vanhaecke, *Spectrochim. Acta, Part B*, 1998, **53**(12), 1739–1763.

51 R. N. Taylor, T. Warneke, J. A. Milton, I. W. Croudace, P. E. Warwick and R. W. Nesbitt, *J. Anal. At. Spectrom.*, 2003, **18**, 480–484.

52 J. A. McLean, J. S. Becker, S. F. Boulyga, H. J. Dietze and A. Montaser, *Int. J. Mass Spectrom.*, 2001, **208**, 193.

53 S. F. Boulyga, C. Testa, D. Desideri and J. S. Becker, *J. Anal. At. Spectrom.*, 2001, **16**, 1283–1289.

54 D. Larivière, V. F. Taylor, R. D. Evans and R. J. Cornett, *Spectrochim. Acta, Part B*, 2006, **61**(8), 877–904.

55 M. G. Minnich and R. S. Houk, *J. Anal. At. Spectrom.*, 1998, **13**, 167–174.

56 J. Zheng, *J. Nucl. Radiochem. Sci.*, 2015, **15**(1), 7–13.



57 Z. Varga, G. Surányi, N. Vajda and Z. Štefánka, *Microchem. J.*, 2006, **85**, 39–45.

58 J. S. Becker, *Spectrochim. Acta, Part B*, 2003, **58**, 1757–1784.

59 M. Hollenbach, J. Grohs, S. Mamich and M. Kroft, *J. Anal. At. Spectrom.*, 1994, **9**, 927–933.

60 J. H. Aldstadt, J. M. Kuo, L. L. Smith and M. D. Erickson, *Anal. Chim. Acta*, 1996, **319**, 135–143.

61 E. H. Hansen and M. Miró, *Trends Anal. Chem.*, 2007, **26**(1), 18–26.

62 N. Vajda and C.-K. Kim, *J. Radioanal. Chem.*, 2010, **284**, 341–366.

63 J. Qiao, X. Hou, P. Roos and M. Miró, *J. Anal. At. Spectrom.*, 2010, **25**, 1769–1779.

64 J. Ruzicka, *Analyst*, 2000, **125**, 1053–1060.

65 S. F. Boulyga, D. Desideri, M. A. Meli, C. Testa and J. S. Becker, *Int. J. Mass Spectrom.*, 2003, **226**, 329–339.

66 M. D. Seltzer, *Appl. Spectrosc.*, 2003, **57**(9), 1173–1177.

67 J. S. Becker, *Int. J. Mass Spectrom.*, 2005, **242**, 183–195.

68 L.-S. Chen, T. Wang, Y.-K. Hsieh, C.-H. Hsu, J. C.-T. Lin and C.-F. Wang, *J. Membr. Sci.*, 2014, **456**, 202–208.

69 S. Bürger and L. R. Riciputi, *J. Environ. Radioact.*, 2009, **100**(11), 970–976.

70 Z. Varga, *Anal. Chim. Acta*, 2008, **625**, 1–7.

71 F. Pointurier, A. Hubert and A. C. Pottin, *J. Radioanal. Nucl. Chem.*, 2013, **296**, 609–616.

72 J. V. Cizdziel, M. E. Ketterer, D. Farmer, S. H. Faller and V. F. Hodge, *Anal. Bioanal. Chem.*, 2008, **390**, 521–530.

73 J. S. Becker and H. J. Dietz, *Fresenius' J. Anal. Chem.*, 2000, **368**, 23–30.

74 J. S. Becker, C. Pickhardt and H.-J. Dietze, *Int. J. Mass Spectrom.*, 2000, **202**, 283–297.

75 Viridiscan, <http://www.viridian-tc.co.uk/viridiscan.html>, accessed 17/08/16.

76 R. C. Marin, J. E. S. Sarkis and M. R. L. Nascimento, *J. Radioanal. Nucl. Chem.*, 2013, **295**, 99–104.

77 P. Grinberg, S. Willie and R. E. Sturgeon, *J. Anal. At. Spectrom.*, 2007, **22**(11), 1409–1414.

78 J. S. Santos, L. S. G. Teixeira, W. N. L. dos Santos, V. A. Lemos, J. M. Godoy and S. L. C. Ferreira, *Anal. Chim. Acta*, 2010, **674**, 143–156.

79 M. Song, T. U. Probst and N. G. Berryman, *Fresenius' J. Anal. Chem.*, 2001, **370**(6), 744–751.

80 J. B. Truscott, L. Bromley, P. Jones, E. Hywel Evans, J. Turner and B. Fairman, *J. Anal. At. Spectrom.*, 1999, **14**, 627–631.

81 P. Grinberg, S. Willie and R. E. Sturgeon, *J. Anal. At. Spectrom.*, 2005, **20**, 717–723.

82 L. A. De las Heras, E. Hrnecek, O. Bildstein and M. Betti, *J. Anal. At. Spectrom.*, 2002, **17**, 1011–1014.

83 M. Betti and L. A. de las Heras, *Spectrochim. Acta, Part B*, 2004, **59**(9), 1359–1376.

84 S. F. Wolf, D. L. Bowers and J. C. Cunnane, *J. Radioanal. Nucl. Chem.*, 2005, **263**(3), 581–586.

85 I. Günther-Leopold, N. Kivel, J. K. Waldes and B. Wernli, *Anal. Bioanal. Chem.*, 2008, **309**, 503–510.

86 A. P. Vonderheide, M. V. Zoriy, A. V. Izmer, C. Pickhardt, J. A. Caruso, P. Ostapczuk, R. Hille and J. S. Becker, *J. Anal. At. Spectrom.*, 2004, **19**(5), 675–680.

87 M. V. Zoriy, P. Ostapczuk, L. Halicz, R. Hille and J. S. Becker, *Int. J. Mass Spectrom.*, 2005, **242**(2–3), 203–209.

88 A. R. Timerbaev and R. M. Timerbeav, *Trends Anal. Chem.*, 2013, **51**, 44–50.

89 C. Möser, R. Kautenburger and H. P. Beck, *Electrophoresis*, 2012, **33**(9–10), 1482–1487.

90 C. Bresson, E. Ansoborlo and C. Vidaud, *J. Anal. At. Spectrom.*, 2011, **26**, 593–601.

91 Perkin Elmer, Elan II DRC brochure, <http://www.esc.cam.ac.uk/esc/files/Department/facilities/icp-ms/drcii-b.pdf>, accessed 18/05/2016.

92 D. R. Bandura, V. I. Baranov, A. E. Litherland and S. D. Tanner, *Int. J. Mass Spectrom.*, 2006, **235**–**236**, 312–327.

93 U. Nygren, I. Rodushkin, C. Nilsson and D. C. Baxter, *J. Anal. At. Spectrom.*, 2003, **18**(12), 1426–1434.

94 M. Moldovan, E. M. Krupp, A. E. Holliday and O. F. X. Donard, *J. Anal. At. Spectrom.*, 2004, **1**(9), 815–822.

95 M. E. Ketterer and S. C. Szechenyi, *Spectrochim. Acta, Part B*, 2008, **63**, 719–737.

96 M. Hamester, D. Wiederin, J. Wills, W. Kerl and C. B. Douthitt, *Fresenius' J. Anal. Chem.*, 1999, **364**(5), 495–498.

97 D. Solatie, P. Carbol, M. Betti, F. Bocci, T. Hiernaut, V. V. Rondinella and J. Cobos, *Fresenius' J. Anal. Chem.*, 2000, **368**, 88–94.

98 Z. Varga, *Anal. Chim. Acta*, 2007, **587**, 165–169.

99 M. E. Wieser and J. B. Schwieters, *Int. J. Mass Spectrom.*, 2005, **242**(2–3), 97–115.

100 Spectro, <http://www.spectro.com/products/icp-ms-spectrometers>, Overview of ICP-MS spectrometers, accessed 18/05/2016.

101 N. L. Sanders, S. Kothari, G. Huang, G. Salazar and R. G. Cooks, *Anal. Chem.*, 2010, **82**, 5313–5316.

102 J. K. Dalglish, K. Hou, Z. Ouyang and R. G. Cooks, *Anal. Lett.*, 2012, **45**, 1440–1446.

103 J. M. Wells, M. J. Roth, A. D. Keil, J. W. Grossenbacher, D. R. Justes, G. E. Patterson and D. J. Barket Jr, *J. Am. Soc. Mass Spectrom.*, 2008, **19**(10), 1419–1424.

104 A. Malcolm, S. Wright, R. R. A. Syms, N. Dash, M.-A. Schwab and A. Finlay, *Anal. Chem.*, 2010, **82**, 1751–1758.

105 P. I. Hendricks, J. K. Dalglish, J. T. Shelley, M. A. Kirleis, M. T. McNicholas, L. Li, T.-C. Chen, C.-H. Chen, J. S. Duncan, F. Boudreau, R. J. Noll, J. P. Denton, T. A. Roach, Z. Ouyang and R. G. Cooks, *Anal. Chem.*, 2014, **86**, 2900–2908.

106 S. Kumano, M. Sugiyama, M. Yamada, K. Nishimura, H. Hasegawa, H. Morokuma, H. Inoue§ and Y. Hashimoto, *Anal. Chem.*, 2013, **85**(10), 5033–5039.

107 J. M. Giaquinto, J. M. Keller and A. M. Meeks, *J. Radioanal. Nucl. Chem.*, 1998, **234**(1–2), 137–141.

108 F. Pilon, S. Lorthioir, J. Biroilleau and S. Lafontan, *J. Anal. At. Spectrom.*, 1996, **11**(9), 759–764.

109 J. I. G. Alonso, D. Thoby-Schultzendorff, B. Giovanonne, L. Koch and H. Wiesmann, *J. Anal. At. Spectrom.*, 1993, **8**, 673–679.

110 J. D. Burraston, PhD thesis, *GAU-Radioanalytical, Ocean and Earth Science*, University of Southampton, National Oceanography Centre, 2014.



111 R. Forsyth and U.-B. Eklund, *Spent nuclear fuel corrosion: SKB Technical Report 95-04*, Swedish Nuclear Fuel and Waste Management Company, 1995.

112 M. Betti, G. Rasmussen, T. Hiernaut and L. Koch, *J. Anal. At. Spectrom.*, 1994, **9**, 385–391.

113 M. R. Smith, O. T. Farmer III, J. H. Reeves and D. W. Koppenaal, *J. Radioanal. Nucl. Chem.*, 1995, **194**(1), 7–13.

114 J. M. Barrero Moreno, M. Betti and J. I. Garcia Alonso, *J. Anal. At. Spectrom.*, 1997, **12**, 355–361.

115 O. B. Egorov, M. J. O'Hara, O. T. Farmer III and J. W. Grate, *Analyst*, 2000, **126**, 1594–1601.

116 M. Krachler, R. Alvarez-Sarandes and S. V. Winckel, *J. Anal. At. Spectrom.*, 2014, **29**, 817–824.

117 I. W. Croudace, P. E. Warwick, R. Taylor and S. Dee, *Anal. Chim. Acta*, 1998, **371**, 217–225.

118 C. S. Kim, C.-K. Kim, P. Martin and U. Sansone, *J. Anal. At. Spectrom.*, 2007, **22**, 827–841.

119 I. W. Croudace, P. E. Warwick, D. G. Reading and B. C. Russell, *Trends Anal. Chem.*, 2016, **85**, 120–129.

120 R. Bock, *A Handbook of Decomposition Methods in Analytical Chemistry*, International Textbook Company Limited, London, 1979.

121 B. Parsa, *J. Radioanal. Nucl. Chem.*, 1992, **157**, 65–73.

122 U.S. Environmental Protection Agency, *Rapid Method for Sodium Hydroxide/Sodium Peroxide Fusion of Radioisotope Thermoelectric Generator Materials in Water and Air Filter Matrices Prior to Plutonium Analyses for Environmental Remediation Following Radiological Incidents*, 2014, EPA/600/F-14/284.

123 S. Fisher and R. Kunin, *Anal. Chem.*, 1957, **29**, 400–402.

124 C. Galindo, L. Mougin and A. Nourreddine, *Appl. Radiat. Isot.*, 2007, **65**, 9–16.

125 C. W. Sill, K. W. Puphal and F. D. Hindman, *Anal. Chem.*, 1974, **46**, 1725–1737.

126 J. S. Fedorowich, J. P. Richards, J. C. Cain, R. Kerrich and J. Fan, *Chem. Geol.*, 1993, **106**, 229–249.

127 M. Dong, D. Oropeza, J. Chirinos, J. J. González, J. Lu, X. Mao and R. E. Russo, *Spectrochim. Acta, Part B*, 2015, **109**, 44–50.

128 K. Subedi, T. Trjos and J. Almirall, *Spectrochim. Acta, Part B*, 2015, **103–104**, 76–83.

129 Y. Lee, S.-H. Nam, K.-S. Ham, J. Gonzalez, D. Oropeza, D. Quarles Jr, J. Yoo and R. E. Rosso, *Spectrochim. Acta, Part B*, 2016, **118**, 102–111.

130 L. Ashton, P. Warwick and D. Giddings, *Analyst*, 1999, **124**, 627–632.

131 M. Baxter, L. Castle, H. M. Crews, M. Rose, C. Garner, G. Lappin and D. Leong, *Food Addit. Contam., Part A*, 2009, **26**, 139–144.

132 X. Hou, L. F. Østergaard and S. P. Nielsen, *Anal. Chem.*, 2007, **79**, 3126–3134.

133 A. Zulaf, S. Happel, P. Warwick, B. M. Mokili, A. Bombard and H. Junglas, [http://www.triskem-international.com/fr/iso\\_album/poster\\_rrmc\\_2011\\_cl\\_resin.pdf](http://www.triskem-international.com/fr/iso_album/poster_rrmc_2011_cl_resin.pdf), accessed 17/08/16.

134 M. Martschini, P. Andersson, O. Fortsner, R. Golser, D. Hanstorp, A. O. Lindahl, W. Kutschera, S. Pavetich, A. Priller, J. Rohlén, P. Steier, M. Suter and A. Wallner, *Nucl. Instrum. Methods Phys. Res., Sect. B*, 2013, **294**, 115–120.

135 P. W. Kubik, D. Elmore, N. J. Conard, K. Nishiizumi and J. R. Arnold, *Nature*, 1986, **319**, 568–570.

136 P. Müller, B. A. Bushaw, K. Blaum, S. Diel, C. Geppert, A. Nähler, N. Trautmann, W. Nörterhäuser and K. Wendt, *Anal. Chem.*, 2001, **370**, 508–512.

137 K. D. A. Wendt, C. Geppert, M. Miyabe, P. Müller, W. Nörterhäuser and N. Trautmann, *J. Nucl. Sci. Technol.*, 2002, **39**(4), 303–307.

138 C. Hennessy, M. Berglund, M. Ostermann, T. Walczyk, H.-A. Synal, C. Geppert, K. Wendt and P. D. P. Taylor, *Nucl. Instrum. Methods Phys. Res., Sect. B*, 2005, **299**, 281–292.

139 D. Hampe, B. Gleisberg, S. Akhmadaliev, G. Rugel and S. Merchel, *J. Radioanal. Nucl. Chem.*, 2013, **296**, 617–624.

140 G. S. Jackson, D. J. Hillegonds, P. Muzikar and B. Goehring, *Nucl. Instrum. Methods Phys. Res., Sect. B*, 2013, **313**, 14–20.

141 S. Merchel, L. Benedetti, D. L. Bourlès, R. Braucher, A. Deqald, T. Faestermann, R. C. Finkel, G. Korschinek, J. Masarik, M. Poutivtsev, P. Rochette, G. Rugel and K.-O. Zell, *Nucl. Instrum. Methods Phys. Res., Sect. B*, 2010, **268**, 1179–1184.

142 X. Hou, *Radiochim. Acta*, 2005, **93**, 611–617.

143 P. E. Warwick, I. W. Croudace and D. J. Hillegonds, *Anal. Chem.*, 2009, **81**, 1901–1906.

144 G. Jörg, Y. Amelin, K. Kossert, C. Lierse and L. V. Gostomski, *Geochim. Cosmochim. Acta*, 2012, **88**, 51–65.

145 E. Nottoli, D. Bourlès, P. Bienvenu, A. Labet, M. Arnold and M. Bertaux, *Appl. Radiat. Isot.*, 2013, **82**, 340–346.

146 X. Hou, L. F. Østergaard and S. P. Nielsen, *Anal. Chim. Acta*, 2005, **535**(1–2), 297–307.

147 E. Holm, P. Roos and B. Skwarzec, *Appl. Radiat. Isot.*, 1992, **43**(1–2), 371–376.

148 I. Gresits and S. Tölgyesi, *J. Radioanal. Nucl. Chem.*, 2003, **258**(1), 107–122.

149 P. E. Warwick and I. W. Croudace, *Anal. Chim. Acta*, 2006, **567**, 277–285.

150 A. A. Marchetti, L. J. Hainsworth, J. E. McAninch, M. R. Leivers, P. R. Jones, I. D. Proctor and T. Straume, *Nucl. Instrum. Methods Phys. Res., Sect. B*, 1997, **123**(1–4), 230–234.

151 P. Persson, M. Kiisk, B. Erlandsson, M. Faarinen, R. Hellborg, G. Skog and K. Stenström, *Nucl. Instrum. Methods Phys. Res., Sect. B*, 2000, **172**(1–4), 188–192.

152 M. E. Mount, D. W. Layton, N. M. Lynn and T. F. Hamilton, *Report UCRL-JC-130412*, Lawrence Livermore National Laboratory, USA, 1998.

153 S. Aguerre and C. Frechou, *Talanta*, 2006, **69**(3), 565–571.

154 J. Compte, P. Bienvenu, E. Brochard, J.-M. Fernandez and G. Andreoletti, *J. Anal. At. Spectrom.*, 2003, **18**, 702–707.

155 P. Bienvenu, P. Cassette, G. Andreoletti, M.-M. Be, J. Compte and M.-C. Lépy, *Appl. Radiat. Isot.*, 2007, **65**(3), 355–364.



156 S. Brun, S. Bessac, D. Uridat and B. Boursier, *J. Radioanal. Nucl. Chem.*, 2002, **253**(2), 191–197.

157 W. Bu, J. Zheng, X. Liu, K. Long, S. Hu and S. Uchida, *Spectrochim. Acta, Part B*, 2016, **119**, 65–75.

158 J. Feuerstein, S. F. Boulyga, P. Galler, G. Steding and T. Prohaska, *J. Environ. Radioact.*, 2008, **99**(11), 1764–1769.

159 V. Taylor, R. D. Evans and R. J. Cornett, *Anal. Bioanal. Chem.*, 2007, **387**(1), 343–350.

160 Y. Takagai, M. Furukawa, Y. Kameo and K. Suzuki, *Anal. Methods*, 2014, **6**(2), 355–362.

161 M. Sakama, Y. Nagano, T. Saze, S. Higaki, T. Kitade, N. Izawa, O. Shikino and S. Nakayama, *Appl. Radiat. Isot.*, 2013, **81**, 201–207.

162 M. A. Amr, A.-F. I. Helal, A. T. Al-Kinani and P. Balakrishnan, *J. Environ. Radioact.*, 2016, **153**, 73–87.

163 E. P. Steinberg and L. E. Glendenin, *Phys. Rev.*, 1950, **78**, 624.

164 J. I. G. Alonso, D. Thoby-Schultzendorff, B. Giovanonne, J.-P. Glatz, G. Pagliosa and L. Koch, *J. Anal. At. Spectrom.*, 1994, **9**, 1209–1215.

165 F. Chartier, H. Isnard, J. P. Degros, A. L. Faure and C. Fréchou, *Int. J. Mass Spectrom.*, 2008, **270**(3), 127–133.

166 S. Dulanská, B. Remenec, V. Gardoňová and L. Máťel, *J. Radioanal. Nucl. Chem.*, 2012, **293**, 635–640.

167 P. Cassette, F. Chartier, H. Isnard, C. Fréchou, I. Laszak, J. P. Degros, M. M. Bé, M. C. Lépy and I. Tartes, *Appl. Radiat. Isot.*, 2010, **68**, 122–130.

168 K. Shi, J. Qiao, W. Wu, P. Roos and X. Hou, *Anal. Chem.*, 2012, **84**, 6783–6789.

169 K. Shi, X. Hou, P. Roos and W. Wu, *Anal. Chim. Acta*, 2012, **709**, 1–20.

170 T. Y. Su, T. L. Tsay, H. C. Wu and L. C. Men, *J. Radioanal. Nucl. Chem.*, 2015, **303**, 1245–1248.

171 K. Shi, X. Hou, P. Roos and W. Wu, *Anal. Chem.*, 2012, **84**, 2009–2016.

172 K. H. Chung, S. D. Choi, G. S. Choi and M. J. Kang, *Appl. Radiat. Isot.*, 2013, **81**, 57–61.

173 L. S. Chen, T. H. Wang, Y. K. Hsieh, L. W. Jian, W. H. Chen, T. L. Tsai and C. F. Wang, *J. Radioanal. Nucl. Chem.*, 2014, **299**, 1883–1889.

174 N. E. Bibler, W. T. Boyce, C. J. Coleman and W. F. Kinard, *Report WSRC-MS-97-0011*, Office of Scientific and Technical Information, Oak Ridge, USA, 1997.

175 C. J. Bannochie, N. E. Bibler and D. P. DiPrete, *WM2009 conference proceedings, March 1–5 2009*, Phoenix, USA, 2009.

176 P. G. Bienvenu, E. A. Brochard and E. A. Excoffier, in *Application of inductively coupled plasma mass spectrometry to radionuclide determinations: second volume*, ed. R.W. Morrow and J.S. Crain, ASTM, West Conshohocken, USA, 1998.

177 V. Hansen, P. Roos, A. Aldahan, X. Hou and G. Possnert, *J. Environ. Radioact.*, 2011, **102**, 1096–1104.

178 V. Hansen, P. Yi, X. Hou, A. Aldahan, P. Roos and G. Possnert, *Sci. Total Environ.*, 2011, **412–413**, 296–303.

179 Ž. Ežerinskis, A. Spolaor, T. Kirchgeorg, G. Cozzi, P. Valletlonga, H. A. Kjaer, J. Šapolaité, C. Barbante and R. Druteikiené, *J. Anal. At. Spectrom.*, 2014, **29**, 1827–1834.

180 C. Vockenhuber, N. Casacuberta, M. Christl and H.-A. Synal, *Nucl. Instrum. Methods Phys. Res., Sect. B*, 2015, **361**, 510–516.

181 E. Englund, A. Aldahan, X. L. Hou, G. Possnert and C. Söderström, *Nucl. Instrum. Methods Phys. Res., Sect. B*, 2010, **268**, 1139–1141.

182 R. Michel, A. Daraoui, M. Gorny, D. Jakob, R. Sachse, L. Tosch, H. Nies, I. Goroncy, J. Herrman, H. A. Synal, M. Stocker and V. Alfimov, *Sci. Total Environ.*, 2012, **419**, 151–169.

183 X. Hou, P. Povinec, L. Zhang, K. Shi, D. Biddulph, C.-C. Chang, Y. Fan, R. Golser, Y. Hou, M. Ješkovský, A. J. Tim Jull, Q. Liu, M. Luo, P. Steier and W. Zu, *Environ. Sci. Technol.*, 2013, **47**(7), 3091–3098.

184 Y. Muramatsu, H. Matsuzaki, C. Toyama and T. Ohno, *J. Environ. Radioact.*, 2015, **139**, 344–350.

185 J. M. Gómez-Guzmán, S. M. Enamorado-Báez, A. R. Pinto-Goméz and J. M. Abril-Hernández, *Int. J. Mass Spectrom.*, 2011, **303**, 103–108.

186 V. Alfimov and H.-A. Synal, *Nucl. Instrum. Methods Phys. Res., Sect. B*, 2010, **268**, 769–772.

187 H. Fujiwara, K. Kawabata, J. Suzuki and O. Shikino, *J. Anal. At. Spectrom.*, 2011, **26**, 2528–2533.

188 J. Lehto, T. Räty, X. Hou, J. Paatero, A. Aldahan, G. Possnert, J. Flinkman and H. Kankaanpää, *Sci. Total Environ.*, 2012, **419**, 60–67.

189 T. Ohno, Y. Muramatsu, Y. Shikamori, C. Toyama, N. Okabe and H. Matsuzaki, *J. Anal. At. Spectrom.*, 2013, **28**, 1283–1287.

190 J. Zheng, H. Takata, K. Tagami, T. Aono, K. Fujita and S. Uchida, *Microchem. J.*, 2012, **100**, 42–47.

191 R. J. Cox, C. J. Pickford and M. Thompson, *J. Anal. At. Spectrom.*, 1992, **7**, 635–640.

192 E. Englund, A. Aldahan, X. L. Hou, R. Petersen and G. Possnert, *Nucl. Instrum. Methods Phys. Res., Sect. B*, 2010, **268**, 1102–1105.

193 X. Hou, W. Zhou, N. Chen, L. Zhang, Q. Liu, M. Luo, Y. Fan, W. Liang and Y. Fu, *Anal. Chem.*, 2010, **82**, 7713–7721.

194 T. Suzuki, S. Otosaka, J. Kubawara, H. Kawamura and T. Kobayashi, *Biogeosciences*, 2013, **10**, 3839–3847.

195 V. Taylor, R. Evans and R. Cornett, *J. Environ. Radioact.*, 2008, **99**(1), 109–118.

196 J. E. Delmore, D. C. Snyder, T. Tranter and N. R. Mann, *J. Environ. Radioact.*, 2011, **102**(11), 1008–1011.

197 D. C. Snyder, J. E. Delmore, T. Tranter, N. R. Mann, M. L. Abbott and J. E. Olson, *J. Environ. Radioact.*, 2012, **110**, 46–52.

198 T. Ohno and Y. Muramatsu, *J. Anal. At. Spectrom.*, 2014, **29**(2), 347–351.

199 J. Zheng, K. Tagami, W. Bu, S. Uchida, Y. Watanabe, Y. Kubota, S. Fuma and S. Ihara, *Environ. Sci. Technol.*, 2014, **48**, 5433–5438.

200 J. Zheng, W. Bu, K. Tagami, Y. Shikamori, K. Nakano, S. Uchida and N. Ishii, *Anal. Chem.*, 2014, **86**(14), 7103–7110.

201 B. C. Russell, I. W. Croudace and P. E. Warwick, *Anal. Chim. Acta*, 2015, **890**, 7–20.

202 Y. Shibahara, T. Kubota, T. Fuji, S. Fukutani, T. Ohta, K. Takamiya, R. Okumura, S. Mizuno and H. Yamana, *J. Nucl. Sci. Technol.*, 2014, **51**(5), 575–579.

203 B. C. Russell, P. E. Warwick and I. W. Croudace, *Anal. Chem.*, 2014, **86**(23), 11890–11896.

204 J. M. B. Moreno, J. I. G. Alonso, P. Arbore, G. Nicolaou and L. Koch, *J. Anal. At. Spectrom.*, 1996, **11**(10), 929–935.

205 S. Asai, Y. Hanzawa, K. Okamura, N. Shinohara, J. Inagawa, S. Hotoku, K. Suzuki and S. Kaneko, *J. Nucl. Sci. Technol.*, 2011, **48**(5), 851–854.

206 J. Eliades, X.-L. Zhao, A. E. Litherland and W. E. Kieser, *Nucl. Instrum. Methods Phys. Res., Sect. B*, 2013, **294**, 361–363.

207 H. Isnard, M. Granet, C. Caussignac, E. Ducarme, A. Nonell, B. Tran and F. Chartier, *Spectrochim. Acta, Part B*, 2009, **64**(11–12), 1280–1286.

208 A. Pitois, L. A. De Las Heras and M. Betti, *Int. J. Mass Spectrom.*, 2008, **270**, 118–126.

209 M. Granet, A. Nonell, G. Favre, F. Chartier, H. Isnard, J. Moureau, C. Caussignac and B. Tran, *Spectrochim. Acta, Part B*, 2008, **63**(11), 1309–1314.

210 V. V. Lavrov, V. Blagojevic, G. K. Koyanagi, G. Orlova and D. K. Bohme, *J. Phys. Chem. A*, 2004, **108**(26), 5610–5624.

211 T. Lee, K. The-Lung, L. Hsiao-Ling and C. Ju-Chin, *Geochim. Cosmochim. Acta*, 1993, **57**(14), 3493–3497.

212 L. Pibida, C. McMahon and B. A. Bushaw, *Appl. Radiat. Isot.*, 2004, **60**(2–4), 567–570.

213 C. Macdonald, C. R. J. Charles, R. J. Cornett, X. L. Zhao, W. E. Kieser and A. E. Litherland, *Congress de l'ACP, Contribution ID: 155 Type: oral, Session Classification : (T2-9) Instrumentation-DIMP/Instrumentation-DPIM*, 2014.

214 J. I. G. Alonso, F. Sena, P. Arbore, M. Betti and L. Koch, *J. Anal. At. Spectrom.*, 1995, **10**, 381–393.

215 A. Meeks, J. Giaquinto and J. Keller, *J. Radioanal. Nucl. Chem.*, 1998, **234**(1), 131–136.

216 J. M. B. Moreno, M. Betti and G. Nicolaou, *J. Anal. At. Spectrom.*, 1999, **14**(5), 875–879.

217 M. Liezers, O. T. Farmer and M. Thomas, *J. Radioanal. Nucl. Chem.*, 2009, **282**(1), 309–313.

218 J. E. Martin, in *Environmental Radiochemical Analysis*, ed. G. W. A. Newton, Royal Society of Chemistry, London, UK, 1999.

219 S. Sumiya, N. Hayashi, H. Katagiri and O. Narita, *Sci. Total Environ.*, 1993, **130**–**131**, 303–315.

220 M. Yoshida, S. Sumiya, H. Watanabe and K. Tobit, *J. Radioanal. Nucl. Chem.*, 1995, **197**, 219–227.

221 L. Vio, G. Crétier, F. Chartier, V. Geertsen, A. Gourgiotis, H. Isnard and J.-L. Rocca, *Talanta*, 2012, **99**, 586–593.

222 H. Isnard, R. Brennetot, C. Caussignac, N. Caussignac and F. Chartier, *Int. J. Mass Spectrom.*, 2005, **246**, 66–73.

223 M. Baskaran, *J. Environ. Radioact.*, 2011, **102**, 500–513.

224 M. A. Amr, K. A. Al-Saad and A. I. Helal, *Nucl. Instrum. Methods Phys. Res., Sect. A*, 2010, **615**, 237–241.

225 A. E. M. Khater and W. F. Bakr, *J. Environ. Radioact.*, 2011, **102**, 527–530.

226 D. Larivière, K. M. Reiber, R. D. Evans and R. J. Cornett, *Anal. Chim. Acta*, 2005, **549**, 188–196.

227 Z. Varga, *Anal. Bioanal. Chem.*, 2008, **390**, 511–519.

228 T. Zhang, D. Bain, R. Hammack and R. D. Vidic, *Environ. Sci. Technol.*, 2015, **49**(5), 2969–2976.

229 Y.-T. Hsieh and G. M. Henderson, *J. Anal. At. Spectrom.*, 2011, **26**, 1338–1346.

230 M. Bourquin, P. Van Beek, J. L. Reyss, J. Riotte and R. Freydier, *Mar. Chem.*, 2011, **126**, 132–138.

231 M. Leermakers, Y. Gao, J. Navez, A. Poffijn, K. Croes and W. Baeyens, *J. Anal. At. Spectrom.*, 2009, **24**, 1115–1117.

232 Y. Gao, W. Baeyens, S. De Galan, A. Poffijn and M. Leermakers, *Environ. Pollut.*, 2010, **158**, 2439–2445.

233 G. Sharabi, B. Lazar, Y. Kolodny, N. Teplyakov and L. Halicz, *Int. J. Mass Spectrom.*, 2010, **294**, 112–115.

234 M. S. Choi, R. Francois, K. Sims, M. P. Bacon, S. Brown-Leger, A. P. Fleer, L. Ball, D. Schneider and S. Pichat, *Mar. Chem.*, 2001, **76**, 99–112.

235 D. A. Pickett, M. T. Murrell and R. W. Williams, *Anal. Chem.*, 1994, **66**(7), 1044–1049.

236 C.-C. Shen, H. Cheng, R. L. Edwards, S. B. Moran, H. N. Edmonds, J. A. Hoff and R. B. Thomas, *Chem. Geol.*, 2002, **3**–**4**, 165–178.

237 M. Regelous, S. P. Turner, T. R. Elliott, K. Rostami and C. J. Hawkesworth, *Anal. Chem.*, 2004, **76**, 3584–3589.

238 R. A. Mortlock, R. G. Fairbanks, T.-C. Chiu and J. Rubenstein, *Geochim. Cosmochim. Acta*, 2005, **69**(3), 649–657.

239 C.-C. Shen, R. L. Edwards, H. Cheng, J. A. Dorale, R. B. Thomas, S. B. Moran, S. E. Weinstein and H. N. Edmonds, *Chem. Geol.*, 2002, **185**, 165–178.

240 H. Cheng, R. L. Edwards, C.-C. Shen, V. J. Polyak, Y. Asmerom, J. Woodhead, J. Hellstrom, Y. Wang, X. Kong, C. Spötl, X. Wang and E. C. Alexander Jr, *Earth Planet. Sci. Lett.*, 2013, **371**–**372**, 82–91.

241 H. Cheng, R. L. Edwards, J. Hoff, C. D. Gallup, D. A. Richards and Y. Asmerom, *Chem. Geol.*, 2000, **169**, 17–33.

242 Y. Shi, R. Collins and C. Broome, *J. Radioanal. Nucl. Chem.*, 2013, **269**, 509–515.

243 S. K. Aggarwal, *Radiochim. Acta*, 2016, **104**(7), 445–455.

244 E. W. Hoppe, N. R. Overman and B. D. LaFerriere, Low Radioactivity Techniques, *AIP Conf. Proc.*, 2013, **1549**, 58–65.

245 J. S. Becker, M. Burow, M. V. Zoriy, C. Pickhardt, P. Ostapczuk and R. Hille, *J. Anal. At. Spectrom.*, 2004, **25**(5), 197–202.

246 M. L. Cozzella and R. Pettirossi, *Radiation Protection Institute ENEA*, Casaccia, Rome, Italy, 2012.

247 H. E. L. Palmieri, E. A. N. Knupp, L. M. L. A. Auler, L. M. F. Gomes and C. C. Windmöller, *International Nuclear Atlantic Conference- INAC*, 2011.

248 J. Avivar, L. Ferrer, M. Cass and V. Cerà, *J. Anal. At. Spectrom.*, 2012, **27**, 327–334.

249 H. Tuovinen, D. Vesterbacka, E. Pohjolainen, D. Read, D. Solatie and J. Lehto, *J. Geochem. Explor.*, 2015, **148**, 174–180.

250 A. Habibi, B. Boulet, M. Gleizes, D. Larrioviére and G. Cote, *Anal. Chim. Acta*, 2015, **883**, 109–116.



251 A. Borylo, *J. Radioanal. Nucl. Chem.*, 2013, **295**, 621–631.

252 P. J. Gray, L. Zhang, H. Zu, M. McDiarmid, K. Squibb and J. A. Centeno, *Microchem. J.*, 2012, **105**, 94–100.

253 J. G. Arnason, C. N. Pellegrini and P. J. Parsons, *J. Anal. At. Spectrom.*, 2013, **28**, 1410–1419.

254 J. G. Arnason, C. N. Pellegrini and P. J. Parsons, *J. Anal. At. Spectrom.*, 2015, **30**, 126–138.

255 C. Liu, B. Hu, J. Shi, J. Li, X. Zhang and H. Chen, *J. Anal. At. Spectrom.*, 2011, **26**, 2045–2051.

256 S. F. Boulyga, J. L. Matusevich, V. P. Mironov, V. P. Kudrjashov, L. Halicz, I. Segal, J. A. McLean, A. Montaser and J. S. Becker, *J. Anal. At. Spectrom.*, 2002, **17**, 958–964.

257 M. Tanimizu, N. Sugiyama, E. Ponzevera and G. Bayon, *J. Anal. At. Spectrom.*, 2013, **28**, 1372–1376.

258 S. Uchida, R. García-Tenorio, K. Tagami and M. García-León, *J. Anal. At. Spectrom.*, 2000, **15**, 889–892.

259 R. S. Pappas, B. G. Ting, J. M. Jarrett, D. C. Paschal, S. P. Caudill and D. T. Miller, *J. Anal. At. Spectrom.*, 2002, **17**, 131–134.

260 S. L. Maxwell III and V. D. Jones, *Talanta*, 2009, **80**, 143–150.

261 J. W. Ejnik, T. I. Todorov, F. G. Mullick, K. Squibb, M. A. McDiarmid and J. A. Centeno, *Anal. Bioanal. Chem.*, 2005, **382**, 73–79.

262 P. Krystek and R. Ritsema, *Anal. Bioanal. Chem.*, 2002, **374**, 226–229.

263 M. Magara, T. Sakakibara, S. Kurosawa, M. Takahashi, S. Sakurai, Y. Hanzawa, F. Esaka, K. Watanabe and S. Usada, *J. Anal. At. Spectrom.*, 2002, **17**, 1157–1160.

264 R. R. Parrish, M. F. Thirlwall, C. Pickford, M. Horstwood, A. Gerdes, J. Anderson and D. Coggon, *Health Phys.*, 2006, **90**(2), 127–138.

265 X. Dai and S. K. Tremblay, *J. Radioanal. Nucl. Chem.*, 2011, **289**, 461–466.

266 P. Thakur and G. P. Mulholland, *Appl. Radiat. Isot.*, 2012, **70**, 1747–1778.

267 Y.-Q. Ji, J.-Y. Li, S.-G. Luo, T. Wu and J.-L. Liu, *Fresenius' J. Anal. Chem.*, 2001, **371**, 49–53.

268 J. B. Truscott, P. Jones, B. E. Fairman and E. H. Evans, *Anal. Chim. Acta*, 2001, **433**, 245–253.

269 T. C. Kenna, *J. Anal. At. Spectrom.*, 2002, **17**, 1471–1479.

270 C. S. Kim, C. K. Kim and K. J. Lee, *J. Anal. At. Spectrom.*, 2004, **19**, 743–750.

271 Q. C. Chen, H. Dahlgaard, S. P. Nielsen and A. Aarkrog, *J. Radioanal. Nucl. Chem.*, 2002, **253**(3), 451–458.

272 M. Ayranov, U. Krähenbühl, H. Sahli, S. Röllin and M. Burger, *Radiochim. Acta*, 2005, **93**, 631–635.

273 P. Lindahl, P. Roos, E. Holm and H. Dahlgaard, *J. Environ. Radioact.*, 2005, **82**, 285–301.

274 T. C. Kenna, *J. Environ. Radioact.*, 2009, **100**, 547–557.

275 S. L. Maxwell, B. K. Culligan, V. D. Jones, S. T. Nichols, M. A. Bernard and G. W. Noyes, *Anal. Chim. Acta*, 2010, **682**, 130–136.

276 Y. Shi, X. Dai, C. Li, R. Collins, S. Kramer-Tremblay, R. Riopel and C. Broome, *J. Anal. At. Spectrom.*, 2014, **29**, 1708–1713.

277 P. Zhao, R. M. Tinnacher, M. Zavarin and A. B. Kersting, *J. Environ. Radioact.*, 2014, **137**, 163–172.

278 N. Guérin, M.-A. Langevin, K. Nadeau, C. Labrecque, A. Gagné and D. Larivière, *Appl. Radiat. Isot.*, 2010, **68**, 2132–2139.

279 J. Qiao, X. Hou, P. Roos and M. Miró, *Anal. Chem.*, 2011, **83**, 374–381.

280 B. S. Matteson, S. K. Hanson, J. L. Miller and W. J. Oldham Jr, *J. Environ. Radioact.*, 2015, **142**, 62–67.

281 S. Jerome, P. Ivanov, C. Larijani, D. H. Parker and P. H. Regan, *J. Environ. Radioact.*, 2014, **138**, 315–322.

282 A. Gourgiotis, M. Granet, H. Isnard, A. Nonell, C. Gautier, G. Stadelmann, M. Aubert, D. Durand, S. Legand and F. Chartier, *J. Anal. At. Spectrom.*, 2010, **25**, 1939–1945.

283 B. Kuczewski, C. M. Marquardt, A. Seibert, H. Geckeis, J. V. Kratz and N. Trautmann, *Anal. Chem.*, 2003, **75**(24), 6769–6774.

284 S. Röllin, H. Sahli, R. Holzer, M. Astner and M. Burger, *Appl. Radiat. Isot.*, 2009, **67**, 821–827.

285 J. Qiao, X. Hou, M. Miró and P. Roos, *Anal. Chim. Acta*, 2009, **652**, 66–84.

286 T. Warneke, PhD thesis, *GAU-Radioanalytical, Ocean and Earth Science*, University of Southampton, 2002.

287 J. Zheng, T. Aono, S. Uchida, J. Zhang and M. C. Honda, *Geochem. J.*, 2012, **46**, 361–369.

288 N. Erdmann, G. Hermann, G. Huber, S. Köhler, J. V. Kratz, A. Mansel, M. Nunneman, G. Passler, N. Trautmann, A. Turchin and A. Waldek, *Fresenius' J. Anal. Chem.*, 1997, **359**, 378–381.

289 Y. Ohtsuka, Y. Takaku, K. Nishimura, J. Kimura, S. Hisamatsu and J. Inaba, *Anal. Sci.*, 2006, **22**, 309–311.

290 D. Larivière, T. A. Cumming, S. Kiser, C. Li and R. J. Cornett, *J. Anal. At. Spectrom.*, 2007, **22**, 1–9.

291 B. G. Ting, R. S. Pappas and D. C. Paschal, *J. Anal. At. Spectrom.*, 2003, **18**, 795–797.

292 J. Qiao, X. Hou, P. Roos and M. Miró, *Anal. Chem.*, 2013, **85**, 2853–2859.

293 S. Cagno, K. Hellemans, O. C. Lind, L. Skipperud, K. Janssens and B. Salbu, *Environ. Sci.: Processes Impacts*, 2014, **16**, 306–312.

294 Z. Varga, A. Nicholl, M. Wallenius and K. Mayer, *J. Radioanal. Nucl. Chem.*, 2015, **307**(3), 1919–1926.

295 K. Bu, J. V. Cizdziel and D. Dasher, *J. Environ. Radioact.*, 2013, **124**, 29–36.

296 M. Jäggi, S. Röllin, J. A. C. Alvaredo and J. Eikenberg, *Appl. Radiat. Isot.*, 2012, **70**, 360–364.

297 S. Salminen-Paatero, U. Nygren and J. Paatero, *J. Environ. Radioact.*, 2012, **113**, 163–170.

298 T. Shinonaga, P. Steier, M. Lagos and T. Ohkura, *Environ. Sci. Technol.*, 2014, **48**, 3608–3814.

299 H. Hernández-Mendoza, E. Chamizo, A. Delgado, M. García-León and A. Yllera, *J. Anal. At. Spectrom.*, 2011, **26**, 1509–1513.

300 F. N. Pointurier, N. Baglan and P. Hémet, *Appl. Radiat. Isot.*, 2004, **60**, 561–566.

301 V. N. Epov, R. D. Evans, J. Zheng, O. F. X. Donard and M. Yamada, *J. Anal. At. Spectrom.*, 2007, **22**, 1131–1137.



302 M. L. D. P. Godoy, J. M. Godoy and L. A. Roldão, *J. Environ. Radioact.*, 2007, **97**, 124–136.

303 M. V. Zoriy, L. Halicz, M. E. Ketterer, C. Pickhardt, P. Ostapczuk and J. S. Becker, *J. Anal. At. Spectrom.*, 2004, **19**, 362.

304 O. F. X. Donard, F. Bruneau, M. Moldovan, H. Garraud, V. N. Epov and D. Boust, *Anal. Chim. Acta*, 2007, **587**, 170–179.

305 S. K. Aggarwal, *Mass Spectrom. Rev.*, 2016, DOI: 10.1002/mas.21506.

306 G. Xiao, D. Saunders, R. L. Jones and K. L. Caldwell, *J. Radioanal. Nucl. Chem.*, 2014, **301**, 285–291.

307 M. Agarande, S. Benzoubir, P. Bouisset and D. Calmet, *Appl. Radiat. Isot.*, 2001, **55**(2), 161–165.

308 W. Hang, L. Zhu, W. Zhong and C. Mahan, *J. Anal. At. Spectrom.*, 2004, **19**, 966–972.

309 Z. Wang, J. Zheng, L. Cao, K. Tagami and S. Uchida, *Anal. Chem.*, 2016, **88**(14), 7387–7394.

310 H. Kurosaki, J. R. Cadieux and S. B. Clark, *J. Anal. At. Spectrom.*, 2014, **29**, 2419–2423.

311 A. Gourgiotis, H. Isnard, M. Aubert, E. Dupont, I. AlMahamid, G. Tiang, L. Rao, W. Lukens, P. Cassette, S. Panebianco, A. Letourneau and F. Chartier, *Int. J. Mass Spectrom.*, 2010, **291**(3), 101–107.

312 A. Gourgiotis, H. Isnard, A. Nonell, M. Aubert, G. Stadelmann, E. Dupont, I. AlMahamid, G. Tiang, L. Rao, W. Lukens, P. Cassette, S. Panebianco, A. Letourneau and F. Chartier, *Talanta*, 2013, **106**, 39–44.

